Microphysical Modeling of Ultrafine Hydrocarbon-Containing Aerosols in Aircraft Emissions

by

Mina Jun
B.S, Seoul National University (2004)
S.M., Massachusetts Institute of Technology (2007)

Submitted to the Department of Aeronautics and Astronautics
in partial fulfillment of the requirements for the degree of
Doctor of Philosophy in Aeronautics and Astronautics
at the
MASSACHUSETTS INSTITUTE OF TECHNOLOGY
June 2011

Author .....
Department of Aeronautics and Astronautics
May 17, 2011

Certified by .....
Ian A. Waitz
Dean of Engineering and Jerome C. Hunsaker Professor of
Aeronautics and Astronautics
Thesis Supervisor

Certified by .....
Richard C. Miake-Lye
Director of Center for Aero-Thermodynamics, Aerodyne Research

Certified by .....
Jesse H. Kroll
Assistant Professor of Civil and Environmental Engineering and
Chemical Engineering

Accepted by .....
Eytan H. Modiano
Associate Professor of Aeronautics and Astronautics
Chair, Graduate Program Committee

Microphysical Modeling of Ultrafine Hydrocarbon-Containing Aerosols in Aircraft Emissions

by

Mina Jun

Submitted to the Department of Aeronautics and Astronautics
on May 17, 2011, in partial fulfillment of the
requirements for the degree of
Doctor of Philosophy in Aeronautics and Astronautics

Abstract

Combustion engines emit precursors of fine particulate matter (PM) into the atmosphere. Numerous gaseous species, soot particles, and liquid aerosols in the aircraft exhaust are involved in PM formation, and these very fine, nanometer-size particles potentially have significant impacts on climate, human health, and air quality. In particular, the organic content of the particles is important to determine physical and chemical properties of PM and consequently their potential impacts on the environment.

The main objective of this thesis is to understand the role of organic compounds in PM evolution by developing a microphysical model that incorporates organic compounds into the formation mechanism of binary aqueous aerosols. While binary aerosol models with sulfuric acid and water have been widely studied, the understanding of the effect of organics on the formation and growth of aerosols is still insufficient. This work demonstrates important interactions and competitions in the formation of multi-component aerosols with organic compounds, sulfuric acid, and water in aircraft emissions.

Hydrocarbon-containing aerosols have been identified as a major component of ground-level aircraft emission, especially at low power operations. This thesis describes selected surrogates of organic species and introduces estimation techniques for their thermophysical properties. The surrogates of organic species include water-insoluble hydrocarbons and water-soluble oxygenated hydrocarbons. Simulation results suggest that certain hydrocarbon compounds play an important role in the formation of aviation aerosol with interactions with both homogeneous sulfuric acid-water aerosols and soot particles in the organic-rich aircraft plume. Hydrocarbons contribute to the growth of existing homogeneous liquid particles, whereas their contribution to aerosol number density is negligible compared to that of sulfuric acid and water, which largely determine the formation of homogeneous aerosols. Also, low volatility hydrocarbons (e.g., benzopyrene, coronene) are observed to be partitioned into soot particles and induce competition with the uptake of water-soluble species, while light water-soluble oxygenated hydrocarbons enhance the uptake of water and

sulfuric acid on soot particles.

Thesis Supervisor: Ian A. Waitz
Title: Dean of Engineering and Jerome C. Hunsaker Professor of Aeronautics and Astronautics

Acknowledgments

I deeply thank my advisor, Prof. Ian Waitz, for his guidance and support through all my MIT years. He always encouraged and motivated me with insightful comments.

I am also grateful to my committee members and readers, Dr. Richard Miake-Lye, Prof. Jesse Kroll, Prof. Steven Barrett, and Dr. Hsi-Wu Wong. I would like to express my sincere appreciation to Dr. Richard Miake-Lye and Dr. Hsi-Wu Wong from Aerodyne Research, who have worked with this research and provided me critical advice and support.

I am thankful to my friends in PARTNER group at MIT, and also to my Korean friends, for their support.

I specially thank Jun-geun for all his love and support. I can finish this thesis without getting discouraged because of his kindness encouragement and love. I also thank Norang, Flocke, and my little friends. They gave me smiles everyday.

Finally, I thank my parents, my grandmother, and my sister and brother for their unconditional love.

Contents

List of Figures

List of Tables

Chapter 1

Introduction

In an aircraft exhaust plume, particulate matter (PM) evolves with contributions from 1) solid particles distributed from a few nanometers to sizes approaching a micrometer; 2) liquid droplets formed from condensable gases or directly emitted as a fragment of lubricating oil; and 3) a large number of exhaust gaseous species. As a result of being cooled and diluted with ambient air, the properties and sizes of PM are drastically changed through microphysical processes during even the first few minutes. Nanoparticles directly emitted from aircraft engines and generated subsequently in the downstream plumes may have significant impacts on climate, human health, and air quality [3]. To understand impacts of aircraft emitted PM as well as to possibly formulate strategies to mitigate these impacts, it is important to understand the microphysical processes and the atmospheric evolution of PM.

1.1 Background

Combustion engines emit particles in the size range of a few nanometers to micrometers, such as the nucleation mode particles (smaller than 10 nm in diameter), the Aitken mode particles (between 10 and 100 nm in diameter), and the accumulation mode particles in the submicrometer range [4]. Nano-sized particles smaller than 100 nm in diameter are also called ultrafine particles or $PM_{0.1}$ [5]. Primary particles in nanometer-size in the aircraft emission exhaust include soot particles directly emitted

in a solid form and liquid droplets nucleated from condensable gases. Nanoparticles continue to grow to larger size particles and shift toward accumulation mode by microphysical processes during dilution and cooling of the exhaust.

A number of studies have reviewed the potential impacts of nanoparticles on climate change and human health [6]. Black carbon, which is the core component of soot, influences climate by warming the atmosphere. While black carbon has positive radiative forcing by absorbing sunlight, most other aerosols such as sulfate and organic carbon aerosols have negative radiative forcing by scattering light. For example, aviation radiative forcing was estimated as -3.5 mW/m^2 for sulfate aerosol and 2.5 mW/m^2 for soot [7]. However, aerosols having a cooling effect themselves can also contribute to the climate warming by coating soot surfaces through condensation or coagulation [8]. Soot particles coated with nonradiation absorbing aerosols show an enhanced absorption of light compared to bare soot particles. Also, hydrophilicity of aerosols is an important factor for cloud formation and influences climate indirectly [9]. From a human health point of view, ultrafine particles can cause respiratory and cardiopulmonary diseases by entering and accumulating in the lung alveoli and the health risk is closely related to the size of the particles [10, 11]. Large surface area per unit mass of ultrafine particles may induce greater inflammatory effects with greater reactivity compared with larger size particles [12]. The chemical composition of particles is also a critical factor, as well as the particle size, because toxic PAHs or acidity in PM could cause negative health issues [13].

It has been demonstrated that soot particles in aircraft emissions are a major precursor of contrails and potentially of cirrus, through the interaction of water, sulfur, and organic gases; especially sulfate plays an important role for the hygroscopic growth of small particles to act as cloud condensation nuclei (CCN) by activating hydrophobic soot surface [14, 15]. Kanakidou *et al.* [9] reviewed the role of organic aerosols for climate modeling and summarized the importance of their contributions. While water-soluble inorganic species are more important at high relative humidity (RH), it was observed that the organic compounds become important at low RH because the effect of RH is critical for the water-soluble species but not for water-

insoluble organic compounds. The contribution of organic compounds to atmospheric particulates has been discussed increasingly [16, 17, 18, 19]. Organic aerosols are involved in the PM evolution and change the thermodynamic and physical properties of soot surface through the influence of surface tension and solubility. Petzold *et al.* [20] investigated how organic matter and sulfuric acid from exhaust emission affect CCN activation based on the data set of the European PartEmis project. Their results showed that the fraction of organic carbon in the soot particles decreases CCN activation by competing with the coating effect of sulfuric acid. While water-insoluble organic species reduce the water absorption, water-soluble organic species such as organic acids enhance the hydroscopic growth by increasing hydrophilic fraction and decreasing surface tension [21]. Du and Yu [22] reported that organics contribute to the non-volatile particle growth in exhaust from ultra-low sulfur fuel for ground vehicles.

In most studies, particle growth was modeled with an equilibrium partitioning with assumption of wettable surface and/or soluble particles for water absorption [23]. Kulmala *et al.* [24] investigated the early stage growth of aerosol particles in the nanometer size range. They discussed that organic vapors that are soluble in aerosol clusters contribute to the growth of nanometer-size aerosol particles that are not solid particles. Jacobson [25] used different distributions for different coating fractions of black carbon. In his model, particles can move between bins as the fractional coating changed by condensation. However, the change in hydrophobic and hydrophilic surface and the effect of organics on the surface are not tracked.

To better assess the potential impacts of PM on the environment, it is necessary to adequately estimate the evolution of size, mass, and composition of PM. Field and laboratory measurements have been conducted extensively over the past decades. Accumulated data from measurements help to understand the physics and estimate PM formation and subsequent processes, however, there is a possibility of bias in measurement results because collection of particles itself can change the gas-particle partitioning of condensable gases [26]. In addition, since aircraft emitted PM and exhaust gases are sensitive to the ambient conditions and engine operating parameters

such as ambient temperature, relative humidity (RH), engine power, and fuel sulfur content and the high temperature, high velocity exhaust plume is a challenging measurement environment, accurate and repeatable measurements are very challenging. Quantifying sensitivity of those parameters is even more difficult because ambient conditions are very hard to be controlled in the field. Cooperating with theoretical models is also required therefore. Theoretical understanding will help also to enhance the capability of measurement systems through exploring PM behaviors in sampling systems and instruments.

Enhancing models to include organic species will make them complicated as a lot of unidentified organic compounds are involved. Aircraft simultaneously emit many organic species and soot particles from incomplete combustion of fuel, as well as sulfate due to sulfur in the fuel. Microphysical processes evolve dynamically in the hot exhaust from the engine exit and include many complex interactions between exhaust gases and soot particles. In that circumstance, a role of primary organic compounds could be important to the size distribution and properties of PM compared to secondary organic aerosols having low vapor pressure, which are not emitted from engine directly but generated from gas phase oxidation and subsequent microphysical processes. A lot of studies have focused on studying the effect of sulfate of fuel on the PM formation, but modeling and understanding of the contribution of organics on the particle formation is still limited.

The objective of this thesis is to understand the role of organic compounds in the aerosol formation and demonstrate important interactions involved with organic compounds. This thesis describes a kinetic microphysical multi-component model incorporating the hydrocarbons into an aqueous system of sulfuric acid and water with soot particles emitted from aircraft engines. Parametric studies exploring the effect of ambient conditions and engine operating parameters as well as identifying sensitivity associated with modeling parameters are also discussed. Figure 1-1 provides a schematic of the microphysical model for the formation of hydrocarbon-containing aerosols.

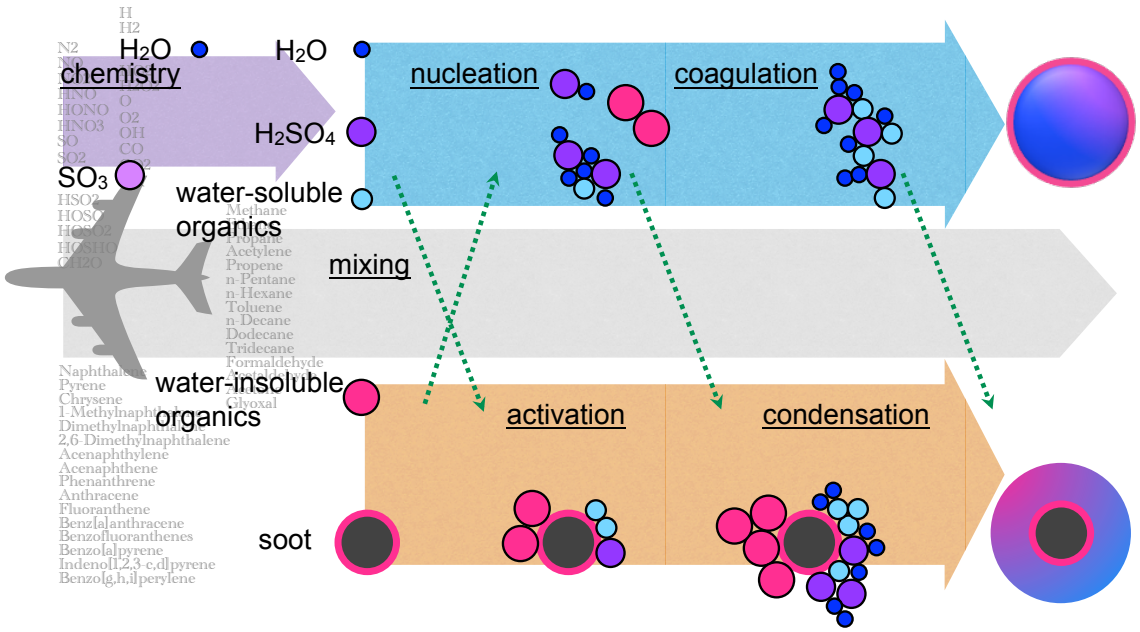

Figure 1-1: Overview of formation of hydrocarbon-containing aerosols in aircraft emissions

1.2 Previous Work

A one-dimensional multi-component model developed in this thesis work follows the scheme of the binary model of Wong *et al.* [27]. This section presents major details of their model focused on the microphysical processes of the H_2SO_4–H_2O binary system. The main equation for the time evolution of the volume mixing ratio X of gaseous or particulate species in jet engine exhaust is defined as

$$\frac{dX_i}{dt} = \left.\frac{dX_i}{dt}\right|_{chemistry} + \left.\frac{dX_i}{dt}\right|_{mixing} + \left.\frac{dX_i}{dt}\right|_{microphysics} \tag{1.1}$$

The first term in Equation (1.1) represents the contribution from chemical reactions written as

$$\left.\frac{dX_i}{dt}\right|_{chemistry} = M_{\omega,i} \cdot \dot{\omega}_i \cdot \frac{1}{\rho_{pl}} \tag{1.2}$$

where $M_{\omega,i}$ is the molecular weight of species i, $\dot{\omega}_i$ is the overall molar chemical reaction rate of species i, and ρ_{pl} is the plume density.

The second term in Equation (1.1) for the contribution of wake dilution and mixing

is calculated as

$$\left.\frac{dX_i}{dt}\right|_{mixing} = (X_i - X_{amb,i}) \cdot \frac{df(t)}{dt} \cdot \frac{1}{f(t)} \tag{1.3}$$

where $f(x)$ describes the extent of plume dilution and was calculated using Davidson-Wang algorithm semi-empirically [see Appendix of Wong *et al.* [27] for detailes].

The contribution of microphysical processes in the last term of equation (1.1) is composed of nucleation, coagulation, and microphysical processes of sulfuric acid and water on the soot surface:

$$\left.\frac{dX_i}{dt}\right|_{microphysics} = \left.\frac{dX_i}{dt}\right|_{nucleation} + \left.\frac{dX_i}{dt}\right|_{coagulation} + \left.\frac{dX_i}{dt}\right|_{soot} \tag{1.4}$$

Binary homogeneous nucleation of sulfuric acid and water was modeled with the kinetic quasi-unary nucleation (KQUN) theory (see Sectioin 4.1.1). In the KQUN theory, sulfuric acid controls the nucleation kinetics while water is assumed to immediately equilibrate with embryos and droplets. With this assumption, the classic binary nucleation of H_2SO_4−H_2O can be treated as the quasi-unary nucleation of sulfuric acid. The rates of embryo formation due to homogeneous binary nucleation are derived as

$$\begin{aligned}
\frac{dn_1}{dt} &= 2\gamma_2 n_2 + \sum_{i=3}^{m} \gamma_i n_i - \sum_{1}^{m-1} \beta_i n_i & (i = 1) \\
\frac{dn_2}{dt} &= \frac{1}{2}\beta_1 n_1 - \gamma_2 n_2 - \beta_2 n_2 + \gamma_3 n_3 & (i = 2) \\
\frac{dn_i}{dt} &= \beta_{i-1} n_{i-1} - \gamma_i n_i - \beta_i n_i + \gamma_{i+1} n_{i+1} & (i > 2)
\end{aligned} \tag{1.5}$$

where n_i is the concentration of embryos with i acid molecules (referred to as i-mers), β_i is the growth rate coefficient of i-mers, γ_i is the evaporation rate coefficient of i-mers, and m is the size of the largest embryo tracked in a simulation.

Coagulation contributes to the particle growth by forming larger particles from collisions of smaller liquid embryos or droplets. In typical aircraft plume conditions, the coagulation process becomes important soon after a start of particle formation by nucleation. The rate of change in the droplet number density by coagulation is

given by

$$\frac{dn_k}{dt} = \frac{1}{2}\sum_{i+j=k} K_{ij} n_i n_j - \sum_{i=1}^{l} K_{ik} n_i n_k \tag{1.6}$$

where K_{ij} is the Brownian coagulation kernel calculated as

$$K_{ij}(d_i, d_j) = \frac{8\pi \bar{d}\bar{D}}{\bar{d}/\left(\bar{d}+\bar{\delta}\right) + 4\bar{D}/\left(\bar{d}+\bar{c}\right)} \tag{1.7}$$

where $\bar{d} = (d_i + d_j)/2$, $\bar{D} = (D_i + D_j)/2$, $\bar{c} = (c_i^2 + c_j^2)^{1/2}$, and $\bar{\delta} = (\delta_i^2 + \delta_j^2)^{1/2}$.

The third term of equation (1.4) describes the size evolution of soot particles by interactions between nucleated liquid particles/gaseous species and the solid soot surface. This soot microphysics term will be visited in Section 3.1 in detail, while describing the extended equations for organic compounds. The relative importance of microphysical terms is closely associated with ambient conditions and engine operating parameters.

1.3 Thesis Outline

This thesis describes how to incorporate hydrocarbon species into the binary sulfuric acid and water system with following structure of chapters:

Chapter 2 describes how to select hydrocarbon surrogates for representing aviation emissions and what estimation methods were employed to model their thermophysical properties.

Chapter 3 addresses the contributions of water-insoluble and water-soluble hydrocarbons to the soot particle growth and providing parametric studies to analyze sensitivities of the soot particle growth associated with key modeling parameters and ambient conditions.

Chapter 4 develops nucleation and coagulation modeling approaches for multicomponent homogeneous aerosols with sulfuric acid, water, and hydrocarbon species and discusses simulation results for suggested pathways for the new particle formation in near-field aircraft emissions.

Chapter 5 presents simulation results including complete microphysical modes

to explore sensitivities of mass distribution to ambient conditions and hydrocarbon parameters.

Finally, Chapter 6 provides a summary and conclusions of this thesis.

1.4 Thesis Contributions

The main focus of this thesis is to understand the role of hydrocarbons in the initial formation of aircraft emitted aerosols through detailed microphysical modeling of hydrocarbon-containing aerosols. Listed below are the major contributions of this thesis work:

- **Development of a multi-component microphysical model incorporating multiple organic species into a binary sulfuric acid and water aerosol model.** General modeling methods are introduced for an easy extension of building hydrocarbon surrogates. The developed model can work with both water-soluble and water-insoluble hydrocarbon compounds and therefore capture the competition effect between different solubility species, which is a major advance of the multicomponent model developed in this work over aqueous aerosol models.

- **Evaluation of modeling parameters in the ranges relevant to aircraft emissions.** Parametric studies of modeling parameters and emission properties allow estimating the uncertainty effect on model predictions from limited accurate measurements of key parameters.

- **Studies of the effect of ambient conditions.** A comprehensive study of the model sensitivity to ambient conditions provides a better understanding of important interactions between constituents of aircraft emissions.

Chapter 2

Modeling of Hydrocarbon Surrogates

Chapter 2 describes estimation methods for thermal and physical properties of hydrocarbon species and selected surrogates of organic species, selected based on recent field measurement of aircraft emissions [28, 29]. Surrogates of organic species include both water-insoluble hydrocarbons and watersoluble oxygenated hydrocarbons listed in Table 2.1, which were chosen to cover a wide range of saturation vapor pressure from 10 times higher than the vapor pressure of water and to 10^{-6} lower than the vapor pressure of sulfuric acid at 300 K (See Figure 2-2 for estimation of saturation vapor pressure of sulfuric acid, water, and selected hydrocarbons.) While a species lumping approach [30, 31] may be more general to model the evolution of aircraft emitted PMs further downstream where equilibrium is almost reached, tracking the evolution of each individual hydrocarbon species is more appropriate in simulating PM evolution in nearfield aircraft plumes where PM microphysics is kinetically controlled. To allow this implementation, general estimation techniques were employed, such as group contribution methods, to estimate species properties for easy extension to include a wide variety of organic compounds.

2.1 Solubility

The water solubility of organic species involved in the PM formation is one of the critical properties affecting hydrophilicity of the soot surface and consequent water uptake, which is a major mechanism of particle growth in the atmosphere. Turpin *et al.* [26] listed *water-soluble* and *water-insoluble* organic compounds measured or expected to exist in atmospheric aerosols:

Water-soluble organics dicarboxylic acid, glyoxal, ketoacids, polyols, hydroxyamines, amino acids, nitrophenol

Water-insoluble organics n-alkanes, n-alkanoic acids, diterpenoid acids, aromatic polycarboxylic acids, polycyclic aromatic hydrocarbons, polycyclic aromatic ketones, polycyclic aromatic quinones

where organic compounds are classified as water-soluble if their solubility is greater than 1 g/(100g of water) [10^4 mg/L of water].

The same criterion was employed in this work. If an organic compound has very low aqueous solubility, the water-insoluble organic compound is assumed to exist on a soot surface as a separate liquid phase from the aqueous solution of water, sulfuric acid, and water-soluble organics. In general, heavier hydrocarbon species are less soluble in water. Table 2.1 lists the solubility of selected hydrocarbon species in water at 25 °C.

2.2 Density of Liquid Mixture

The density of a liquid mixture of sulfuric acid, water, and water-soluble organics or a mixture of water-insoluble hydrocarbons was estimated with the Rackett equation

using Li's method for the mixing rule [2].

$$
\begin{aligned}
\rho_m &= \frac{x_i M_i}{V_m} \\
V_m &= R\left(\sum_i \frac{x_i T_{c,i}}{P_{c,i}}\right) Z_{RA,m}^{\left[1+(1-T_r)^{0.2857}\right]} \\
Z_{RA,m} &= \sum x_i Z_{c,i} \\
T_r &= \frac{T}{T_{cm}} \\
T_{cm} &= \sum \phi_i T_{c,i} \\
\phi_i &= \frac{x_i V_{c,i}}{\sum_j x_j V_{c,j}}
\end{aligned}
\tag{2.1}
$$

where x is the mole fraction, M_i is the molecular weight, T_c is the critical temperature, P_c is the critical pressure, V_c is the critical volume, and Z_c is the critical compressibility factor. The group contribution method by Nannoolal *et al.* [33, 34] wasused to estimate critical properties of individual species required for the density calculation.

Organic Compounds		Aqueous Solubility [mg/L of water][a]	
Propanoic Acid	$C_3H_6O_2$	water-soluble	1×10^6
Butanoic Acid	$C_4H_8O_2$		6×10^4
Acetone	C_3H_6O		1×10^6
Propanol	C_3H_8O		1×10^6
Naphthalene	$C_{10}H_8$	water-insoluble	31
Anthracene	$C_{14}H_{10}$		0.0434
Pyrene	$C_{16}H_{10}$		0.135
Chrysene	$C_{18}H_{12}$		0.002
Benzo[a]pyrene	$C_{20}H_{12}$		0.0004
Benzo[ghi]perylene	$C_{22}H_{12}$		2.6×10^{-4}
Coronene	$C_{24}H_{12}$		1.4×10^{-4}

[a]: Aqueous solubility at 25 °C from experimental database in U.S. EPA Estimation Program Interface Suite™[32]

Table 2.1: Solubility of selected organic compounds

2.3 Surface Tension

Surface tension is required in many calculations for microphysical processes such as the Kelvin equation (Equation 2.2), which is an important factor for an increment of vapor pressure over a curved surface.

$$P = P^{sat} exp\left(\frac{2\sigma M}{RT\rho_l R_p}\right) \tag{2.2}$$

where σ is the surface tension, M is the molecular weight, ρ_l is the liquid-phase density, and R_p is the particle radius.

Surface tension of a liquid mixture was assumed to be the molar fraction weighted summation of the contributions of each component:

$$\sigma_m^r = \sum_i^n x_i \sigma_i^r \tag{2.3}$$

where x_i is the mole fraction of compound i in the mixture. σ_i is the surface tension of pure compound i, and r=1 is recommended for most hydrocarbon mixtures [2].

While the composition of the bulk phase is different from the composition of surface phase in general, this approximation approach is acceptable for thin liquid coatings on the surface of a solid core, where the surface composition dominates the overall layer composition.

Surface tension of a pure hydrocarbon compound can be estimated from temperature and thermodynamics properties of a compound. This work used empirical equations by Brock and Bird for non-polar organics and equations by Sastri and Rao for polar organic liquids [2]. The empirical relationship developed by Brock and Bird

	K	x	y	z	m
Alcohols	2.28	0.25	0.175	0.	0.8
Acids	0.125	0.50	-1.5	1.85	11/9
All others	0.158	0.50	-1.5	1.85	11/9

Table 2.2: Parameters for Sastri-Rao equation [2]

for non-polar organic liquids is:

$$\begin{aligned}
&\sigma\ (\mathrm{N/m}) = 10^{-3} P_c^{2/3} T_c^{1/3} Q (1 - T_r)^{11/9} \\
&Q = 0.1196 \left(1 + \frac{T_{br} ln(P_c/1.01325)}{1 - T_{br}} \right) - 0.279 \\
&T_r = T/T_c \\
&T_{br} = T_b/T_c
\end{aligned} \tag{2.4}$$

where T_b (K) is the normal boiling point, T_c (K) is the critical temperature, and P_c (bar) is the critical pressure.

For polar organic compounds with strong hydrogen-bonding, the estimation can be enhanced using the modified equation by Sastri and Rao [2]:

$$\sigma = K P_c^x T_b^y T_C^z \left[\frac{1 - T_r}{1 - T_{br}} \right]^m \tag{2.5}$$

Constant parameters, K, x, y, z, and m, are given for different type of organic compounds in Table 2.2.

2.4 Activity Coefficient

Activity coefficients of the components in liquid mixtures were evaluated by the CSB approach described in Clegg and Seinfeld [35]. This approach calculates activity coefficients of electrolyte components and organic components in an aqueous mixture with an appropriate estimation method for separate electrolyte and organic mixtures. Interaction effects between water-electrolyte-organics are corrected afterwards. With the assumption that interactions between sulfuric acid and water-soluble organics in the aqueous mixture is negligible, activity coefficients of solutes in the mixture can be calculated from an aqueous sulfuric acid solution and an aqueous organic solution independently. Finally, the water activity of the mixture can be calculated as:

$$a_{\mathrm{w}} = a_{\mathrm{w,\ sulfuric\ acid}}\ a_{\mathrm{w,\ w\text{-}s\ HCs}} \tag{2.6}$$

where $a_{\text{w, sulfuric acid}}$ denotes the water activity of aqueous sulfuric acid solution and $a_{\text{w, w-s HCs}}$ denotes the water activity of aqueous organic solution. This work used the modified UNIversal Functional Activity Coefficient (UNIFAC) group contribution model [36] for the estimation of activity coefficients of aqueous organic solution and the empirical relationship in Taleb *et al.* [37] for activity coefficients of aqueous sulfuric acid solution. Activity coefficients of the water-insoluble organic mixture were estimated using the modified UNIFAC model as well. Interaction between the water-insoluble organic mixture and the aqueous solution was not considered in this work assuming the water-insoluble organic mixture as a separate liquid phase from the aqueous solution.

2.5 Saturation Vapor Pressure

Prediction of saturation vapor pressure of a volatile species is important in the modeling of particle growth by condensation, where the difference between the partial vapor pressure of species and its saturation vapor pressure near soot coatings is the driving force of the condensational process. One of widely used estimation methods for saturation vapor pressure is using the Antoine equation:

$$\log_{10} P = A - \frac{B}{T + C} \tag{2.7}$$

where P is the vapor pressure of species, T is the temperature, and A, B, and C are the interpolation parameters fitted from experimental data. Interpolation parameters can be found in chemical references such as NIST chemistry webbook (Standard References Database Number 69). The Antoine equation can estimate saturation vapor pressure of a volatile species simply as a function of temperature; however, it requires parameters fitted from compound specific measurements, thus for most heavy hydrocarbons, these parameters are not available due to difficulties in measuring very low vapor pressures.

For more general implementation of modeling of organic species in a wide range

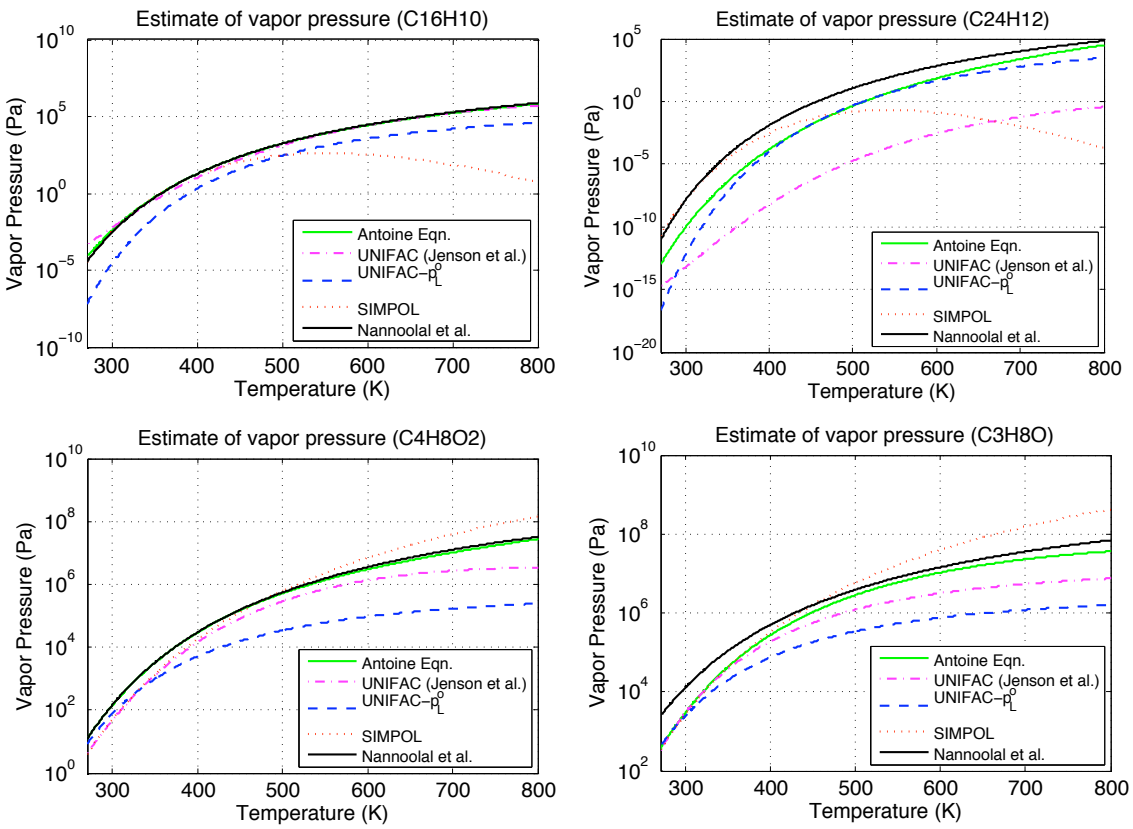

Figure 2-1: Saturation vapor pressure curves estimated from the Antoine equation and from group contribution methods for $C_{16}H_{10}$, $C_{24}H_{12}$ (water-insoluble), C_3H_8O, and $C_4H_8O_2$ (water-soluble)

of saturation vapor pressure, instead group contribution methods was applied to estimate saturation vapor pressure, which are based on the molecular structure of a compound, rather than depending on individual measurement data. Group contribution methods estimate thermodynamic properties of a compound based on the contribution of its structural fragments, such as aromatic carbons, $-CH_2$, and $-CH_3$, and the interactions of interacting groups, such as $-OH$ and $-COOH$, from fitting results using a basis set of compounds in a broad range. Figure 2-1 shows vapor pressure curves estimated using group contribution methods for both water-soluble and water-insoluble organic species with known saturation vapor pressure curves from the Antoine equation. The compared group contribution methods are UNIFAC by Jensen *et al.* [38], UNIFAC-pL° by Asher and Pankow [39], SIMPOL by Pankow and Asher [40], and the approach by Nannoolal *et al.* [41]. This work choose to use the approach

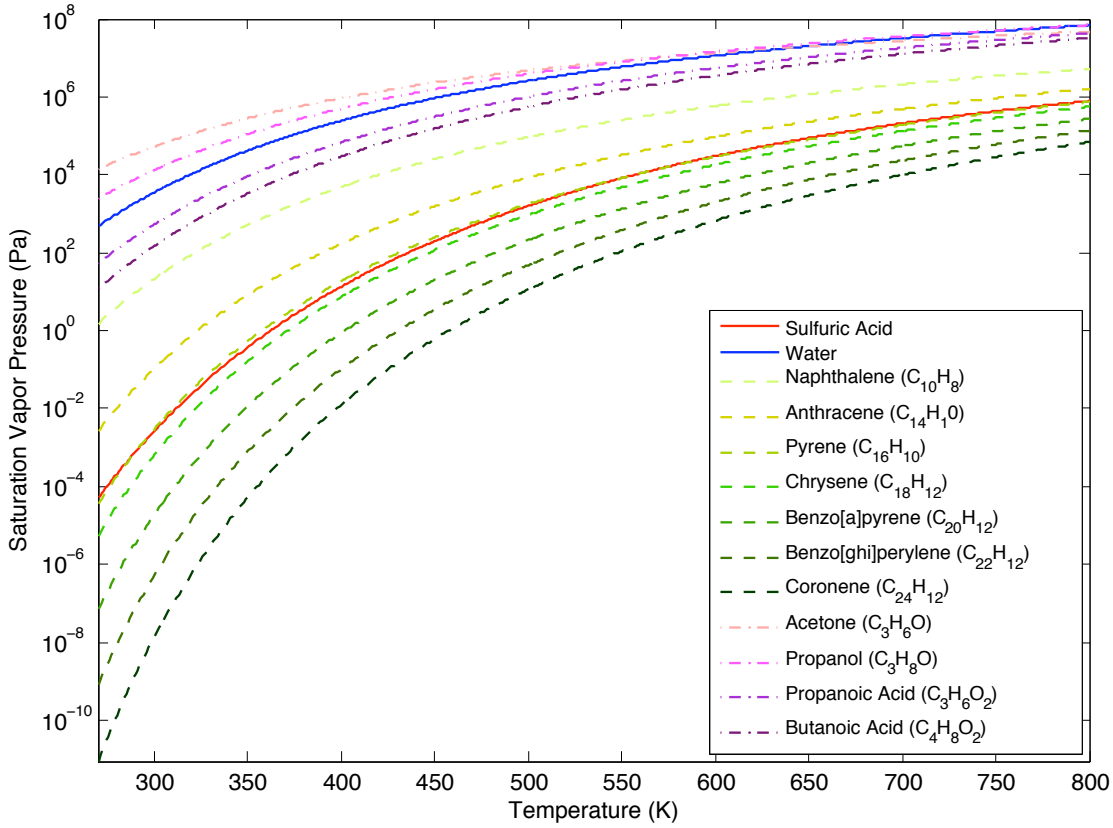

Figure 2-2: Estimation of saturation vapor pressure by the Nannoolal *et al.* approach for selected surrogates of organic species and by Vehkamäki *et al.* [1] for sulfuric acid and water

developed by Nannoolal *et al.* for its good agreements between the estimation and measurements for both types of organic species over a wide range of temperature for exhaust gases. SIMPOL and UNIFAC-pL° show an offset in the high temperature region because their temperature fitting ranges for basis sets are limited as 290-320 K for UNIFAC-pL° and 273-393 K for SIMPOL. The approach by Nannoolal *et al.* is also relatively straightforward to extend the model to incorporate various organic compounds than other methods. Figure 2-2 shows the saturation vapor pressure curves for several organic species selected to cover a range of saturation behaviors as estimated by the Nannoolal *et al.* approach and the saturation vapor pressure for sulfuric acid and water [1].

Chapter 3

Modeling of Soot Particle Growth

3.1 Microphysical Model

While complete microphysical processes include nucleation of embryos, coagulation of liquid particles, and condensation of gaseous species and embryos/droplets on soot particles as seen in Equation (1.4), this chapter focuses on studying the role of organic compounds in the condensational growth of soot particles by enhancing or competing with sulfuric acid and water condensation. The formation of new particles via nucleation and coagulation is not considered in the simulation results in this chapter, but will be discussed in the next chapter.

3.1.1 Microphysics on Surface

Condensation is a mass transfer process through adsorption of molecules from the gaseous state to the liquid state. Adsorption can occur either as the formation of a monolayer or as multilayer coatings [42]. While limited adsorption forming a monolayer is plausible when the vapor pressure of species is low, adsorption proceeds to a multilayer at sufficiently high vapor pressure. The Langmuir isotherm is the famous monolayer adsorption model and fits experimental data well for chemisorption that shows specific interaction between the adsorbent and adsorbate. For multilayer adsorption models, BET (Brunauer, Emmet and Teller) [43] and FHH (Frenkel, Halsey,

and Hill) [44] are well known models. Various models for the particle growth by adsorption were suggested and applied especially to cloud droplet activation to grow as CCN. The Köhler theory [45] describes condensation of water vapor on water-soluble aerosol nuclei. Nano-Köhler theory [24] is analogous to the classical Köhler theory, but it describes activation by water-soluble organic compounds and condensation of water for particle growth on nanometer-size inorganic clusters, where organic and inorganic compounds are mixed together in an aqueous solution. For water-insoluble but perfectly wettable particles, Henson [46] and Sorjamaa and Laaksonen [47] modified the classical Köhler theory with multilayer adsorption isotherms of BET and FHH respectively. These models explain the particle growth with condensation of homogeneous droplets on wettable particles or soluble nuclei, but not for the hydrophobic particle growth.

While soot particles generated from aviation kerosene in laboratory flame have very hydrophobic surfaces, sampled soot particles from aircraft engine were observed as rather hydrophilic [48]. Therefore, it is reasonable to assume that freshly emitted aerosols from combustion engines are hydrophobic, but are transformed to hydrophilic as they age. Since water molecules avoid adsorption on hydrophobic surfaces, a soot surface needs to be activated to be hydrophilic. For example, sulfuric acid can enhance the water absorption of soot by activating the soot surface. The surface of dry particles can be first coated by collision with sulfur containing molecules, and then, water and sulfuric acid can condense on the liquid coating, i.e., the activation layer. In this work, modeling of hydrophobic particle growth followed the scheme of soot activation and condensation afterward in Kärcher's model [49]. However, Kärcher's model works well for partially activated particles but not for the particles fully immersed by water. Partial activation of the soot surface with Langmuir-type adsorption may limit condensation of water vapor and not applicable to aerosols under high RH conditions or when the volume of condensed liquid layers surpasses that of the soot core. Popovicheva *et al.* [48] measured a rapid increase of water adsorption on hydrophobic combustor soot with increasing RH, and they suggested the formation of water film as connecting adsorbed molecules over the soot surface.

A process for the surface activation by condensation is described in Section 3.1.3 to resolve this issue.

3.1.2 Adsorption on Soot Surface

Mass transfer of exhaust gases was modeled in two pathways, which are: 1) into liquid layers and 2) on the solid surface. Since fresh soot surfaces are assumed to completely dry and hydrophobic, activation of the soot surface is prerequisite for condensation on soot. Adsorption of molecules on the soot surface forming a liquid layer can initiate activation as described in Equation (3.1). The soot surface can be activated to be either hydrophilic or hydrophobic by sulfuric acid and water-soluble organics, or by water-insoluble organics, respectively. Water was not considered in this activation process because it is very hard for it to be adsorbed on the hydrophobic soot surface directly. In addition to the adsorption of gas molecules on soot surfaces, there are also collisions between nucleated clusters or droplets with soot surfaces, and this is referred to as scavenging. Scavenging was modeled with Brownian coagulation between particles and scavenged liquid droplets were assumed to activate the surface with πr_k^2 corresponding to a cross-sectional area of hemisphere of droplets.

$$
\begin{aligned}
\left.\frac{d\Theta}{dt}\right|_{\text{activation}} &= \left.\frac{d\Theta}{dt}\right|_{\text{ads,aq}} + \left.\frac{d\Theta}{dt}\right|_{\text{ads,non-aq}} + \left.\frac{d\Theta}{dt}\right|_{\text{scav,aq}} + \left.\frac{d\Theta}{dt}\right|_{\text{scav,non-aq}} \\
\left.\frac{d\Theta}{dt}\right|_{\text{ads,aq}} &= \frac{1}{4}\left[\alpha_{d,\text{S}} \cdot \bar{c}_{\text{S}} \left(C_{\text{H}_2\text{SO}_4} + C_{\text{SO}_3}\right) + \sum_{i=\text{w-s}} \alpha_{d,\text{HC}_i} \cdot \bar{c}_{\text{HC}_i} C_{\text{HC}_i}\right] \frac{(1-\Theta)N_A}{\sigma_0} \\
\left.\frac{d\Theta}{dt}\right|_{\text{ads,non-aq}} &= \frac{1}{4} \sum_{j=\text{w-is}} \alpha_{d,\text{HC}_j} \cdot \bar{c}_{\text{HC}_j} C_{\text{HC}_j} \frac{(1-\Theta)N_A}{\sigma_0} \\
\left.\frac{d\Theta}{dt}\right|_{\text{scav,aq/non-aq}} &= \frac{1}{4} \sum_{\substack{k \\ (j=\text{ws/w-is})}} K_k\left(d_s, d_{k,j}\right) n_{k,j} \left(\frac{d_{k,j}}{d_s}\right)^2 (1-\Theta)
\end{aligned}
\tag{3.1}
$$

where Θ is the activated soot surface fraction ($A_{\text{activated surface}}/A_{\text{total surface}}$), α_d is the mass accommodation coefficient of gaseous species on the dry soot surface (referred to as dry accommodation coefficient), $\bar{c}$ is the mean particle thermal speed, C is the gaseous concentration of species, N_A is the Avogadro number, σ_0 is the number

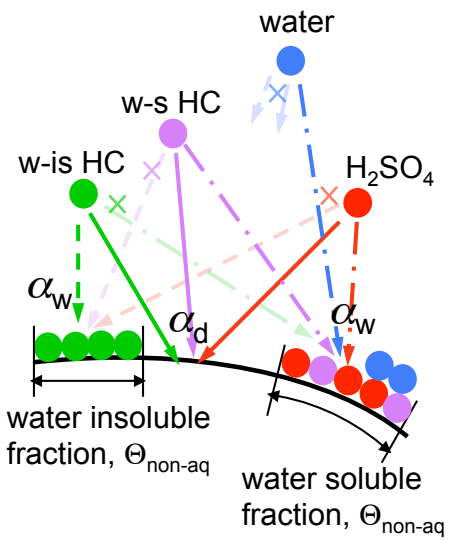

Figure 3-1: Mass accommodation coefficients describing interactions between gas molecules and a soot surface

of sites able to adsorb molecules per unit area of soot surface, K_k is the Brownian coagulation kernel between soot particles and liquid particles in the kth size bin, n_k is the number density of liquid particles in the kth size bin, d_k is the diameter of liquid particles in the kth size bin, d_s is the diameter of the dry soot particles. *w-s* and *w-is* stand for water-soluble and water-insoluble.

The surface activation rate by adsorption is proportional to the gaseous concentration and the dry accommodation coefficient corresponding to the sticking probability of a molecule on the soot activation site. Figure 3-1 shows two types of mass accommodation coefficients in soot microphysics. The dry accommodation coefficient (α_d) is involved in the adsorption on soot surfaces, while the wet accommodation coefficient (α_w) appear in the condensation in Section 3.1.3. For this work, α_d was set to 0.018 for H_2SO_4 and SO_3 [27]. For organic species, an accurate value of α_d is not available, so it was assumed to be 0.01 for this work. To determine experimental values for several organic species, a set of experiments is being conducted by UTRC and Aerodyne Research, Inc. The adsorption activation rate is also proportional to $(1 - \Theta)$ and this factor represents the surface saturation of monolayer like Langmuir adsorption.

The rate of change of mass by activation is written as

$$\begin{aligned}
\left.\frac{dm}{dt}\right|_{\text{ads},S} &= \frac{1}{4}\alpha_{d,\text{S}} \cdot \bar{c}_{\text{S}} \cdot N_A \cdot \pi d_s^2 \left(1-\Theta\right)\left(C_{\text{H}_2\text{SO}_4} M_{\text{H}_2\text{SO}_4} + C_{\text{SO}_3} M_{\text{SO}_3}\right) \\
\left.\frac{dm}{dt}\right|_{\text{ads},\text{HC}_j} &= \frac{1}{4}\alpha_{d,\text{HC}_j} \cdot \bar{c}_{\text{HC}_j} \cdot N_A \cdot \pi d_s^2 \left(1-\Theta\right) \cdot C_{\text{HC}_j} M_{\text{HC}_j} \\
\left.\frac{dm}{dt}\right|_{\text{scav,aq/non-aq}} &= \sum_{\substack{k \\ (j=\text{ws/w-is})}} K_k\left(d_s, d_{k,j}\right) n_{k,j} M_{k,j} \left(1-\Theta\right)
\end{aligned} \tag{3.2}$$

where d_s is the diameter of the dry soot particle, M_i is the molecular weight of species, and M_k is the molecular weight of liquid particles in the kth size bin.

3.1.3 Condensation

Condensation can occur only on the activated soot surface and, in addition, it depends on the hydrophilicity of the surface. The activated soot surface can be hydrophilic or hydrophobic according to the water solubility of adsorbed species as described in the above section. Water-soluble species cannot condense on the hydrophobic surface activated by water-insoluble HCs. This dependence on the activated surface fraction (Θ) was included in the classical condensation equation as

$$\begin{aligned}
\left.\frac{dm}{dt}\right|_{\text{cond},S} &= 4\pi D_{\text{H}_2\text{SO}_4} R_p G_{\text{H}_2\text{SO}_4} \Theta_{\text{aq}} \left(\frac{P_{\text{H}_2\text{SO}_4} - \kappa_{\text{aq}} \cdot a_{\text{H}_2\text{SO}_4} P^{sat}_{\text{H}_2\text{SO}_4}}{RT}\right) M_{\text{H}_2\text{SO}_4} \\
\left.\frac{dm}{dt}\right|_{\text{cond,w}} &= 4\pi D_{\text{w}} R_p G_{\text{w}} \Theta_{\text{aq}} \left(\frac{P_{\text{w}} - \kappa_{\text{aq}} \cdot a_{\text{w}} P^{sat}_{\text{w}}}{RT}\right) M_{\text{w}} \\
\left.\frac{dm}{dt}\right|_{\text{cond},\text{HC}_j} &= 4\pi D_{\text{HC}_j} R_p G_{\text{HC}_j} \Theta_{\text{aq/non-aq}} \left(\frac{P_{\text{HC}_j} - \kappa_{\text{aq/non-aq}} \cdot a_{\text{HC}_j} P^{sat}_{\text{HC}_j}}{RT}\right) M_{\text{HC}_j}
\end{aligned} \tag{3.3}$$

where D is the diffusivity of species in air, R_p is the radius of soot particle including liquid layers, G is the correction factor, P is the partial pressure, P^{sat} is the saturation vapor pressure, κ_{aq} is the Kelvin factor for aqueous solution, $\kappa_{\text{non-aq}}$ is the Kelvin factor for water-insoluble hydrocarbons mixture, and a is the activity.

The correction factor (G_i) for the flux matching of the kinetic regime ($R_p \le r \le R_p + \Delta$) and the continuum regime ($r \ge R_p + \Delta$), where distance from the particle surface (Δ)

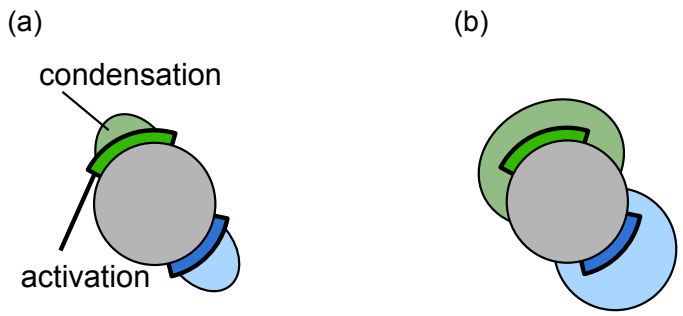

Figure 3-2: Surface coverage by condensation

is an empirical value of the order of mean free path, is given by [4]

$$G_i = \frac{J}{J_c} = \frac{0.75\alpha_{w,i}\left(1 + \mathrm{Kn}_i\Delta/\lambda_i\right)}{0.75\alpha_{w,i} + \mathrm{Kn}_i + \left(\Delta/\lambda_i\right)\mathrm{Kn}_i^2} \tag{3.4}$$

where J is the total flux of species i toward the particle and the J_c is the flux in the continuum regime, $\alpha_{w,i}$ is the mass accommodation coefficient of species on activated soot surface (referred to as wet accommodation coefficient), Kn is the Knudsen number defined as $\mathrm{Kn} = \lambda_i/R_p$, and λ_i is the mean free path. The wet accommodation coefficients were assumed to 1 for all species if they condense on the liquid layers of the same solubility type (see Figure 3-1). For the value of Δ deciding the boundary for regime, a suggestion by Fuchs [50] was used here:

$$\Delta = \lambda_i, \quad \lambda_i = \frac{3D_i}{\bar{c}_i} \tag{3.5}$$

While the rate of change of the surface activation by adsorption in Equation (3.1) is independent of particle size, small particles are easier to be immersed into a liquid drop than large particles in real systems. If the partially activated surface area is compared to the rapidly increasing condensation volume of the liquid films, liquid layers can be piled up higher on a droplet than the underlying activated surface can hold. This will result in increasing the contact angle between liquid films and the soot surface if the activated surface area is kept constant without additional surface activation by adsorption. In this work, it was assumed that the contact angle is constant while the excess volume by condensation can increase the activated soot

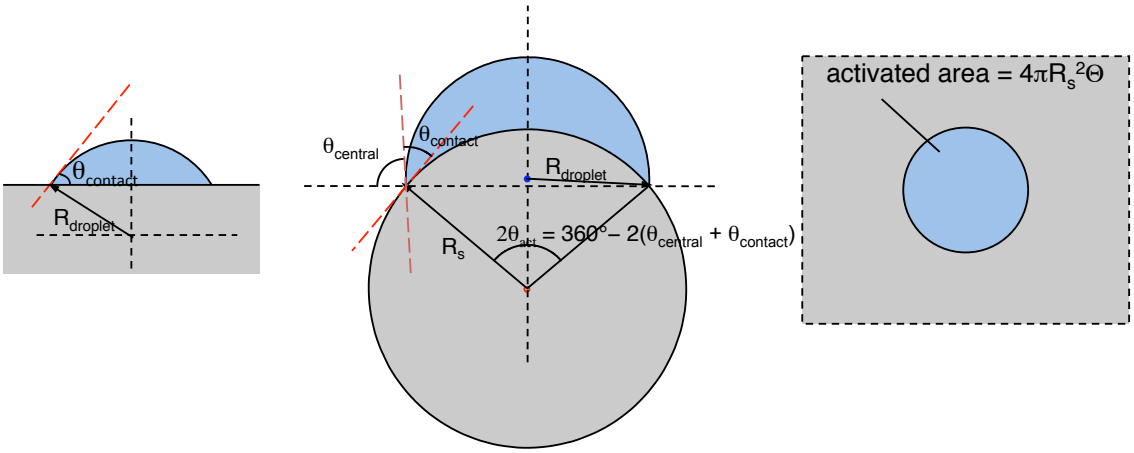

Figure 3-3: Geometry of droplets on the partially wettable surfaces

surface instead. With a constant contact angle the excess volume would be spread over the surface and increase the surface coverage as shown in Figure 3-2. The excess volume by condensation can be calculated from the geometry of a cap shaped drop on the partially wettable surface in Figure 3-3. Therefore, the activated surface area can be modeled as a combination of activation and condensation contribution and written as

$$\begin{aligned} \left.\frac{d\Theta}{dt}\right|_i &= \left.\frac{d\Theta}{dt}\right|_{\text{ads},i} + \left.\frac{d\Theta}{dt}\right|_{\text{scav},i} + \left.\frac{d\Theta}{dt}\right|_{\text{cond},i} \qquad (i = \text{aq, non-aq}) \\ \left.\frac{d\Theta}{dt}\right|_{\text{cond},i} &= f\left(R_s,\ \Theta_i,\ \theta_{\text{contact},i},\ \rho_i\right) \left.\frac{dm}{dt}\right|_{\text{cond},i} \end{aligned} \tag{3.6}$$

where R_s is the radius of dry soot particle, θ_{contact} is the contact angle for liquid solution on the soot surface, and ρ_i is the density of liquid solution. The relationship for excess condensed mass on the surface activated coverage is described in Appendix A. Several measured contact angles of water on the soot surfaces are in the range of 60°-80° including 63° for aircraft combustor soot [51], and the contact angles of H_2SO_4−H_2O droplet was measured to $64° \pm 2°$ on the graphite surface and $55° \pm 2°$ on the OH-treated graphite surface [52]. In this thesis work, $\theta_{\text{contact}} = 60°$ was used for the contact angle of aqueous solutions on the soot surface. Based on the assumption that the hydrophobic soot surface is more wettable with water-insoluble hydrocarbon compounds, $\theta_{\text{contact}} = 30°$ was used for the contact angle of water-

insoluble hydrocarbon mixtures. The sensitivity of the model prediction to the contact angle assumption is provided in Section 3.2.4.

Figure 3-4 shows the contribution of condensation on the surface coverage with several geometric assumptions. N is the number of sites on the surface wetted by liquid drops. For example, the assumption of a curved surface with N=2 means that two cap shaped liquid droplets grow on the site of the surface located on opposite hemispheres of the soot particle. Note that the soot concentrations were adjusted to have the same total surface area for different size particles, and 60° of the contact angle was assumed between a sulfuric acid solution and a soot surface. While the condensational contribution to the surface activation is insignificant for large soot particles, it enhances surface saturation for small particles. Considering surface geometry is also important for nanometer-size particles because the flat surface assumption is likely to estimate the surface activation rate too fast for particles having large surface curvature, as seen in Figure 3-4. If the size distribution of soot particles includes particles in a few nanometers, the growth of fully immersed small particles can be modeled better by considering the effect of condensation on the soot surface coverage.

3.2 Results and Discussion

In this section, the effect of organic species condensation on the PM formation was studied with 1-D kinetic calculations for the near-field aircraft plume up to 1 km downstream. Note that this section focused on the growth of soot particles through activation and condensation of gaseous species in the plume and did not consider the nucleation process. This would result in overestimation of the soot particle growth by excluding mass transfer to nucleated liquid aerosol particles. Results are compared to calculation with binary $H_2SO_4-H_2O$ model in Section 3.2.3, and sensitivities to modeling parameters and initial conditions for organic species as well as ambient conditions are discussed in Section 3.2.4.

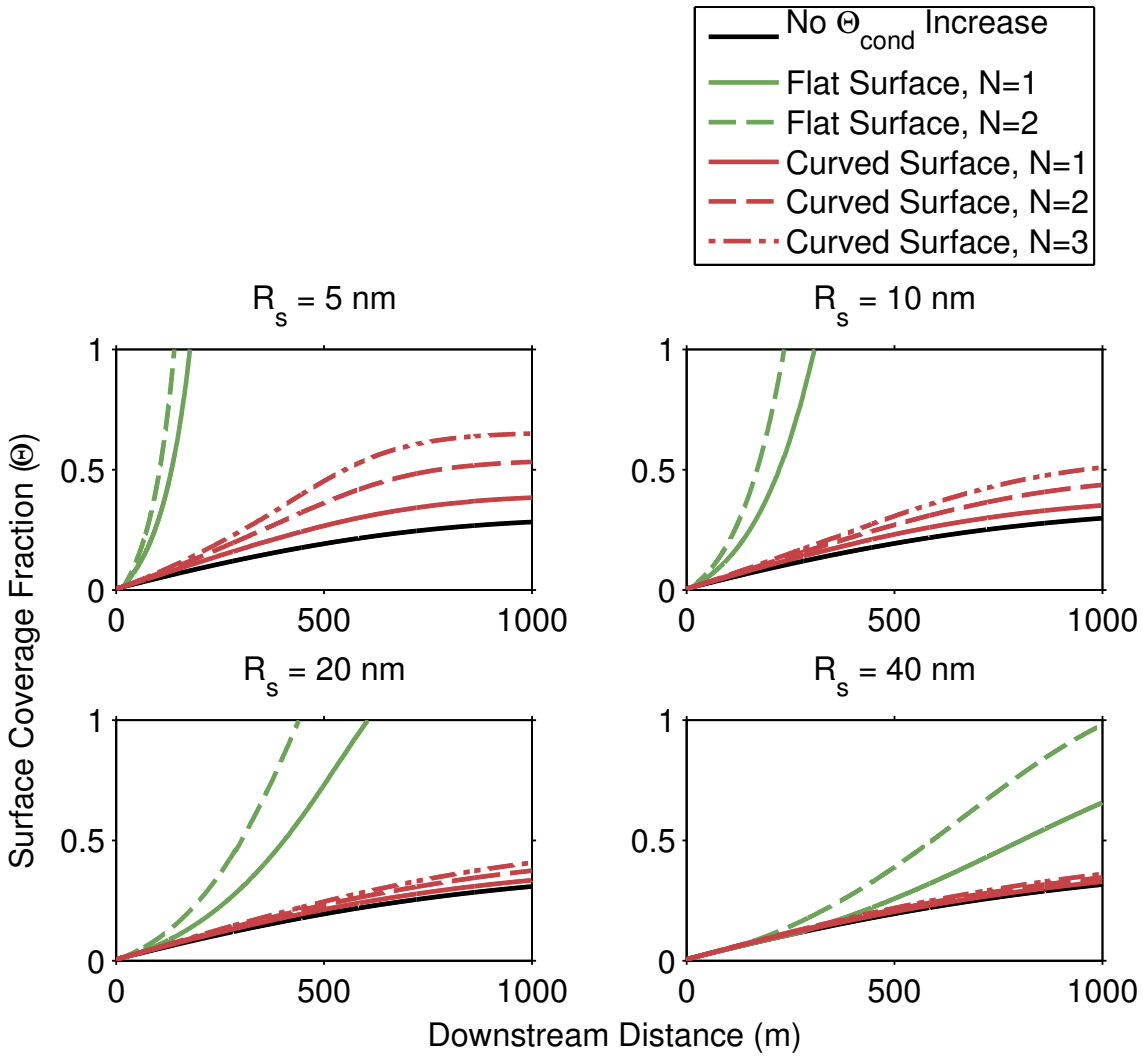

Figure 3-4: Comparison of assumptions for surface coverage

3.2.1 Modeling of Aircraft Plume Properties

Estimation of exhaust properties in aircraft plumes followed the approach in Wong *et al.* [27], where those predictions matched well the measurement data for near-field aircraft plumes. For the simulation results in this section, initial exhaust properties at engine exit were set to 97490 Pa, 677 K, and 66.68 m/s for the core flow that correspond to 7% of maximum rated thrust of the CFM56-2C1 engine used in the Aircraft Particle Emissions eXperiment (APEX); and the ambient conditions were set to 286 K, RH 80%. Figure 3-5 shows plume dilution profiles of temperature and RH as a time-varying function of downstream distance.

Three condensable PAHs, pyrene ($C_{16}H_{10}$), benzo[a]pyrene ($C_{20}H_{12}$), and coronene ($C_{24}H_{12}$), and three oxygenated hydrocarbons, acetone (C_3H_6O), propanoic acid ($C_3H_6O_2$), and butanoic acid ($C_4H_8O_2$), were tested as the potential condensing organic species in aircraft emissions. The selected water-soluble organic compounds are light oxygenates having one or two oxygen atoms to focus on the primary organic aerosol. While secondary organic aerosol is known as a major source of organic PM, its formation occurs via oxidation of emitted hydrocarbons, and such oxidation is expected to be negligible within 15 minutes after emission and/or to 1 km downstream.

Exhaust gas concentrations of organic compounds were set to

$$\begin{aligned} \sum X_{\text{w-soluble}} &= 100\text{ppb}; \quad X_{\text{w-soluble},i} M_{\text{w-soluble},i} = X_{\text{w-soluble},j} M_{\text{w-soluble},j} \\ \sum X_{\text{w-insoluble}} &= 100\text{ppb}; \quad X_{\text{w-insoluble},i} M_{\text{w-insoluble},i} = X_{\text{w-insoluble},j} M_{\text{w-insoluble},j} \end{aligned} \tag{3.7}$$

These numbers are comparable to the field measurements to a reasonable extent. The identified concentration of organic species for the CFM56-2C1 engine operating at 7% engine power during the APEX-1 measurement campaign were calculated as 20 ppb for naphthalene and 38 ppb for acetone with 22000 ppm of CO_2 emission [28]. With this exhaust composition, the initial concentration of each of the selected organic species is of the same order of magnitude as the maximum concentration of $H_2SO_{4/}SO_3$. However, the assumption used here of the same mass fraction for all organic species is likely to overestimate the concentration of heavier compounds and thus provides an upper estimate for condensed mass in that regard.

Soot particles were initially modeled as log-normally distributed between 6 nm to 250 nm in diameters with distribution parameters, 16 nm geometric mean diameter, 1.3 standard deviation, and $8.510^6\,\text{cm}^{-}3$ concentration (see the initial particle distribution in Figure 3-6). The parameters were fitted to the data obtained in APEX-1 for 7% power setting of CFM56-2C1 engines [27]. The size distribution of soot particles was approximated with 10 moving bins, where the initially allocated particle size increases geometrically as the particles grow. In the fully moving bin structure, bins move with initially allocated particles to track the exact size of particles and to

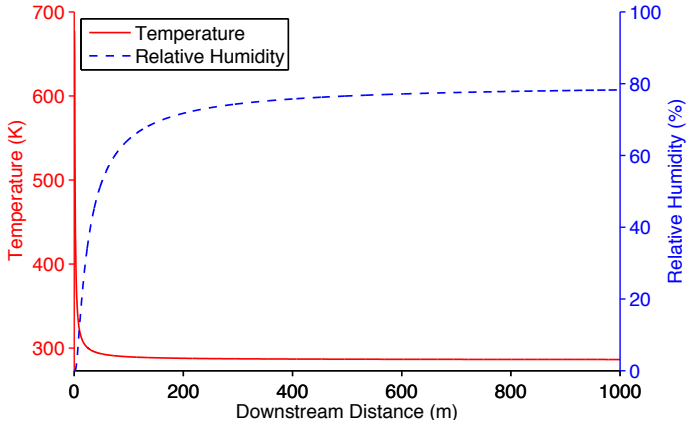

Figure 3-5: Temperature and RH profile for 7 % power setting

allow evaporation to the initial soot core volume [53], and thus the concentration of particles in each bin is maintained unless nucleation generates new particles.

3.2.2 Simulation Results

Figure 3-6 and Figure 3-7 show the evolution of the particle size and the surface activation of soot particles. Log-normally distributed soot particles with initial 16 nm mean diameter grew to 40 nm mean diameter at 1 km downstream after 14 minutes exposure to ambient air. The particle distribution became positively skewed as smaller soot particles grew relatively faster. This indicates that smaller particles underwent significant condensation because adsorption is not dependent on particle size. Additionally, smaller particles reached surface saturation faster due to enhanced surface activation by condensation. Consequently, larger particles having smaller soot core arise for particles that experience surface saturation, depending on the exhaust properties and ambient conditions. For example, particles in the first bin overtook particles in the second bin as shown in Figure 3-6. This is a possible situation when the contribution of enhanced surface coverage becomes more important than the contribution of initial particle size to condensation.

The mass composition of the surface activation layer and the total soot coatings at 1 km downstream are shown in Figure 3-8 and Figure 3-9 respectively. The particle size is a critical factor to determine the composition of the first activation layer of sur-

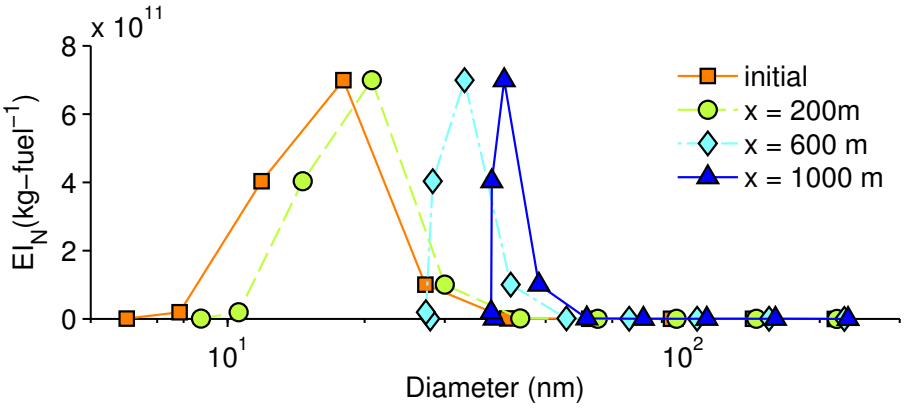

Figure 3-6: Size distribution of soot particles

face. While the activation rate by adsorption is identical for all size particles, the activation rate by condensation is faster for smaller particles, which are easily immersed in the resulting condensed liquid droplet. Simulation results in Figure 3-8 show that soot particles with an initial diameter less than 15 nm (bin1-bin3) reached surface saturation, where condensational growth contributed to more than half of the surface coverage. Condensation of water-insoluble hydrocarbons contributed to increasing hydrophobic surface fractions on these small soot particles compared to large soot particles having negligible condensational contribution. Thus water-insoluble hydrocarbons compete with water-soluble species for surface area and limit the hydrophilic surface activation. Further, because of the enhanced surface activation by condensation, water-soluble species then experienced limited surface area for adsorption. Therefore, smaller particles are relatively easier to be covered with water-insoluble hydrocarbons. The more hydrophobic portion of the soot surface layer resulted in the greater hydrophobic coatings of soot particles that, in turn, preventing the uptake of water as well as promoting the uptake of hydrophobic organic species as shown in Figure 3-9. Note that acidity in Figure 3-9 indicates the acid fraction in the aqueous solution. Small particles tend to be more hydrophobic as well as more acidic.

The simulated mass composition of soot coatings is investigated as a function of downstream distance in Figure 3-10. While water-soluble organics appeared on soot coatings substantially in the young plume where adsorption is the dominating mass transfer process, their fractions became negligible further downstream as particles

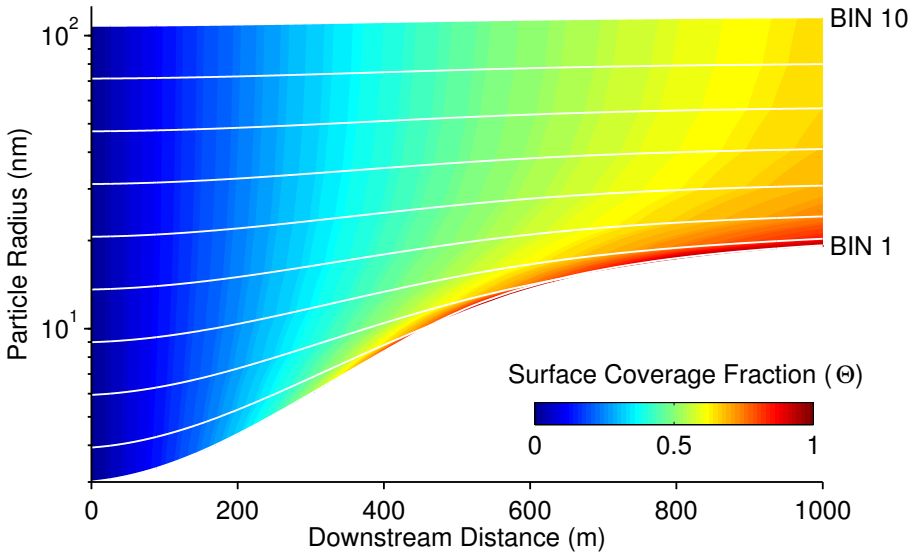

Figure 3-7: Evolution of radius and surface coverage of soot particles

grew by condensation. Since light water-soluble organic species are hard to condense on soot particles due to their high vapor pressure, they do not contribute to the particle growth directly; however, they are involved in the soot particle growth by activating soot surface to be hydrophilic immediately after the engine exit plane. On the other hand, heavy water-insoluble hydrocarbons continued to condense on soot particles as well as activate the surface to be hydrophobic.

Figure 3-11 presents the mass budget evolution between phases, vapor phase and the liquid phase on soot coatings. A substantial mass transfer occurred from vapor phase to soot coatings for low volatile condensable gases. Under the simulation conditions, sulfuric acid gas was almost depleted and two heavy water-insoluble hydrocarbon gases continued to transfer to soot coatings at 1 km downstream. Volatile species such as water-soluble hydrocarbon oxygenates tended to remain in the gas phase. Mass fractions of condensation and activation soot coatings are shown in Figure 3-12. Note that mass transfer between phases accompanied the condensation process. Interestingly, only hydrocarbon species having a lower saturation vapor pressure than sulfuric acid (see Figure 2-2) are able to lead to significant condensation on soot particles.

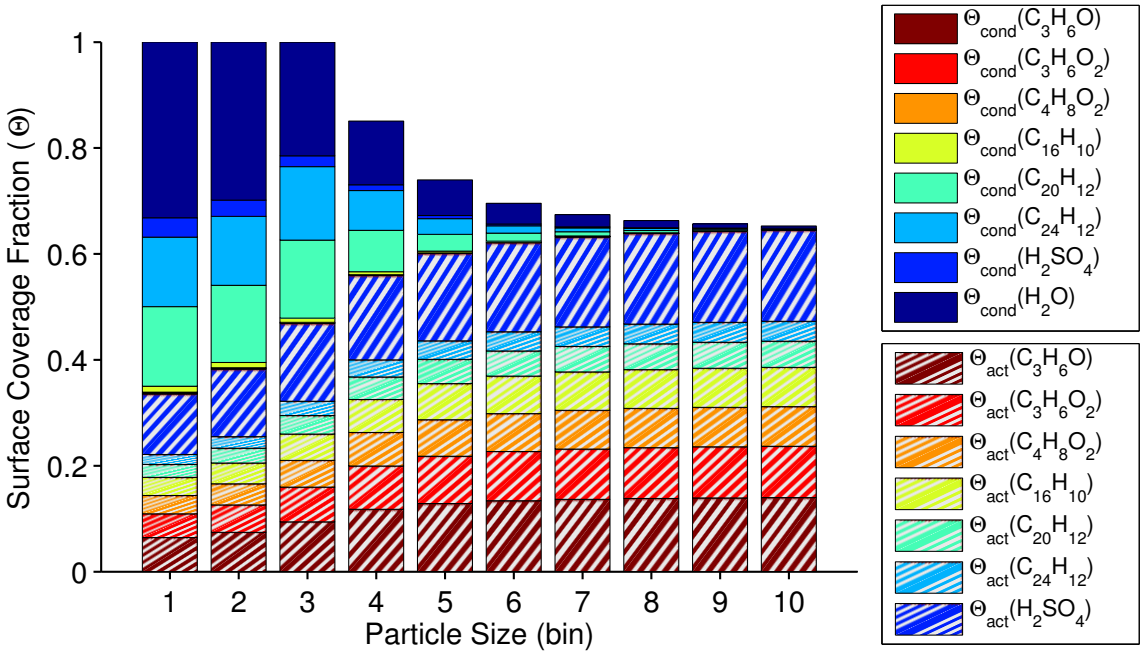

Figure 3-8: Composition of the surface activation layer at 1 km downstream

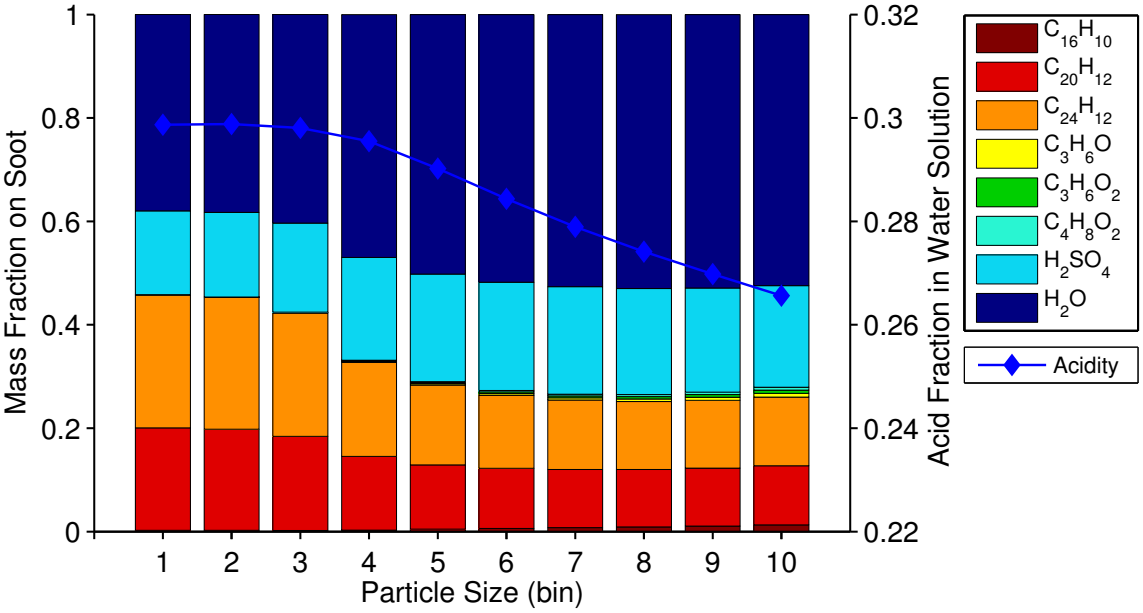

Figure 3-9: Composition of the liquid soot coatings at 1 km downstream

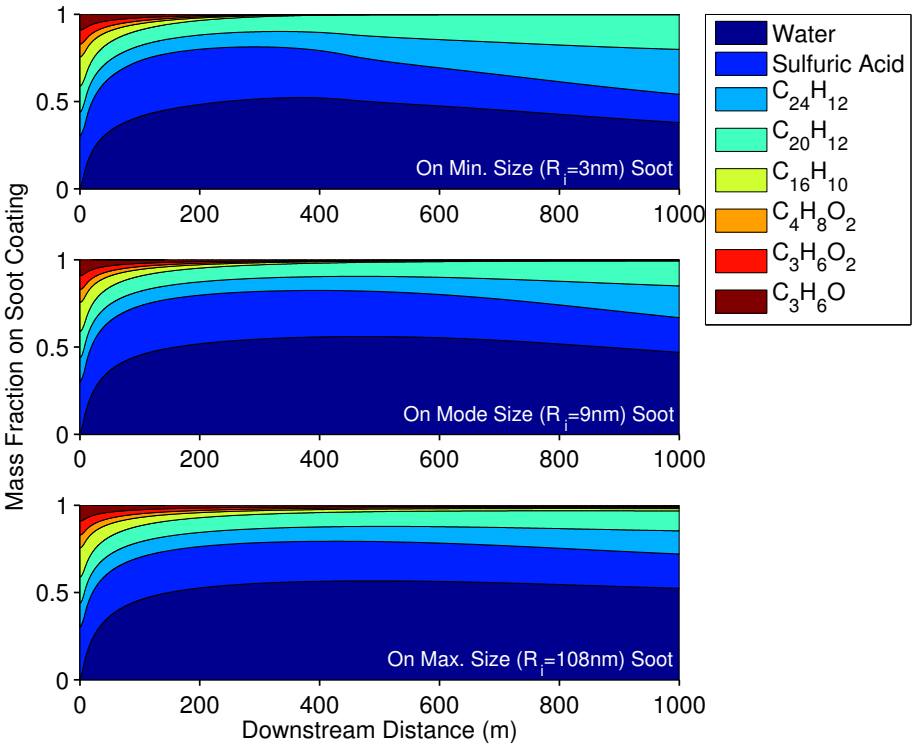

Figure 3-10: Mass fraction of absorbed species in liquid layers on the soot surface

3.2.3 Comparison with Binary H2SO4-H2O Model

This section discusses the role of hydrocarbons in soot microphysics by comparing simulation results from the multi-component model developed through this thesis work to those from the binary $H_2SO_4-H_2O$ model. The contributions of hydrocarbon compounds in aircraft emissions to the size and mass of soot particles is illustrated in Figure 3-13 in terms of percent difference between with and without hydrocarbons for different size of soot particles. Overall, soot particles obtain more mass from the gas phase in the presence of hydrocarbons, with the consequent increased particle size. Interaction with hydrocarbon species also enhances surface activation of soot particles that enable the uptake of gaseous species via condensation. It is important to note that excluding hydrocarbon interactions with soot particles is likely to underestimate soot particle growth therefore. Oxygenated hydrocarbons can enhance the uptake of water and sulfuric acid by increasing hydrophilic surface activation and by decreasing water activity. Water-insoluble hydrocarbons increase hydrophobic surface activation

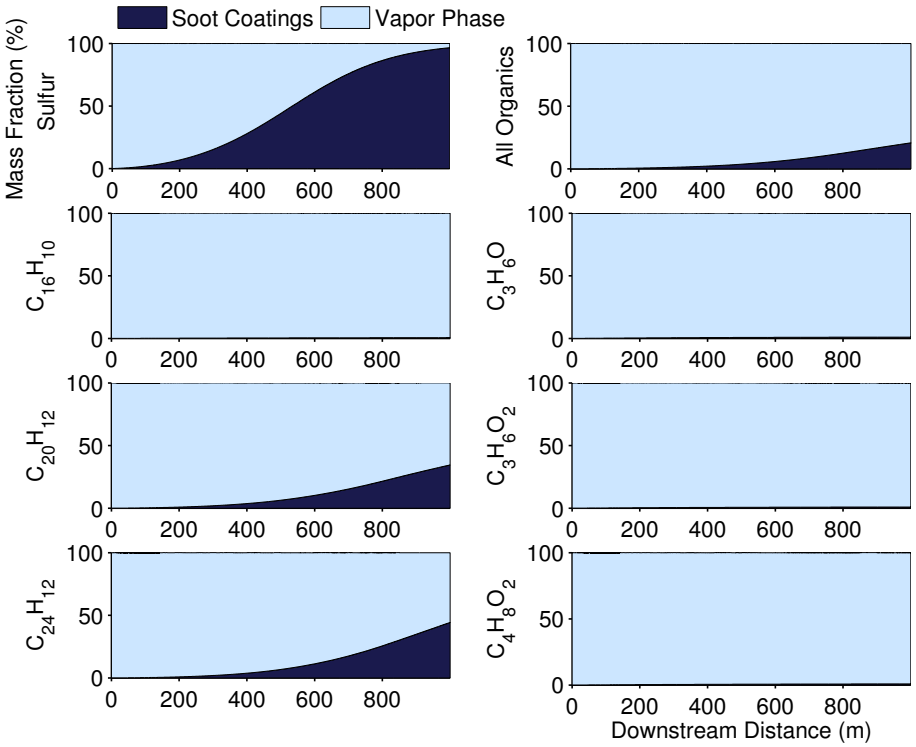

Figure 3-11: Evolution of mass fractions for individual species

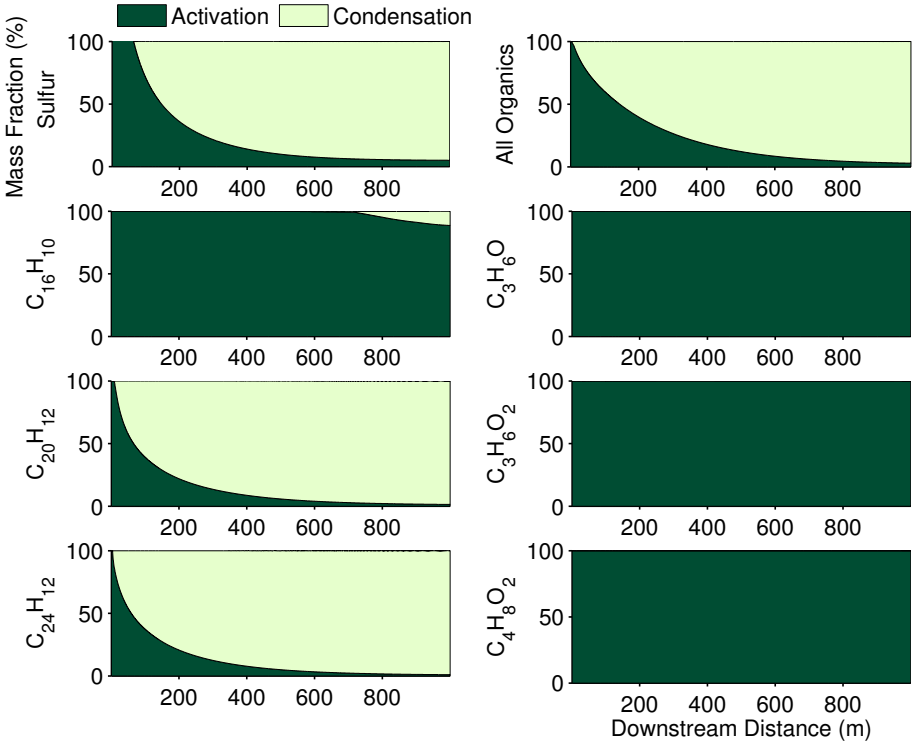

Figure 3-12: Evolution of activation/condensation fractions in liquid layers on soot particles for individual species

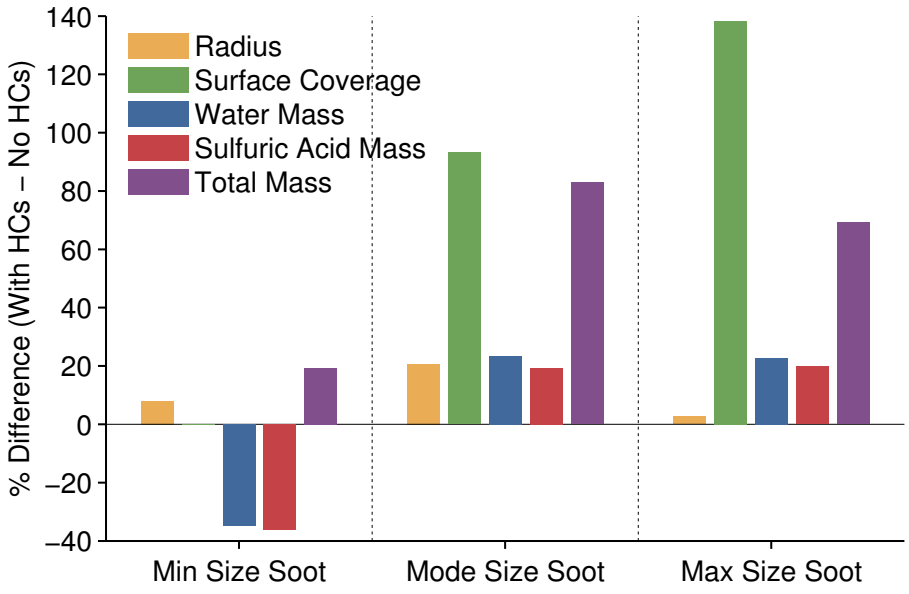

Figure 3-13: Effect of organic compounds on the particle growth

and contribute to increasing mass of soot coating by condensation.

Details of individual species show that there arises competition between water-soluble and water-insoluble species if surface saturation occurs. Competition between water-soluble and water-insoluble species does not appear clearly for large soot particles whose surface for adsorption was not limited through the end of the simulation. For very fine particles, however, the hydrophobic contribution of water-insoluble hydrocarbons prevented the uptake of water and sulfuric acid compared with the binary model. Note that the particle growth in the minimum size soot particles is smaller than that of the mode size particles not undergoing significant competition preventing uptake of water.

3.2.4 Parametric Studies for Modeling Parameters and Ambient Conditions

A set of simulations was performed to study the effect of modeling parameters and ambient conditions. The baseline values of key parameters are summarized in Table 3.1, where varied parametric values explored in these studies are given in brackets. Each parameter was varied one at a time, while keeping other parameters at the baseline

values. The parameters are selected to investigate key properties in four categories: 1) Initial exhaust properties (concentration of organic compounds and soot particles), 2) Properties of organic compounds (mass accommodation coefficients), 3) Properties of the soot surface (contact angle for liquids on the soot surface and initial activation fraction), 4) Ambient conditions for engine operations (temperature and relative humidity).

Figure 3-14, Figure 3-15, and Figure 3-16 show sensitivities of the soot particle growth to the studied parameters for different size of soot particles in minimum, mode, and maximum size bins. In the scatters plots, the results presented are: 1) the baseline, 2) with increasing parameters, and 3) with decreasing parameters and were marked as 1) dashed lines, 2) circles, and 3) diamonds, respectively. A greater size of the symbol indicates a greater change (increasing or decreasing) in the level of that parameter. For bar plots, the mass and final radius of soot coatings were shown in order of decreasing particle growth. For all cases, increasing the initial concentration of water-insoluble hydrocarbons showed strongest effect on the soot particle growth. Decreasing the soot loading also resulted in increased particle growth and had a similar effect as increasing the gaseous concentration of species. Other parameters that led to increased particle growth in common for all sizes of soot particles included both increasing initial hydrophobic surface coverage and increasing contact angle of water-soluble species. On the other hand, common parameters that

Water-soluble organics		Water-insoluble organics	
$\Sigma X_{\text{w-s}} = 10^{-7}$	$[10^{-6}, 10^{-8}]$	$\Sigma X_{\text{w-is}} = 10^{-7}$	$[10^{-6}, 10^{-8}]$
$\alpha_{\text{dry,w-s}} = 0.01$	[0.001, 0.1]	$\alpha_{\text{dry,w-is}} = 0.01$	[0.001, 0.1]
$\alpha_{\text{wet,w-s}} = 1$	[0.5]	$\alpha_{\text{wet,w-is}} = 1$	[0.5]
$\theta_{\text{contact,w-s}} = 60°$	[40°,80°]	$\theta_{\text{contact,w-is}} = 30°$	[10°,50°]
$\Theta_{\text{initial,w-s}} = 0$	[0.2]	$\Theta_{\text{initial,w-is}} = 0$	[0.2]
Ambient conditions		Soot particles	
$T = 286$ K	[293 K, 300 K]	Conc. =	[4.25, 12.75] $\times 10^6$ (1/cc)
RH= 80%	[20% , 40%, 60%]	8.5×10^6 (1/cc)	

Table 3.1: The baseline settings and selected levels (given in brackets) of parameters and ambient conditions for the parametric studies

resulted in decreased soot particle growth included decreased initial concentration, decreased dry accommodation coefficient of water-insoluble hydrocarbons, increased soot loadings, decreased wet accommodation coefficients, and increased contact angle of water-soluble species.

Since the particle size is also an important factor deciding the uptake of hydrophilic and hydrophobic species, some parameters did not result in consistent effects for all soot particles. Regardless of the particle size, however, soot particle growth is most sensitive to parameters directly affecting uptake of water-insoluble hydrocarbons on soot coatings and then indirect parameters related to hydrophilic surface coverage inducing competition with uptake of water-insoluble hydrocarbons as well. At the baseline condition described in Section 3.2.2, only water-insoluble hydrocarbons are condensable and more than half of their mass still remains in the gas phase at 1 km downstream. These key parameters, such as initial concentration and dry accommodation coefficient of hydrocarbons, determine how fast and how much of the hydrocarbons are taken up by soot particles.

3.2.4.1 Initial Exhaust Properties

The most important contributor to the soot particle growth is the initial concentration of water-insoluble hydrocarbons. Figure 3-17 compares the mass evolution of species at different levels of initial concentrations of water-insoluble hydrocarbons. Increasing the initial concentration of water-insoluble hydrocarbons to 1000 ppb, which is more than an order of magnitude higher than the initial mole fraction of precursors of H_2SO_4 in the exhaust, resulted in forming very hydrophobic soot particles downstream, with the mass of water-insoluble hydrocarbons surpassing that of the hydrophilic species. Low volatile hydrocarbons, $C_{20}H_{12}$ and $C_{24}H_{12}$, reached equilibriums with their condensed mass on the soot coatings. On the other hand, with 10 ppb initial concentration of water-insoluble hydrocarbons, the condensation of hydrocarbons was almost completely suppressed, while the condensed sulfate mass was not affected.

The initial concentration of hydrocarbons also affects the sensitivity of the hy-

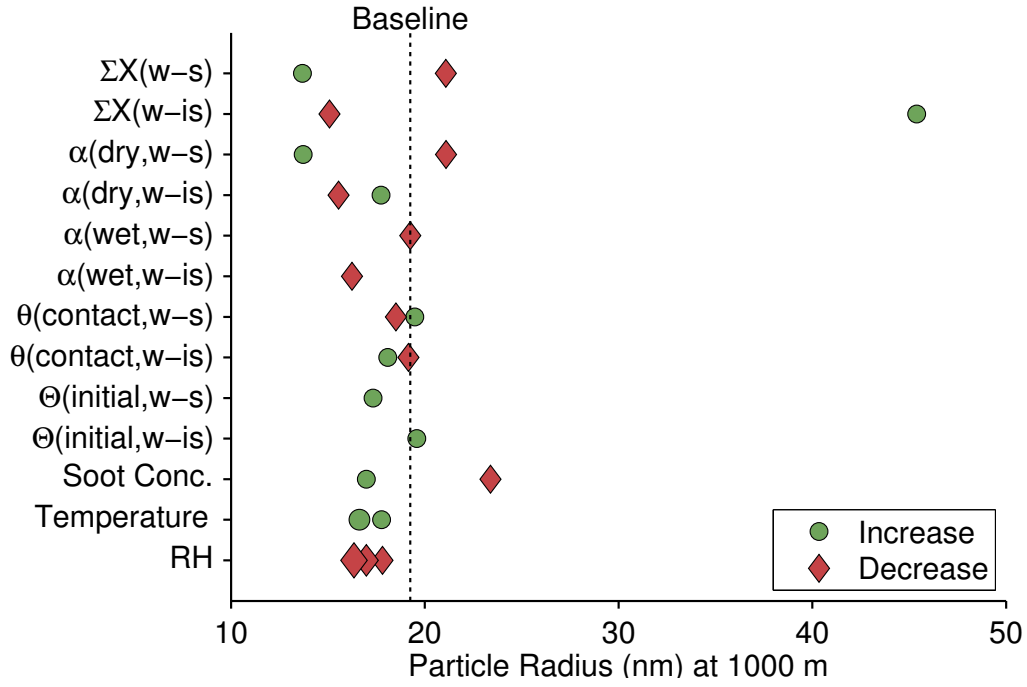

(a)

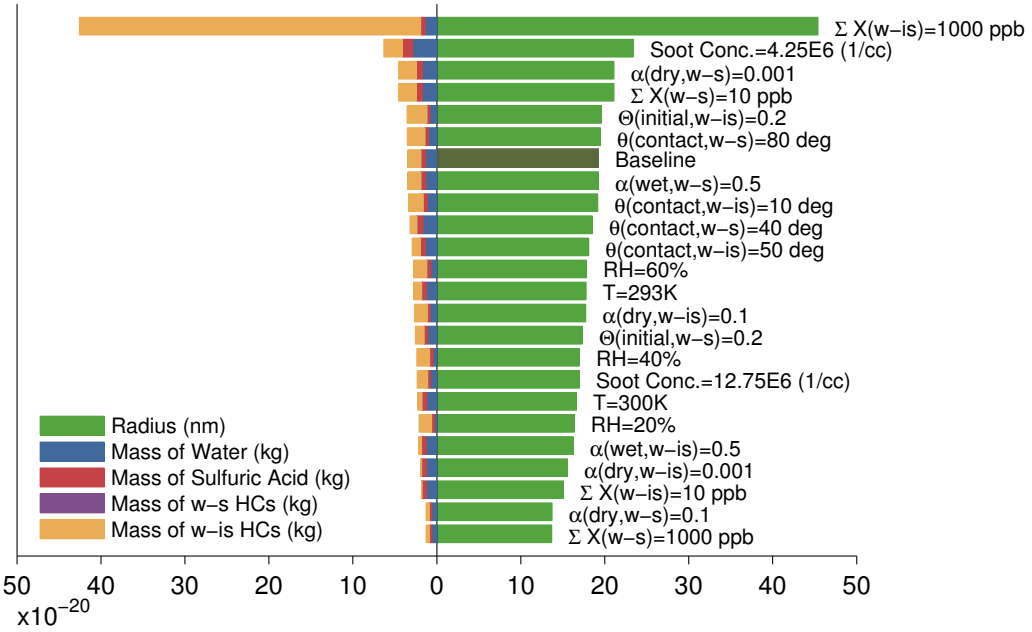

(b)

Figure 3-14: Summary of parametric studies for minimum size particles

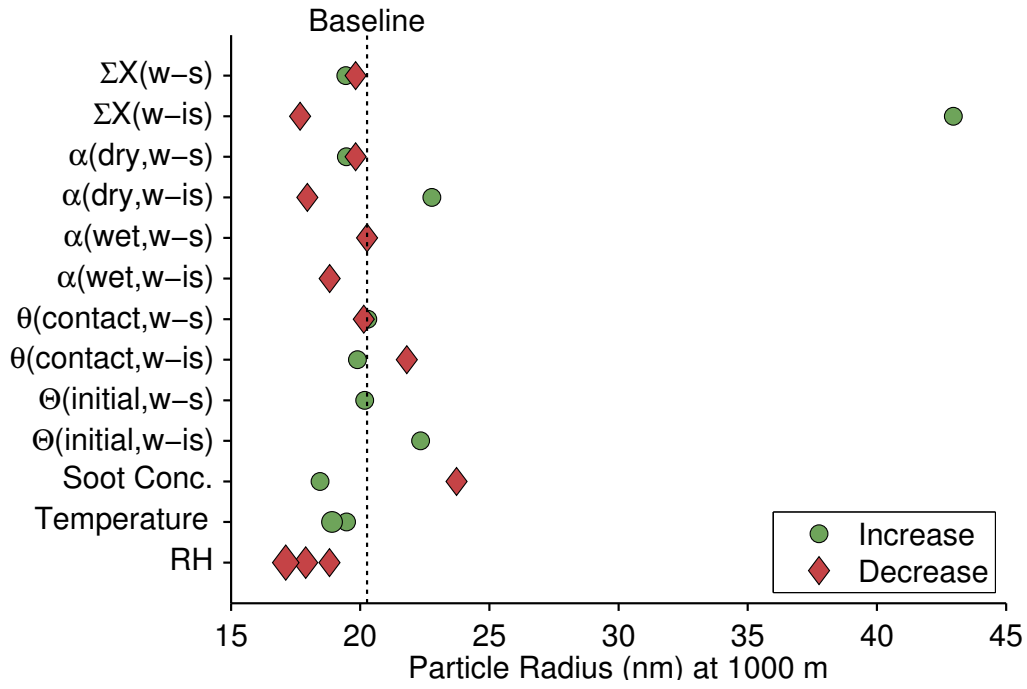

(a)

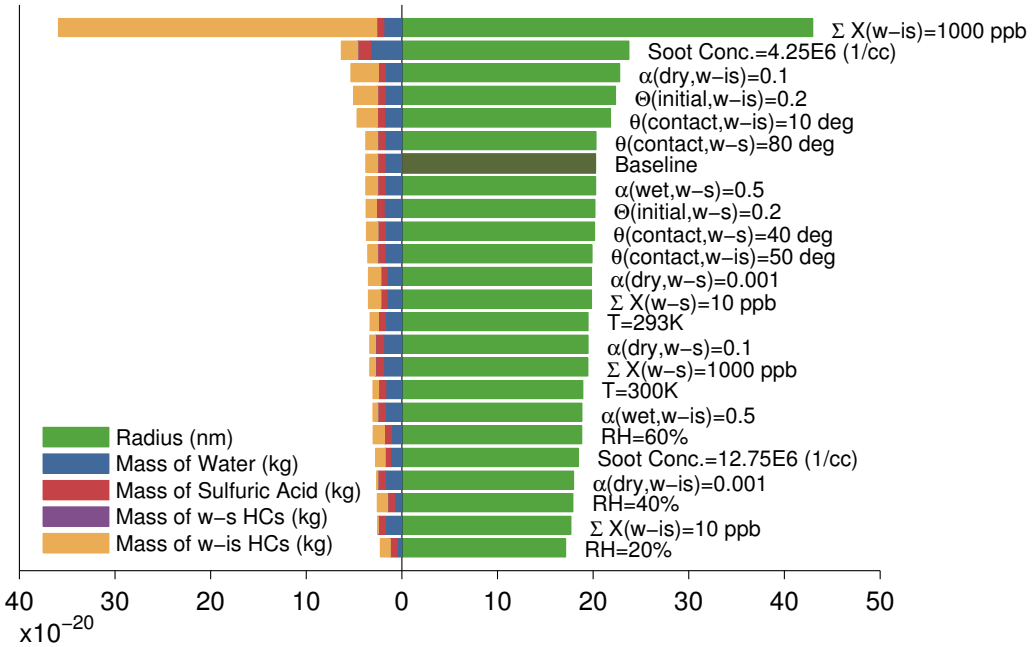

(b)

Figure 3-15: Summary of parametric studies for mode size particles

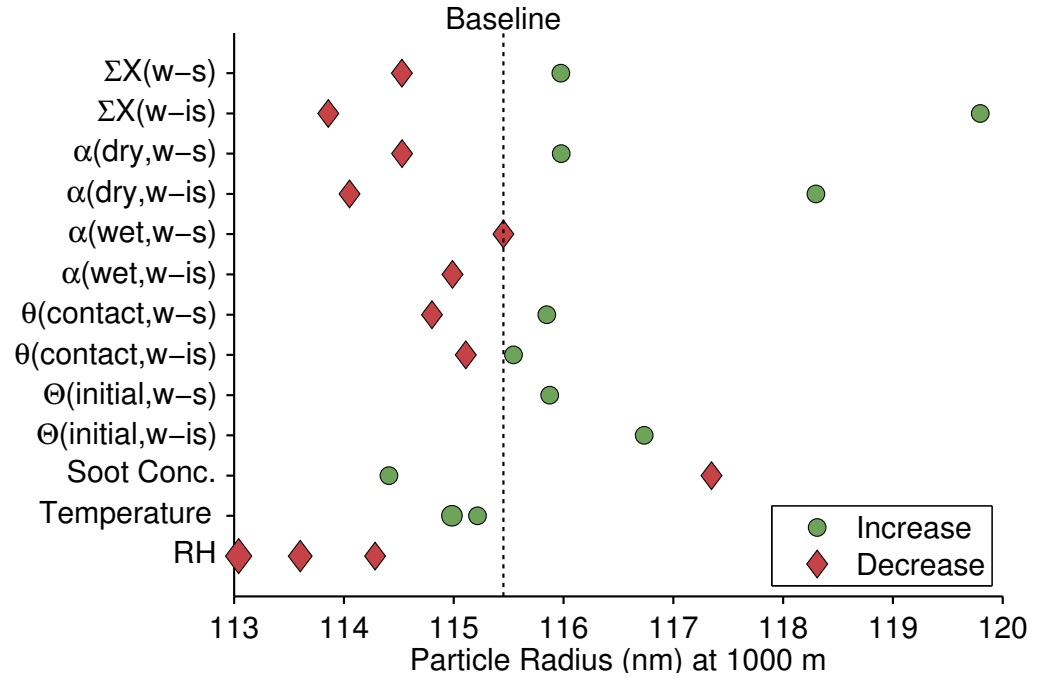

(a)

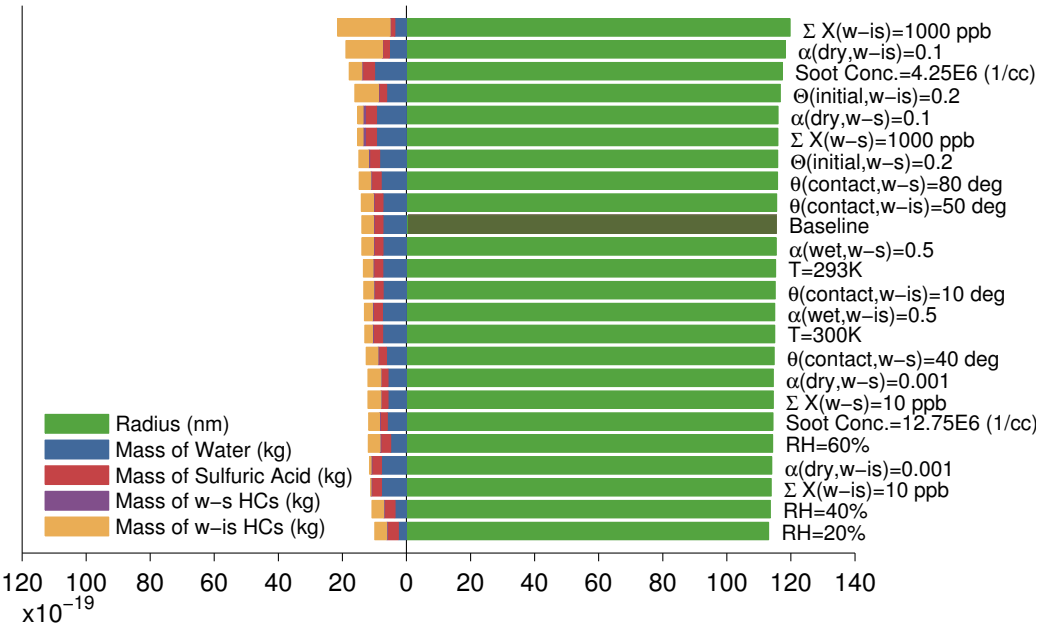

(b)

Figure 3-16: Summary of parametric studies for maximum size particles

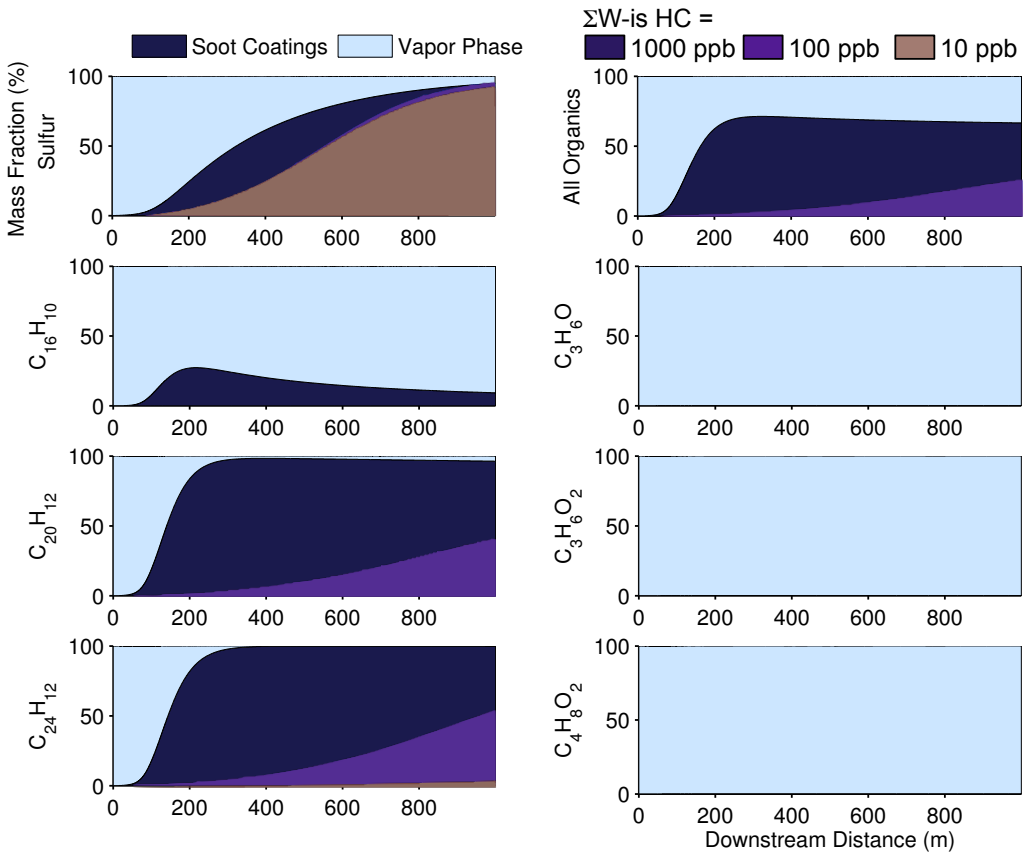

Figure 3-17: Comparison of mass fraction evolution for different levels of initial concentration of water-insoluble hydrocarbons

drocarbon properties to the soot particle growth. For example, varying the dry accommodation coefficient of water-insoluble hydrocarbons from 0.001 to 0.1 did not contribute to the particle growth significantly with 10 ppb initial concentration. With a dry accommodation coefficient of 0.001, the particle growth is negligible at both 10 ppb and 100 ppb initial concentrations, while the growth is significant with 1000 ppb (Figure 3-18). This suggests that interactions of hydrocarbon species with soot particles become more important in the organic-rich condition, and there are exhaust conditions where condensation of hydrocarbons is not important as compared to the condensation of sulfuric acid and water. While the particle growth is sensitive to both the concentration and accommodation coefficients of hydrocarbons in the baseline condition assumed in this thesis work, the sensitivity of the hydrocarbon properties is not apparent in the organic-poor condition.

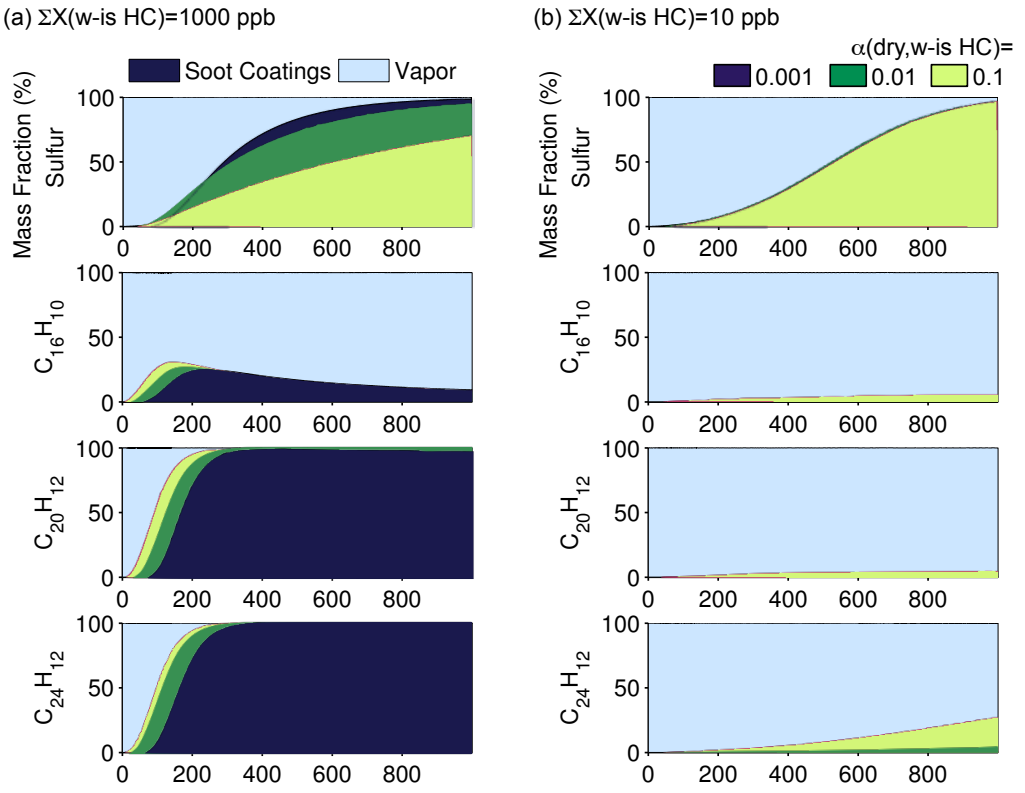

Figure 3-18: Comparison of mass fraction evolution for different levels of dry accommodation coefficients of water-insoluble hydrocarbon: (a) at 1000 ppb, and (b) at 10 ppb of initial concentration of water-insoluble hydrocarbons

On the other hand, the effect of soot loadings is straightforward. Uptake of gaseous species is distributed into increasing soot particles, and the soot coating per one particle decreases consequently.

3.2.4.2 Properties of Hydrocarbons

The dry accommodation coefficient is another important contributor to the hydrocarbon interactions with soot particles. In addition to its substantial impact on the soot particle growth, the dry accommodation coefficient is one of most uncertain modeling parameters. For condensable water-insoluble hydrocarbons, this parameter is closely related with the uptake of species by affecting the available surface. The dry accommodation coefficient of water-soluble hydrocarbons on the other hand, induces competition for surface area with water-insoluble hydrocarbons. For example,

while the decreasing dry accommodation coefficient of water-soluble hydrocarbon decreased the particle growth for large particles, it resulted in increasing particle growth for small soot particles in the minimum size bins by increasing hydrophobic surfaces.

Figure 3-18 presents the effect of dry accommodation coefficients at organic-rich and organic-poor conditions. In the organic-poor condition where the uptake of sulfuric acid is a major contributor to the particle growth, aerosol evolution is less sensitive to dry accommodation of condensable hydrocarbons. In the organic-rich condition, however, it affects the composition of aerosols by preventing the uptake of sulfuric acid.

3.2.4.3 Properties of Soot Surfaces

The properties of the soot surface investigated in this chapter include contact angle and initial activation fraction. The contact angle is one of factors determining the surface activation rate by condensation. A liquid droplet on a wettable surface, that is, having a small contact angle, can be spread over the surface easily. Therefore, the activation rate by condensation increases with decreasing the contact angle. The initial activation fraction represents initial hydrophilic and hydrophobic fractions of soot particles at the engine exit. Aircraft soot particles have been observed having hydrophilic fractions or organic fractions forming under high temperature and pressure conditions [54].

Overall, particle growth is less sensitive to the soot surface properties compared to the hydrocarbon properties. Initial surface activation fraction showed opposite effects according to the particle size since this property is related to surface competition between hydrophilic and hydrophobic fractions.

3.2.4.4 Ambient Conditions

While water condensation strongly depends on the RH condition, microphysical processes on soot particles associated with hydrocarbons are less sensitive to the ambient conditions. Parametric studies with the binary $H_2SO_4-H_2O$ model also indicated that condensation of sulfate on soot was less sensitive to ambient conditions [27]. While

the particle growth is significantly limited by restricted water uptake at low RH, the effect of ambient temperature is relatively small compared to sensitivity from exhaust properties or hydrocarbon properties, although ambient temperature is a more important factor affecting condensation of hydrocarbons than RH. The effect of ambient conditions will be discussed further in Chapter 4 including all microphysical processes where water vapor plays an important role.

3.3 Summary

This chapter presents the modeling approaches to incorporate hydrocarbon species into soot microphysics and discusses the formation of organic coatings on aircraft-emitted soot particles in interactions with sulfuric acid and water. Predictions with the developed model are consistent with other studies (*e.g.* [48], [20]) in that water-soluble organics enhance the water uptake whereas water-insoluble organics prevent it, by forming the hydrophilic and hydrophobic liquid layers on soot surfaces, respectively. This chapter demonstrates that low volatility hydrocarbons, which are water-insoluble in general, can contribute to the particle growth by condensation on soot coatings while preventing the uptake of water-soluble species by inducing competition. Water-soluble hydrocarbons can increase hydrophilic surface coverage and consequently increase the uptake of water and sulfuric acid although they are not condensable on soot coatings directly. Under the assumed conditions of aircraft emissions, where condensation of water-insoluble hydrocarbons is comparable with that of sulfuric acid and water, competition appears between hydrophilic and hydrophobic activation of soot surfaces. This competition is more important for small particles that are easily immersed in liquid coatings.

The sensitivity of the particle growth is explored for modeling parameters and ambient conditions, including initial exhaust properties, properties of hydrocarbons, properties of soot surfaces, and ambient conditions. The growth of soot particles is most sensitive to the properties associated with condensation of water-insoluble hydrocarbons regardless of the particle size. On the other hand, particle size and

therefore surface area available for absorption of gaseous species are critical factors to determine the competition effect. The particle growth is limited by decreasing RH while enhance by increasing the initial concentration of condensable hydrocarbons significantly.

Chapter 4

Modeling of the New Particle Formation with Nucleation and Coagulation

In the previous chapter, aerosol growth by activation and condensation was discussed, focused on the interaction with solid particles directly emitted from aircraft engine. There are also microphysical processes which form and grow new liquid particles from gas, such as nucleation and coagulation as seen in Equation (1.4).

Nucleation processes are classified with following four types in general [4]:

- Homogeneous-homomolecular: nucleation of one species without foreign nuclei.
- Homogeneous-heteromolecular: nucleation of more than one species without foreign nuclei.
- Heterogeneous-homomolecular: nucleation of one species on foreign surfaces.
- Heterogeneous-heteromolecular: nucleation of more than one species on foreign surfaces.

While this identification of nucleation types includes heterogeneous nucleation processes, a nucleation process focused on this thesis is the homogeneous nucleation.

Water is very unlikely to form nuclei by itself at normal ambient conditions or even at supersaturated condition experienced in an exhaust plume. However, the presence of sulfuric acid can induce aqueous binary nucleation at even a subsaturated condition. Binary nucleation can occur if species are supersaturated with respect to their solution in a liquid droplet, even when both components are subsaturated with respect to their pure gas phase. If the nucleated clusters exceed their critical cluster size, the clusters are likely to grow to larger droplets due to the resulting larger growth rate. At the critical cluster size, the net nucleation rate becomes zero as evaporation rate and growth rate are equal. If clusters are smaller than the critical cluster on the other hand, the clusters are prone to evaporate and decay.

Binary $H_2SO_4-H_2O$ nucleation is an important source forming liquid aerosols in aircraft plumes. A binary $H_2SO_4-H_2O$ nucleation model has been widely studied and enhanced for better predictions and modified to capture additional features in atmospheric nucleation: for example, ternary $H_2SO_4-H_2O-NH_3$ nucleation or ion-induced nucleation [55, 4, 56]. A potential role of organic compounds in nucleation has been studied also [9, 57]. However, incorporating more than one hydrocarbon species into a nucleation model is not a straightforward work since handling more than two components with the classical nucleation theory would be very time-consuming and impose a heavy computational burden. For example, finding the minimum free energy configurations and tracking all possible combinations of cluster configurations will be very challenging as the number of species considered in the nucleation process at the same time is increased. Therefore, it will be more practical to apply a simplified model with adequate assumptions applicable to the system being considered as in an aircraft plume conditions in fast equilibrium with water vapor. The following sections discusse several nucleation models that can be easily extended to a multi-component model.

4.1 Review of Nucleation Model

4.1.1 Quasi-unary nucleation model

The binary homogeneous nucleation of H_2SO_4−H_2O can be simplified as a kinetic model simulating quasi-unary nucleation (QUN) of H_2SO_4 in equilibrium with water vapor in atmospheric conditions due to the presence of much higher concentration of water vapor [58, 59]. In these conditions, binary H_2SO_4−H_2O clusters are controlled by collision or evaporation of H_2SO_4 molecules and the amount of water vapor in the cluster reaches equilibrium very quickly due to excess water vapor available. The QUN model can be simulated kinetically with the mass balance equations in Equation (1.5):

$$\begin{aligned}
\frac{dn_1}{dt} &= 2\gamma_2 n_2 + \sum_{i=3}^{m} \gamma_i n_i - \sum_{1}^{m-1} \beta_i n_i \qquad (i = 1) \\
\frac{dn_2}{dt} &= \frac{1}{2}\beta_1 n_1 - \gamma_2 n_2 - \beta_2 n_2 + \gamma_3 n_3 \qquad (i = 2) \\
\frac{dn_i}{dt} &= \beta_{i-1} n_{i-1} - \gamma_i n_i - \beta_i n_i + \gamma_{i+1} n_{i+1} \quad (i > 2)
\end{aligned}$$

The growth rate coefficient β_i, and the evaporation rate coefficient γ_i are given with the kinetic theory of gases for collisions between H_2SO_4 monomers and H_2SO_4−H_2O clusters,

$$\begin{aligned}
\beta_i &= \left(\frac{8\pi kT\,(m_1 + m_i)}{m_1 m_i}\right)^{1/2} (r_1 + r_i)^2\, n_1 \\
\gamma_i &= \left(\frac{8\pi kT\,(m_1 + m_i)}{m_1 m_i}\right)^{1/2} (r_1 + r_i)^2\, n_{a,sol}^{\infty} \exp\left(\frac{2M_a\sigma}{\rho_i RT r_i}\right)
\end{aligned} \tag{4.1}$$

where m_1 and r_1 are the mass and radius of H_2SO_4−H_2O monomers, m_i and r_i are the mass and radius of i-mers, n_1 is the concentration of monomers, and $n_{a,sol}^{\infty}$ is the concentration of H_2SO_4 vapor above a flat surface of a solution having the same composition as the i-mers, M_a is the molecular mass of H_2SO_4, σ is the surface tension of the binary solution, ρ_i is the density of i-mers, R is the ideal gas constant, k is the Boltzmann constant. The kinetic QUN model shows better estimation results than the classical binary nucleation model compared with experimental data. Additionally, the QUN model is applicable for conditions such as diluting engine exhaust where

properties of gases change rapidly.

4.1.2 Multi-component nucleation models

There have been several studies that have used simplified nucleation models for a multi-component system. Some of them can be applicable with the QUN model for binary homogeneous nucleation of $H_2SO_4-H_2O$. Du and Yu [60] developed a ternary nucleation model that extended binary $H_2SO_4-H_2O$ equations. An unknown third species participates in the ternary nucleation equations by reducing the Gibbs free energy from that of binary $H_2SO_4-H_2O$ nucleation. Like the binary nucleation case, sulfuric acid controls the growth and evaporation rate of clusters by colliding with and evaporating from clusters and water influences the composition of the clusters and the evaporation coefficient of sulfuric acid clusters. Du and Yu assumed that the third species plays a similar role as water. The reduced Gibbs free energy by this third species decreases evaporation coefficients of binary clusters and increases stability as a result. The change in Gibbs free energy was expressed as a function of the number of molecules of the third species and empirical parameters by assuming the Gibbs free energy difference between binary and ternary nucleation increases with decreasing cluster size and diminishes to zero with sufficiently large clusters as:

$$\begin{aligned} \gamma_i &= \beta_{i-1} \exp\left(\frac{\Delta G_{i-1,i}}{kT}\right) \\ \Delta G_{i-1,i}^{ternary} &= \Delta G_{i-1,i}^{binary} - dG\,(i) \\ dG\,(i) &= a + \frac{b}{i^c} \end{aligned} \tag{4.2}$$

where γ_i is the evaporation rate of i-mers, β_{i-1} is the collision rate of $(i-1)$-mers to grow to i-mers, $\Delta G_{i-1,i}$ is the Gibbs free energy associated with $(i-1)$-mers and i-mers, and a, b, and c are empirical parameters.

Gorbunov [61] suggested that in the embryos formed from multi-component nucleation, two main species will be dominant in concentration with the reminder species being insignificant. They modeled the multi-component nucleation with two separate

steps extended from binary nucleation: 1) binary nucleation process with two dominant species, and 2) transformation process of minor species afterward. The Gibbs free energy of the embryo formation can be calculated with the sum of the Gibbs free energy for the corresponding steps:

$$\begin{aligned}\Delta G(N_w,N_{sa},N_1,N_2,\cdots,N_{N-2}) &= \Delta G(N_w,N_{sa}) + \Delta G(N_1,N_2,\cdots,N_{N-2}) \\ &= \Delta G_{binary} - RT\sum_{i=1}^{N-2}\left[\ln\left(\frac{P_i}{k_i X_i}\right)+1\right]N_i + \sigma_{e2}\sum_{i=1}^{N-2}\Delta S_i\end{aligned} \tag{4.3}$$

where N_w is moles of water and N_{sa} is moles of sulfuric acid transferred from gas phase to embryo. P_i is the partial pressure of species i, K_i is the Henrys law constant, v_i is the molar volume of species i, r_e is the radius of embryo, σ_{e2} is the interfacial free energy for the embryo formation in the second step, ΔS_i is the change of the embryo surface area due to transfer molecules at the second step.

The composition of minor species forming diluted solution in sulfuric acid and water solution is calculated thermodynamically using Henrys law with respect to the composition of binary major species:

$$N_i = (N_w + N_{sa})\frac{P_i}{K_i}\exp\left(-2\frac{\sigma_e v_i}{RTr_e}\right) \tag{4.4}$$

where radius of embryo, r_i, can be replaced with the radius of embryo in the first step:

$$r_{e1} = \left(\frac{3m_{e1}}{4\pi\rho_{e2}}\right)^{1/3} \tag{4.5}$$

With known mole fraction of all species, coefficients for growth rate and evaporation rate can be calculated,

$$\beta_{e1} = \left[\frac{8\pi k_B T\,(m_1+m_{e1})}{m_1 m_{e1}}\right]^{1/2}(r_1+r_{e1})^2\,n_1 \tag{4.6}$$

$$r_{e2} = \left(\frac{3m_{e2}}{4\pi\rho_{e2}}\right)^{1/3} \tag{4.7}$$

$$\beta_{e2} = \left[\frac{8\pi k_B T\left(m_1 + m_{e2}\right)}{m_1 m_{e2}}\right]^{1/2} \left(r_1 + r_{e2}\right)^2 n_1$$
$$\gamma_{e2} = \beta_{e2} \frac{n_{a,sol}^{\infty}}{n_1} \exp\left(\frac{2M_a \sigma_{e2}}{\rho_{e2} k_B T r_{e2}}\right) \tag{4.8}$$

where σ_{e2} is the interfacial free energy for the embryo formation in the second step but can be replaced with that in the first step since it can be assumed that it depends on only the concentration of the dominant species.

Du and Yus parametric model is applicable to a kinetic nucleation model simply with one additional step, but it is not useful when the values of the empirical parameters are not available. While Gorbunovs approach is more general and applicable to systems with more than three species, it is only applicable to system controlled by two major species and limited to the equilibrium calculation of other insignificant species. In this work, Gorbunovs approach was used to test multi-component nucleation among one of several possible nucleation pathways for hydrocarbons with sulfuric acid and water system.

4.2 Microphysical Model for Hydrocarbon in Nucleation Process

This section provides the modeling approach of hydrocarbon nucleation applicable according to their solubility. Nucleation of water-insoluble hydrocarbons was modeled independently from $H_2SO_4-H_2O$ nucleation because water-insoluble hydrocarbons are not expected to participate in forming aqueous clusters via a nucleation process. Nucleation of water-soluble hydrocarbons was examined among possible pathways, including multi-component nucleation extended from binary sulfuric acid-water nucleation, binary hydrocarbon and water nucleation as well as separate unary nucleation. Clusters formed via nucleation can grow to larger particles via coagulation with other aqueous clusters or hydrocarbon clusters afterward. Coagulation is described in Section 4.3 in detail.

4.2.1 Nucleation of water-insoluble hydrocarbons

In this work, it was assumed that water-insoluble hydrocarbons have no direct effect on the nucleation of aqueous clusters. Therefore, sulfuric acid and water participate in the nucleation process the same way as the previously implemented binary nucleation case, regardless of presence of water-insoluble hydrocarbons. Water-insoluble hydrocarbons are assumed to be involved in the new particle formation via homogeneous nucleation of separate water-insoluble clusters from aqueous nuclei. Water-insoluble hydrocarbon clusters are allowed to contribute to the growth of aqueous embryos or droplets by coagulation afterward.

In contrast to the aqueous cluster formation process, in which clusters grow by gaining or losing hydrated sulfuric acid monomers — $H_2SO_4{-}(H_2O)_n$ would form with abundant water molecules — water-insoluble hydrocarbon molecules nucleate by collisions with molecules of its own kind or other hydrocarbon species. In this work, rather than considering multi-component nucleation of hydrocarbon species, nucleation of water-insoluble hydrocarbons was modeled as unary nucleation. This approach, while does not strictly reflect reality, is a reasonable way of modeling water-insoluble hydrocarbon nucleation in aircraft emissions. This is because nucleation of hydrocarbons is not a favorable pathway to grow to critical clusters compared to binary nucleation of sulfuric acid and water. $H_2SO_4{-}H_2O$ aerosols are most abundant in aircraft plume, and thus, tracking coagulation between hydrocarbon clusters may not be critical because these collisions are rare compared to those between hydrocarbon clusters and $H_2SO_4{-}H_2O$ clusters under the conditions of our interest.

Concentrations of water-insoluble hydrocarbon embryos and $H_2SO_4{-}H_2O$ embryos are compared in Figure 4-1. While $H_2SO_4{-}H_2O$ embryos tend to grow and form larger homogeneous droplets, water-insoluble hydrocarbons remain in the gas phase or form low concentrations of oligomers smaller than the critical cluster size via unary nucleation. We thus conclude that under the conditions of aviation emissions, $H_2SO_4{-}H_2O$ nucleation determines the population of homogeneous aerosols in general and the contribution of water-insoluble hydrocarbon nucleation to the aerosol

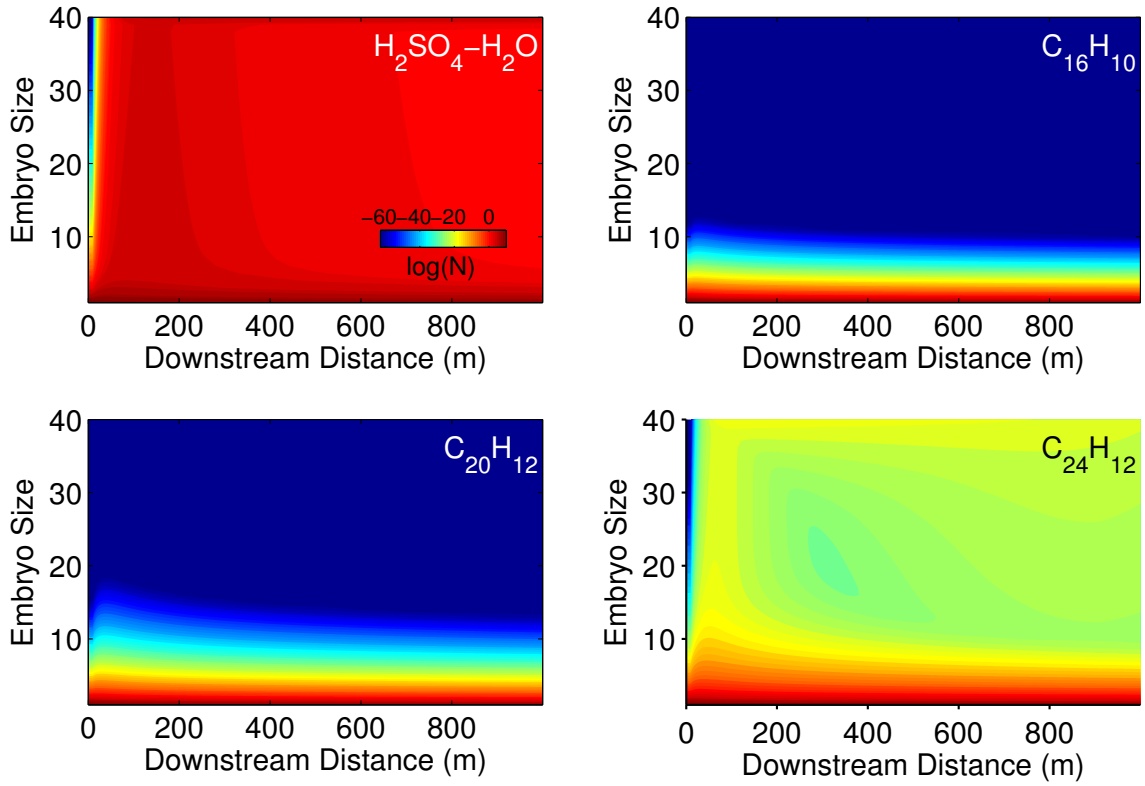

Figure 4-1: Concentrations for binary H2SO4-H2O embryos and unary water-insoluble hydrocarbon embryos

number density is negligible. It is likely, though, that water-insoluble hydrocarbons can contribute to other processes such as particle growth by coagulation and condensation on $H_2SO_4-H_2O$ clusters and form aerosols composed of hydrocarbons as well as sulfuric acid and water.

4.2.2 Nucleation of water-soluble hydrocarbons

For water-soluble hydrocarbons, the possibility of binary or multi-component nucleation of hydrocarbons with sulfuric acid and water should be considered in contrast to unary nucleation of water-insoluble hydrocarbons.

Nucleation mechanisms for water-soluble hydrocarbons examined in this work are:

- Multi-component clusters with sulfuric acid and water. Hydrocarbons may change stability of aqueous clusters and their lifetime. Following Gorbunovs approach of modeling multi-component nucleation with consequent two nucle-

ation steps, the composition of binary clusters with sulfuric acid and water is calculated first by quasi-unary nucleation approach. Transfer of water-soluble hydrocarbons from gas to aqueous clusters is then calculated thermodynamically in terms of the composition of sulfuric acid and water. This calculation is based on the assumption that additional species in the second nucleation step are relatively insignificant compared to the two species participate in the main nucleation process. This assumption of very small fractions of hydrocarbons in embryos compared to those of sulfuric acid and water is acceptable in considering conditions for near-field aircraft emissions with highly volatile water-soluble hydrocarbon species.

- Binary nucleation of water-soluble hydrocarbons and water in addition to binary nucleation of sulfuric acid and water. In this approach, water-soluble hydrocarbons are assumed to play a similar role to sulfuric acid in the binary nucleation, that is, controlling the growth and evaporation of clusters.

- Unary nucleation of water-soluble hydrocarbons as similar to the unary nucleation of water-insoluble hydrocarbons. This approach would be acceptable if the number of water molecules attracted by hydrocarbon clusters is very small.

- Negligible contribution of water-soluble hydrocarbons to the nucleation process because of their high volatility. This assumption would be valid if there is no effect of water-soluble hydrocarbons to mass composition and nucleation rate of liquid particles regardless of approaches applied for water-soluble hydrocarbon nucleation.

Comparisons of different cluster formation mechanisms for water-soluble hydrocarbons are shown in Figure 4-2. Interaction between water-soluble hydrocarbons and sulfuric acid-water clusters in the nucleation process has a minor contribution to the very initial formation of clusters, as shown in the first panel of Figure 4-2 for the difference of embryo concentration between binary $H_2SO_4-H_2O$ nucleation and multi-component nucleation of $H_2SO_4-H_2O$-ws HCs. However, as the residence time

increases, multi-component nucleation does not significantly affect binary nucleation of sulfuric acid and water because light hydrocarbons having high Henrys coefficients tend to remain in the gas phase rather than nucleating with sulfuric acid and water. Also, the hydrocarbon cluster concentration shown in Figure 4-2 suggest that neither binary nucleation of water-soluble hydrocarbons with water nor unary nucleation of water-soluble hydrocarbons is an efficient pathway to grow to larger liquid particles. For binary nucleation of water-soluble hydrocarbons and water, only a small number of water molecules is attracted to hydrocarbon clusters due to high activity coefficient of water in water-soluble hydrocarbon solutions, which is much smaller than that in water-insoluble hydrocarbon solutions but still significantly higher than that in sulfuric acid solutions. This result indicates that binary nucleation of water-soluble hydrocarbon and water is close to unary nucleation of hydrocarbons indeed. Both nucleation models for water-soluble hydrocarbon clusters predict that formation of new particles is difficult to initiate due to high volatility of water-soluble hydrocarbons. These species re-evaporate to the vapor phase quickly due to their high vapor pressure, such that the evaporation rates of clusters are much greater than the growth rates. The analysis of nucleation pathways of water-soluble hydrocarbons presented in this section shows that their contribution to the aerosol formation may be negligible without foreign nuclei under the conditions of interest in this work, similar to our observation of water-insoluble hydrocarbons. Hydrocarbon oilgomers evolved in aircraft plume are unlikely to grow bigger than the critical size of clusters.

4.3 Multi-component Coagulation Model

As discussed in the previous section, nucleation of hydrocarbons in aircraft emissions is not an efficient means to promote new particle formation from gaseous molecules and most of their mass remains in the gas phase or in the form of small oligomers. However, this conclusion does not necessary mean that their involvement in the evolution of homogeneous aerosols is insignificant. Considerable amount of organic fraction has been measured in aircraft emitted volatile particles during recent field missions

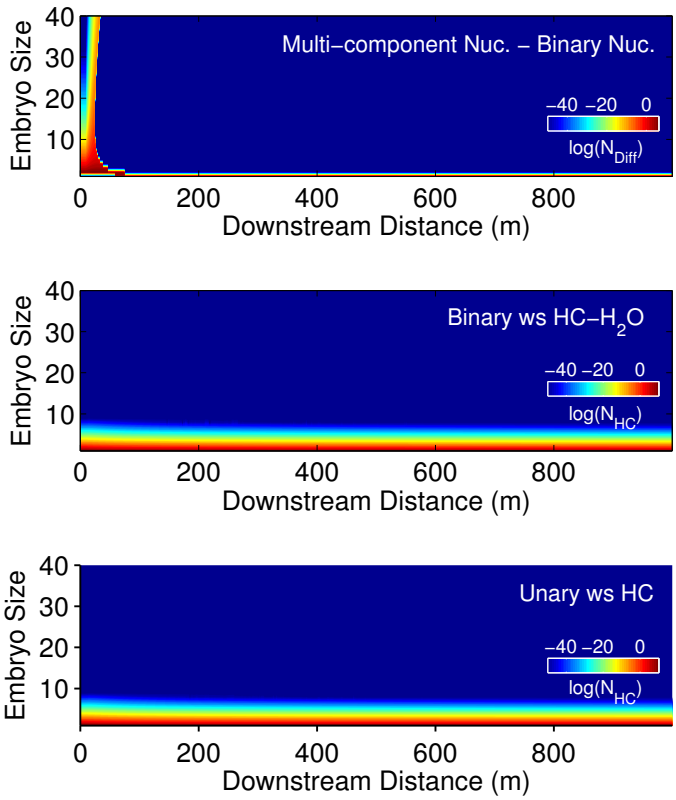

Figure 4-2: Calculated difference in embryo concentrations between binary $H_2SO_4-H_2O$ nucleation and multi-component nucleation of water-soluble hydrocarbon molecules

[62, 63], and several studies have shown that that aerosol particles have an aqueous core with hydrocarbon surface layers forming hydrophobic organic coatings due to their negligible water solubility [64, 65, 66].

Figure 4-3 illustrates mechanisms of forming liquid coatings on a solid core or on a liquid aqueous core considered in this work. Liquid films tend to aggregate with liquid of same type of solubility on a partially wetted solid surface, while hydrophobic liquid films tend to spread on aqueous liquid surfaces. If collisions occur between water-insoluble hydrocarbon clusters and $H_2SO_4-H_2O$ clusters, hydrocarbon mass starts to have uptake on $H_2SO_4-H_2O$ clusters. As $H_2SO_4-H_2O$ clusters grow to larger liquid particles via coagulation, aggregates of $H_2SO_4-H_2O$ clusters and hydrocarbons clusters form multi-component aerosols having a hydrophobic film of hydrocarbons. Coagulation between unary nucleated clusters of different water-insoluble hydrocar-

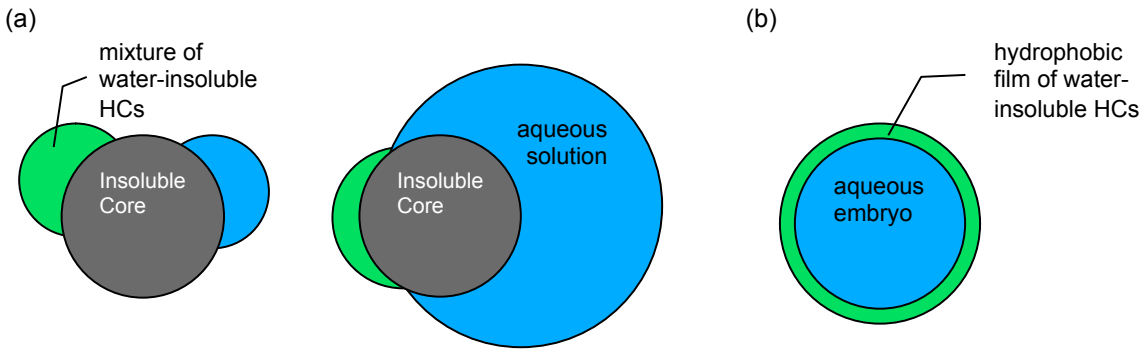

Figure 4-3: Structure for coagulation on: (a) solid core, (b) aqueous core

bon species was not considered in this thesis since this process is less likely compared to the collision between hydrocarbon clusters and much abundant sulfuric acid-water clusters. The coagulation model for multi-component aerosols in this thesis is based on the assumptions that water-insoluble hydrocarbons form a thin oily film on aqueous droplets, where the film is assumed to spread uniformly and quickly after collisions and does not to affect the thermodynamics of the binary droplets and the composition of the sulfuric acid-water core. While some studies have shown that the presence of organic films on aerosol particles can retard the uptake or evaporation of water from an aqueous core [67, 68], Garland *et al.* [69] suggested that the retardation effect is negligible with a thin hydrophobic film. Here it is assumed that ignoring the effect of a thin hydrocarbon film to hygroscopic growth of nanometer-size particles would be acceptable for the rapidly growing particles in the aircraft plume.

The coagulation model for the multi-component aerosols requires additional variables to simulate and track the growth of hydrophobic films, while the composition of binary droplets can be calculated by finding the composition of minimum free energy at the size of particles being considered. Since tracking all possible combinations of aqueous core sizes and hydrocarbon film volumes for volatile particles is impractical, a modified sectional bin approach was implemented in the simulation model to track the evolution of both the aqueous core and the hydrocarbon film.

For the original $H_2SO_4-H_2O$ binary model, Wong *et al.* [27] used the fully stationary sectional bin approach for coagulated droplets bigger than the largest size of embryos, where embryos were tracked with the number of sulfuric acid molecules.

The fully stationary bin approach uses fixed size of bins, forcing all particles in a bin to have the same volume while allowing particles to move between bins if they grow or shrink. To conserve particle number and volume, a coagulated new particle whose volume between two sectional bins is partitioned into two bins adjacent to the size of new particle based on the fraction of volume of the new particle and values of the bins volumes. The composition of binary droplets can be calculated by finding the composition of minimum free energy at the size of the sectional bins. The stationary sectional bin approach is practical generally for simulating coagulation of particles. However, the approach may cause numerical issues when particles grow via condensation and evaporation [70] and it is difficult to track particles having components in separate phases such as aqueous core with hydrophobic coatings. Jacobson and Turco [70] suggested that a hybrid model combining the stationary bin approach and the fully moving bin approach. The hybrid bin approach tracks core and non-core components separately, which applies fixed size bins for the core fraction and allows non-core fraction to grow to its exact size. If a particle is moved to a new bin, its averaged non-core volumes in that bin will also be moved with the particle.

With the hybrid bin approach, the aqueous cores are tracked with the stationary bin approach and the growth of hydrophobic film is tracked to its exact size, where the size of each stationary bin becomes a lower limit of the mean size of whole particles as illustrated in Figure 4-4. If two particles having an aqueous core and hydrophobic film coagulate [in the case of Figure 4-4 (b)], the coagulated particle is partitioned based on the volume of aqueous core into two adjacent bins using the stationary bin approach, whereas the mass of the hydrophobic film on the particles is fractionated into both bins according to how the core is distributed. The hydrocarbon mass composing the hydrophobic film on the partitioned particles entered into bins is averaged with the hydrocarbon mass of the existing particles in those bins. This approach also allows the condensational growth of the hydrophobic film via coagulation of hydrocarbon clusters and sulfuric acid-water droplets as shown in Figure 4-4 (c). Detailed calculations are shown in Table 4.1 and Figure 4-5.

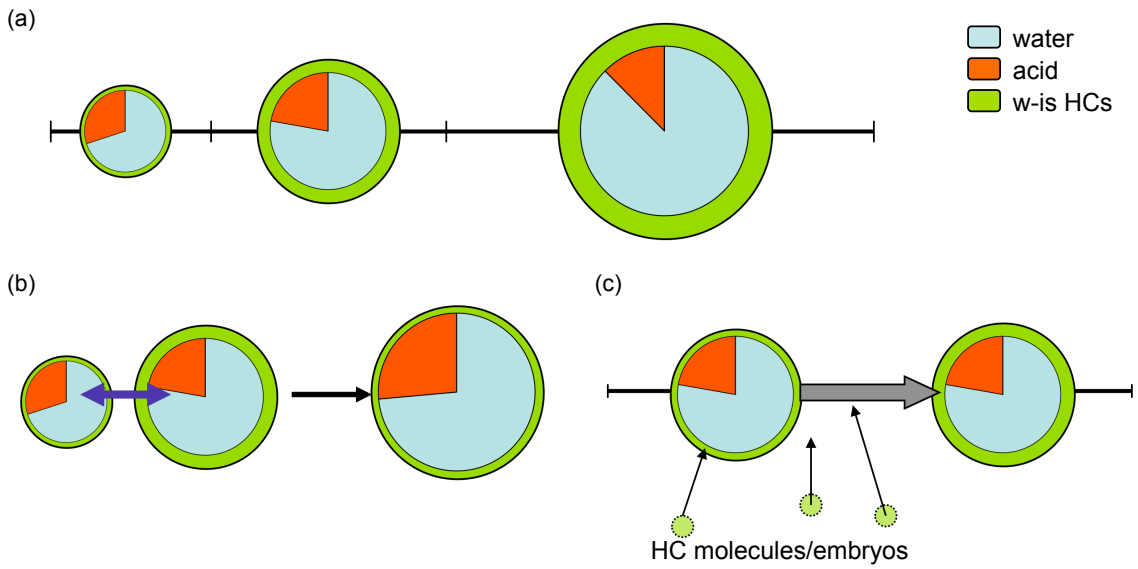

Figure 4-4: Outline for modeling coagulation with the hybrid bin approach (a), applicable to coagulation of sulfuric acid-water droplets having hydrophobic film (b) and coagulation of sulfuric acid-water droplets and hydrocarbon clusters (c)

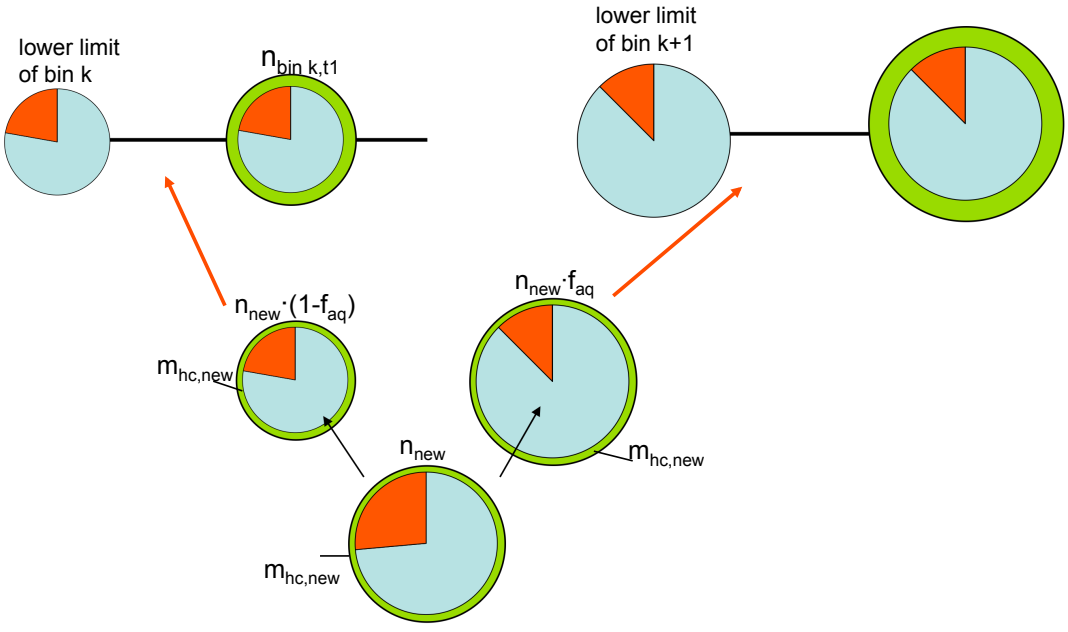

Figure 4-5: Details of the combined bin approach

Particle composition at time t_1:

m_w, m_{ac}, m_{hc} for mass of water, sulfuric acid, hydrocarbon

$$X_w = \frac{m_w}{m_w + m_{ac}}, \quad X_{ac} = \frac{m_{ac}}{m_w + m_{ac}}, \quad X_{hc} = \frac{m_{hc}}{m_w + m_{ac} + m_{hc}}$$

Coagulation of particle in bin i and particle in bin j

---

step i. calculate properties of the new particle:

$m_{ac,new} = m_{ac,i} + m_{ac,j}$, $m_{hc,new} = m_{hc,i} + m_{hc,j}$

find bin k and bin $k+1$ satisfying $m_{ac,k} \leq m_{ac,new} < m_{ac,k+1}$

$X_{ac,new} = (1 - f_{ac} \cdot X_{ac,k} + f_{ac} \cdot X_{ac,k+1})$ where $f_{ac} = \dfrac{m_{ac,new} - m_{ac,k}}{m_{ac,k+1} - m_{ac,k}}$

$m_{ac,new} + m_{w,new} = m_{aq,new} = \dfrac{m_{ac,new}}{X_{ac,new}}$

---

step ii. find bin l and bin $l+1$ satisfying $m_{aq,l} \leq m_{aq,new} < m_{aq,l+1}$

where $f_{aq} = \dfrac{m_{aq,new} - m_{aq,l}}{m_{aq,l+1} - m_{aq,l}}$

---

step iii. calculate properties of partitioned particles:

n_{new} = the number of coagulated particles

Δn_l = the number of partitioned particles entering into bin $l = n_{new}(1 - f_{aq})$

Δn_{l+1} = the number of partitioned particles entering into bin $l+1 = n_{new} f_{aq}$

---

step iv. update averaged properties of particles in bin l and bin $l+1$ after coagulation

$n_{l,new} = n_{l,t_1} + n_{new}(1 - f_{aq})$

$m_{aq,new} = m_{aq,l,t_1}$

$$m_{hc,l,new} = \frac{n_{l,t_1} m_{hc,l,t_1} + n_{new}(1 - f_{aq}) m_{hc,new}}{n_{l,t_1} + n_{new}(1 - f_{aq})}$$

$n_{l+1,new} = n_{l+1,t_1} + n_{new} f_{aq}$

$m_{aq,l+1,new} = m_{aq,l+1,t_1}$

$$m_{hc,l+1,new} = \frac{n_{l+1,t_1} m_{hc,l+1,t_1} + n_{new} f_{aq} m_{hc,new}}{n_{l+1,t_1} + n_{new} f_{aq}}$$

Table 4.1: Calculation for tracking coagulation with the hybrid bin approach

4.4 Summary for pathways for new particle formation

This section summarizes possible interactions and mechanisms of the nucleation and coagulation processes and compares their contributions to the formation of hydrocarbon-containing aerosols. Figure 4-6 shows a schematic of new liquid particle formation pathways via nucleation (indicated as alphabet letters) or coagulation (indicated as Roman numerals) processes. Table 4.2 lists five different approaches of including different particle formation pathways discussed in Section 4.2. Figure 4-7 shows simulated liquid particle size distributions at 1 km downstream of a CFM56-2C1 engine at 80% ambient relative humidity and 286 K ambient temperature using the approaches in Table 4.2. Coagulation between water-insoluble hydrocarbon clusters and aqueous clusters forms hydrocarbon films on aqueous cores like particles having green coating shown in Figure 4-6. Our analysis shows that the coagulation between water insoluble hydrocarbon clusters and sulfuric acid-water particles (process iii) is the most critical pathway. The growth of hydrophobic organic films increased aerosol size of about 1.5 (mode size) to 2.5 (min size) times greater compared to aerosols formed merely from binary nucleation of sulfuric acid and water without hydrocarbons (i.e. Approach 5). The contribution of water-soluble hydrocarbons, on the other hand, is insignificant (see the comparison between Approach 4 and Approach 1 or 3 in Figure 4-7) since they remain mostly in the gas phase, as shown in Table 4.3. The predicted particle size distribution from Approaches 1 and 3 are almost identical, suggesting that the interaction between water-soluble hydrocarbon and water (process b) is insignificant. While the interaction between water-soluble hydrocarbons with $H_2SO_4-H_2O$ clusters via coagulation (process i) is identified as an inefficient pathway to change aerosol size distribution, the interaction between water-soluble hydrocarbon molecules and $H_2SO_4-H_2O$ nuclei in the nucleation step (process e in Figure 4-6) has minor contributions to aerosol growth by decreasing evaporation rate by decreasing surface tension.

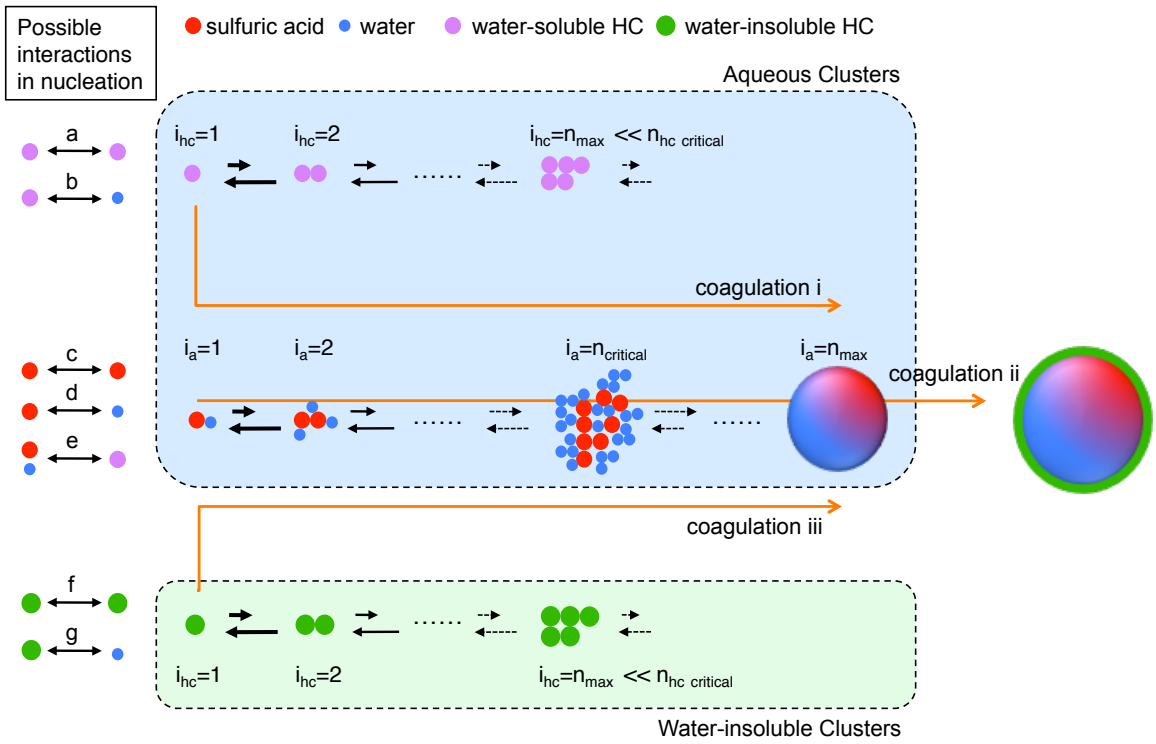

Figure 4-6: Interaction and pathways for new particle formation

4.5 Results and Discussion

4.5.1 Simulation Result

This section provides simulation results for the evolution of aviation PM emissions at ground level with all microphysical processes considered. The role of hydrocarbons to the particle growth is also discussed. Initial exhaust properties are identical to those used in the simulations for the soot particle growth [see Section 3.2.1 for details], and ambient conditions were set to 286 K temperature and 80% relative humidity. Also, 100 ppb of three water-insoluble hydrocarbons, $C_{16}H_{10}$, $C_{20}H_{12}$, $C_{24}H_{12}$, and 100 ppb of three water-soluble hydrocarbon oxygenates, C_3H_6O, $C_3H_6O_2$, $C_4H_8O_2$, were used as hydrocarbon surrogates in the exhaust plume, and the same initial gas concentrations were employed as described in Equation (3.7). $H_2SO_4-H_2O$ clusters were tracked as embryos that are no larger than 40 sulfuric acid molecules, and larger particles having more than 40 acid molecules were tracked using 10 bins that initially log-normally distributed between 3 nm to 250 nm. Hydrocarbon clusters were

	Binary nucleation of H_2SO_4-H_2O	Multi-component nucleation of H_2SO_4-H_2O-water soluble Hydrocarbons (HCs)	Binary nucleation of w-s HCs	Unary nucleation of w-s HCs	Negligible effect of nucleation of w-s HCs	Unary Nucleation of water insoluble HCs
included interactions	c,d,ii	c,d,e,ii	a,b,i	a,i	-	f,iii
Approach 1	v		v			v
	a, b, c, d, f, i, ii, iii					
Approach 2		v				v
	c, d, e, f, ii, iii					
Approach 3	v			v		v
	a, c, d, f, i, ii, iii					
Approach 4	v				v	v
	c, d, f, ii, iii					
Approach 5	v					
	c, d, ii					

Table 4.2: Nucleation and coagulation approaches for new particle formation

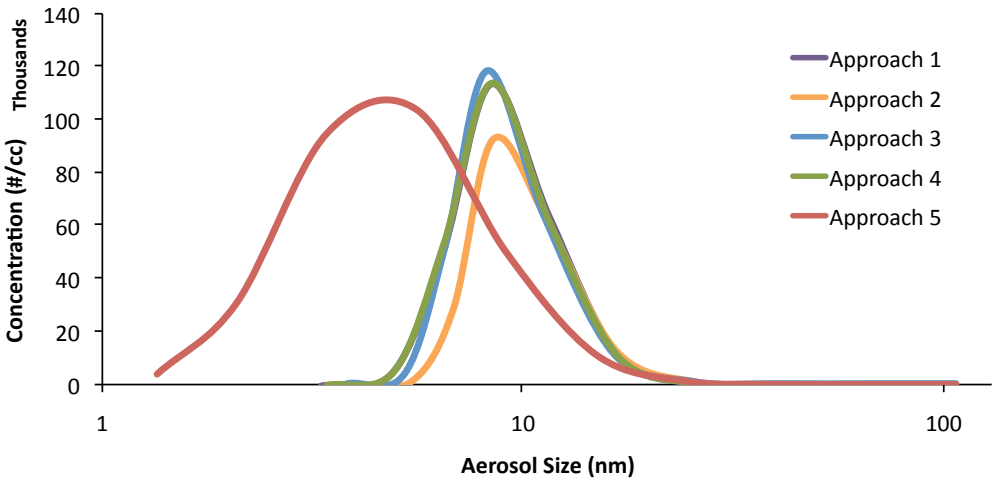

Figure 4-7: Comparison of predicted particle size distributions of liquid aerosols at 1 km downstream of a CFM56-2C1 engine by involved different interactions in nucleation and coagulation processes

	Mass fraction (%) of species in nucleation mode		
	Sulfur	Water-insoluble HCs	Water-soluble HCs
Approach 1	100	99.8	0.007
Approach 2	100	99.7	0
Approach 3	100	99.8	0.36
Approach 4	100	99.7	-
Approach 5	99	-	-

Table 4.3: Comparison of mass fraction transferred to the nucleation mode

tracked up to a size of 5 monomer units since larger embryos are present a negligible concentration as discussed previously in Figure 4-1. Monodisperse soot particles were employed with an initial diameter of 16 nm and an initial concentration of 9.75×10^6 cm^{-3}, which represents the emitted soot surface area at low power of a CFM56-2C1 engine that was examined during the APEX measurement campaign.

Figure 4-8 compares the evolution of particle size distribution of homogeneous nucleation mode particles formed from two mechanisms: (a) binary homogeneous $H_2SO_4-H_2O$ particles without hydrocarbons and (b) multi-component liquid particles with $H_2SO_4-H_2O$ cores and hydrophobic film coatings of hydrocarbons. For both cases, the particles number densities evolved similarly. Small embryos were formed via binary $H_2SO_4-H_2O$ nucleation and grew to larger liquid particles via coagulation. At around 500 m downstream of the engine, liquid particles reached equilibrium size and then their concentrations started to decrease because of mixing with ambient air. Under the exhaust conditions where sufficient amounts of condensable hydrocarbons are present, the particle growth also had contributions from water-insoluble hydrocarbon coagulation even though the formation of liquid particles is primarily driven by binary $H_2SO_4-H_2O$ nucleation. Due to coagulation with water-insoluble hydrocarbons, small particles had hydrophobic film coatings as thick as the radii of their aqueous cores at 1 km downstream. The mean radius of liquid particle distribution increased from 5.4 nm to 10.5 nm when hydrocarbons were included in the model.

Figure 4-9 and Figure 4-10 show evolution of mass compositions of liquid particles and soot coatings predicted from the model, respectively. The predicted mass composition of soot coatings is not significantly different from that of the soot coating

without nucleation and coagulation modes as seen in Figure 3-10; however, the soot particle growth is suppressed significantly as a result of decreasing total soot coating mass. About 80% of the total sulfate mass and about 50% of water-insoluble hydrocarbon mass was found moving to the nucleation mode as compared to the results shown in Section 3.2.2, where only soot mode microphysics were considered. The mass composition of liquid particles, on the other hand, demonstrated that aqueous liquid aerosols in the initial aircraft plume started to have a substantial amount of water-insoluble hydrocarbons as they grew downstream. Smaller liquid particles tend to obtain more hydrocarbon mass fractions, and these particles with small aqueous cores and thick hydrocarbon films could be considered as primarily organic aerosols. This suggests that organics constitute a significant mass fraction in very fine aerosols, where species with low volatility (e.g., $C_{20}H_{12}$ and $C_{24}H_{12}$) could account for a significant amount of organic mass. The contribution of water-soluble hydrocarbons is almost negligible in the nucleation and coagulation processes, but they still can contribute to the growth of soot particle by enhancing the hydrophilic fraction of the soot surfaces and consequently the hygroscopic growth of soot particles.

In Figure 4-11, the mass budget for individual species is divided into three modes: 1) soot coatings due to activation and condensation, 2) liquid aerosol droplets and embryos formed via nucleation and coagulation, 3) vapor phase including monomers and gases. Under the same condition studied earlier, sulfate mass in aerosol droplets and soot coatings increased with downstream distance, and 100% of sulfate mass was transferred from vapor phase to liquid phase at 1 km downstream. Under high ambient relative humidity levels (such as 80% in this case), binary $H_2SO_4-H_2O$ nucleation becomes a dominant process to transfer sulfate mass into aerosol droplets, even at short distance downstream. This is significantly different from the prediction when the nucleation process is turned off in the simulation (see Figure 3-11), where all sulfate mass condensed on soot coatings. Soot particle growth, however, continues to increase after depletion of sulfuric acid gas via scavenging of liquid aerosols on soot particles. For condensable water-insoluble hydrocarbons, similar evolutions were observed that hydrocarbon mass in the vapor phase was transferred relatively quickly

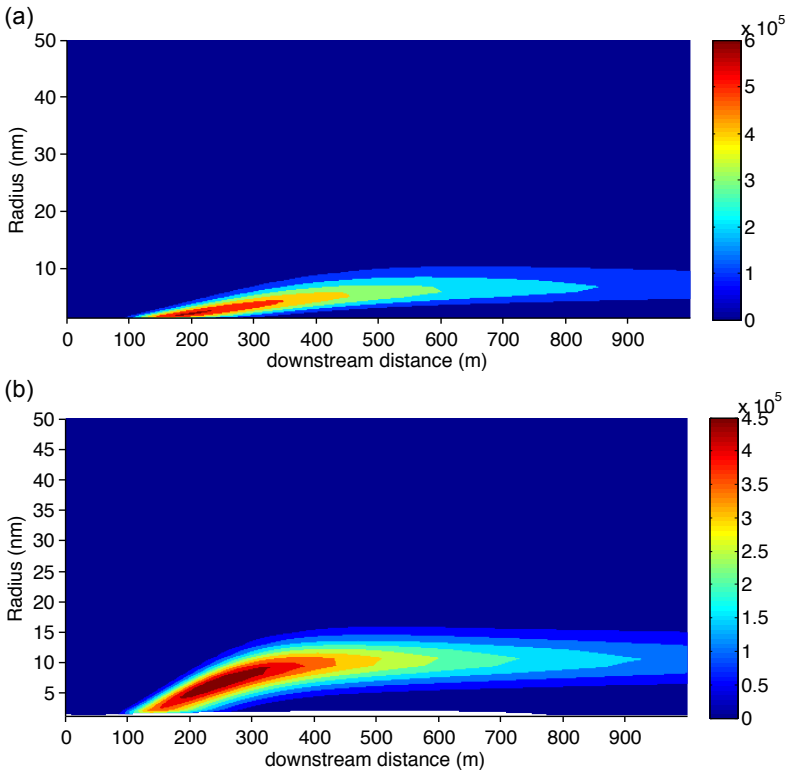

Figure 4-8: Concentration and size evolution of liquid droplets predicted from the model with (a) only sulfuric acid and water binary nucleation, and (b) the presence of hydrocarbons in addition to sulfuric acid and water

into homogeneous liquid aerosols via condensation on or coagulation with homogeneous $H_2SO_4-H_2O$ aerosols followed by gradual coagulation of these particles with soot. Note, however, that benzopyrene ($C_{20}H_{12}$) mass fraction in the liquid droplets initially increased but started to decrease at about 500 m downstream. Consequently, its mass fraction in the vapor phase increased because evaporation of the hydrocarbon species from smaller droplets occurred due to the Kelvin effect. This result implies that the nucleation mode is likely to be more sensitive to the volatility of species than the soot mode because much smaller clusters and droplets are involved in the process. Water-soluble hydrocarbons, on the other hand, are not favorable to be partitioned into homogeneous liquid particles or soot particles because of their high vapor pressure.

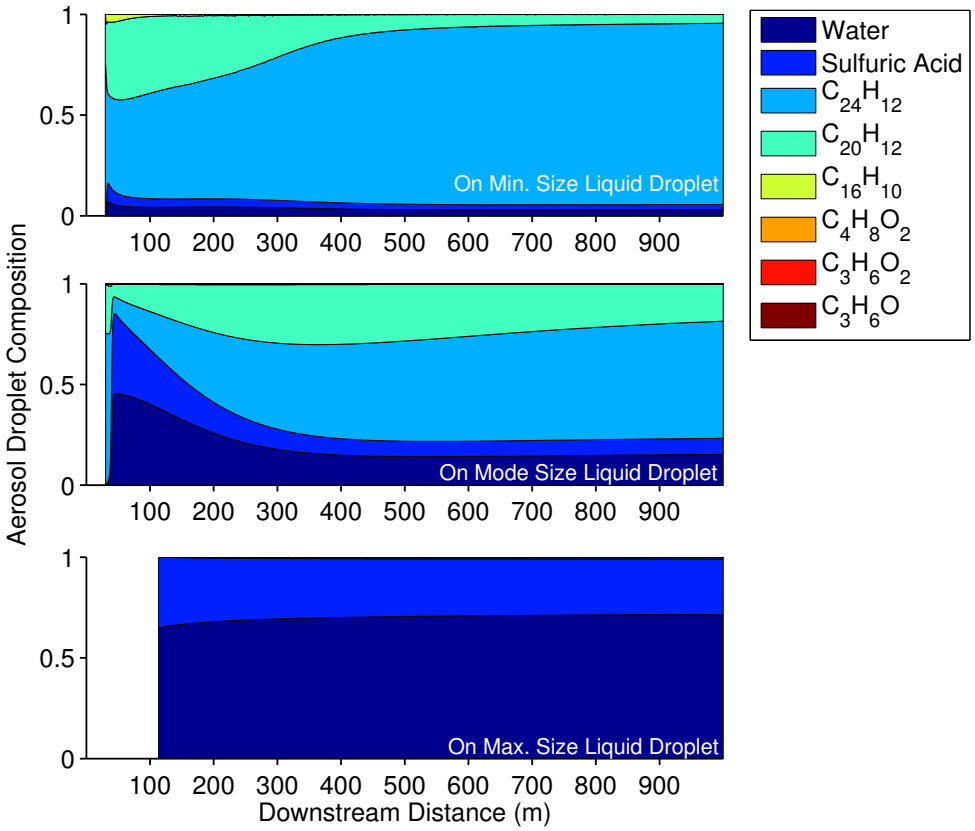

Figure 4-9: Composition evolution of homogeneous particles in minimum, mode, maximum size

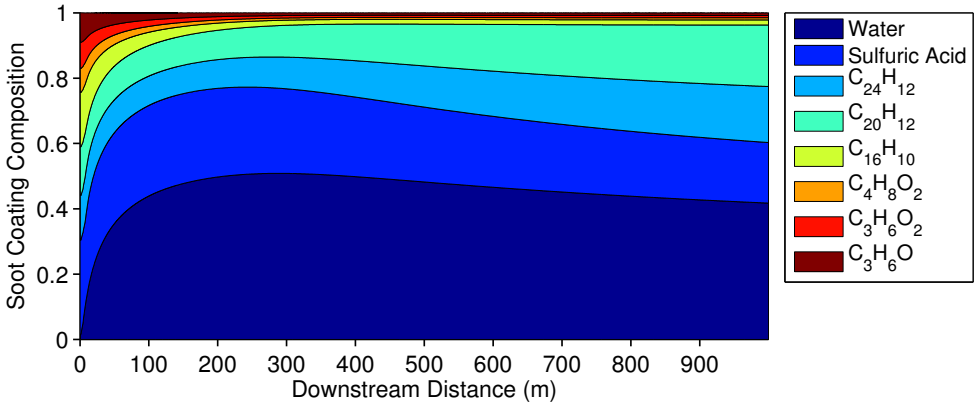

Figure 4-10: Composition evolution of soot coatings

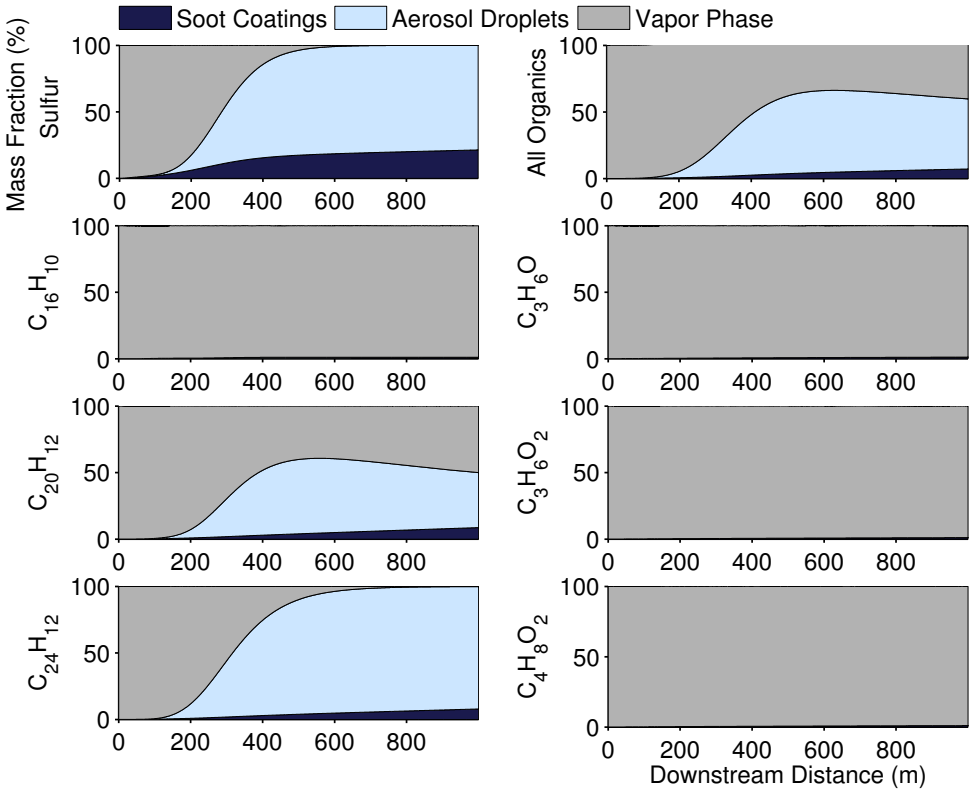

Figure 4-11: Evolution of sulfate and hydrocarbon mass fractions under the conditions described in Section 4.5.1

4.5.2 Comparison with Binary System

4.5.2.1 Role of Hydrocarbons

The effect of hydrocarbons on aerosol formation is examined in this section. Three systems were studied and compared, binary sulfuric acid-water system without hydrocarbons, binary system with water-insoluble hydrocarbon species only, and binary system with all hydrocarbon species included. The contributions of the species to the size and mass growth of both types of particles can be seen in Figure 4-12. Incorporating water-insoluble hydrocarbons contributes to increased size of liquid aerosols while preventing the uptake of water-soluble species on soot coatings. The addition of water-soluble hydrocarbons on the other hand, improves the uptake of water and sulfuric acid on soot particles by competing with the hydrophobic effect of water-insoluble hydrocarbons on soot surfaces. It is important to note that hydrocarbons can contribute to the aerosol formation directly or indirectly via adding condensa-

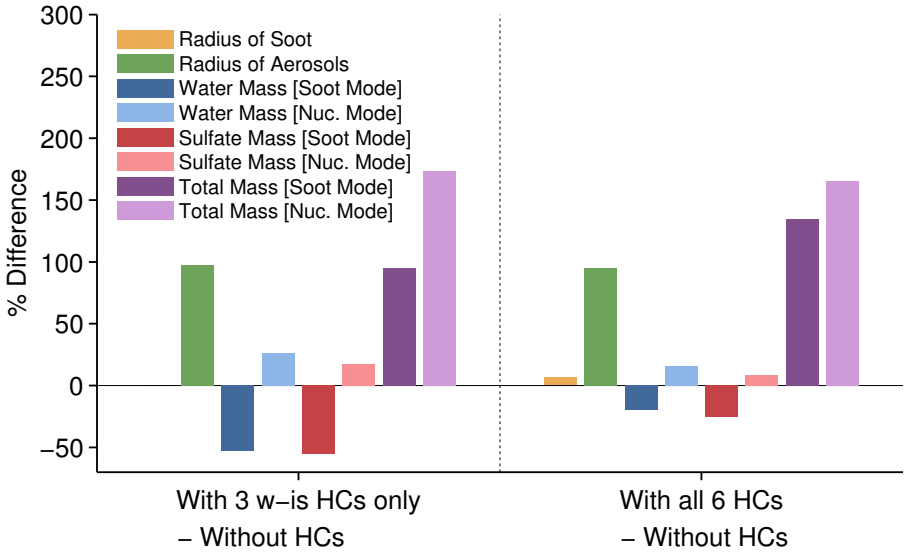

Figure 4-12: Effect of hydrocarbons

tion mass directly and/or inducing competition between condensable species through microphysical processes.

4.5.2.2 Competition Across Microphysical Modes

Nucleation is the most dominant microphysical process at high levels of ambient relative humidity. When ambient relative humidity was set to 80% in our simulations, the nucleation mode accounts for 80% of sulfate mass at 1 km downstream, whereas the soot mode was limited to the remaining 20% of sulfate mass. Consequently, the decreased contribution of nucleation mode at lower ambient relative humidity conditions can lead to increased sulfate mass budget in the soot mode. Figure 4-13 shows that the contribution of the nucleation mode was completely suppressed when 20% ambient relative humidity was used in our simulation. As a result, the contribution of soot mode increased as compared to the 80% ambient RH case. Note that this result that increased sulfate mass on the soot mode with decreasing ambient RH does not agree with the result shown in Section 3.2.4, where sulfate mass on soot mode decreased with decreasing ambient RH when the nucleation process was turned off in the simulation. This indicates that competition between nucleation and soot modes is also important to the evolution of aerosols in addition to competition

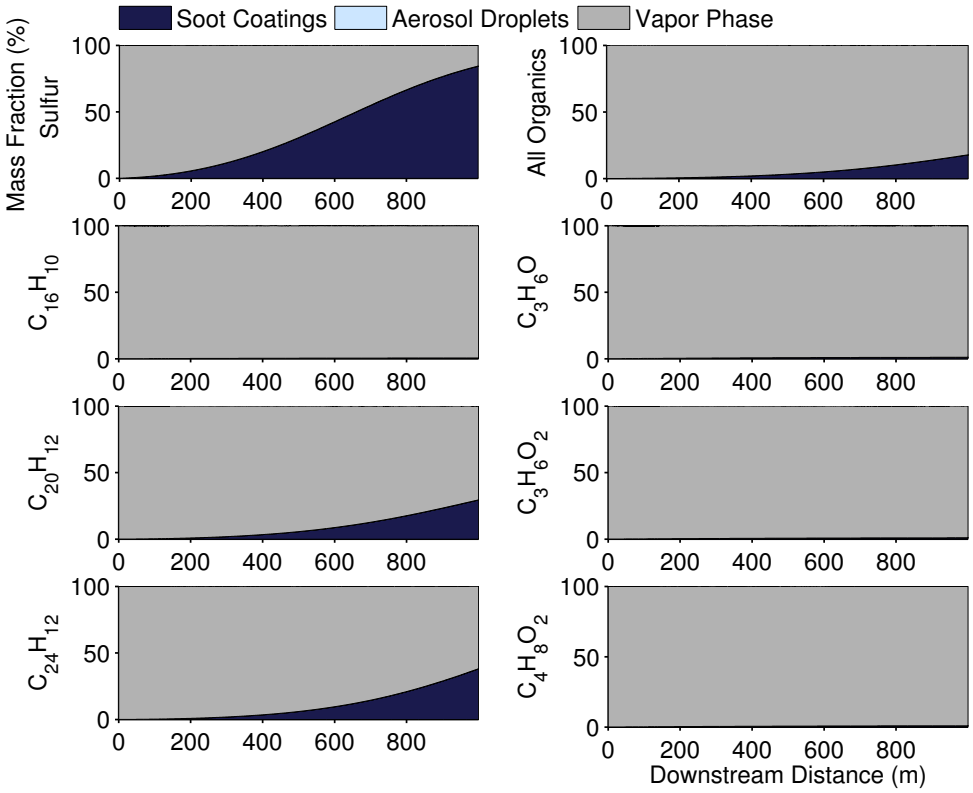

Figure 4-13: Evolution of mass fraction at 20% RH

between exhaust species.

The effect of RH on aerosol formation is examined with and without including hydrocarbons as shown in Figure 4-14a, and the effect of hydrocarbons is further discussed at different RH conditions, in terms of percent difference as shown in Figure 4-14b. Regardless of the presence of hydrocarbons, decreasing RH restricted aerosol nucleation and consequently sulfuric acid preferred to condense on soot coatings as opposed to liquid aerosols. The effect of RH on the soot mode is strengthened by the presence of hydrocarbons. At lower ambient RH levels, hydrocarbons have a stronger effect on soot particle growth. While water-insoluble hydrocarbons substantially contributed to soot particle growth via condensation, water-soluble hydrocarbons enhanced the uptake of water and sulfuric acid on soot coating by increasing hydrophilic surface area. At high ambient RH levels, competition between nucleation and soot modes and competition between hydrocarbons and sulfuric acid on soot surfaces occur at the same time. Delayed sulfuric acid adsorption on soot surfaces

due to competition with water-insoluble hydrocarbons during initial activation process allowed more mass transfer to nucleation mode. Consequently, water-insoluble hydrocarbons decreased the uptake of water and sulfuric acid in the soot mode.

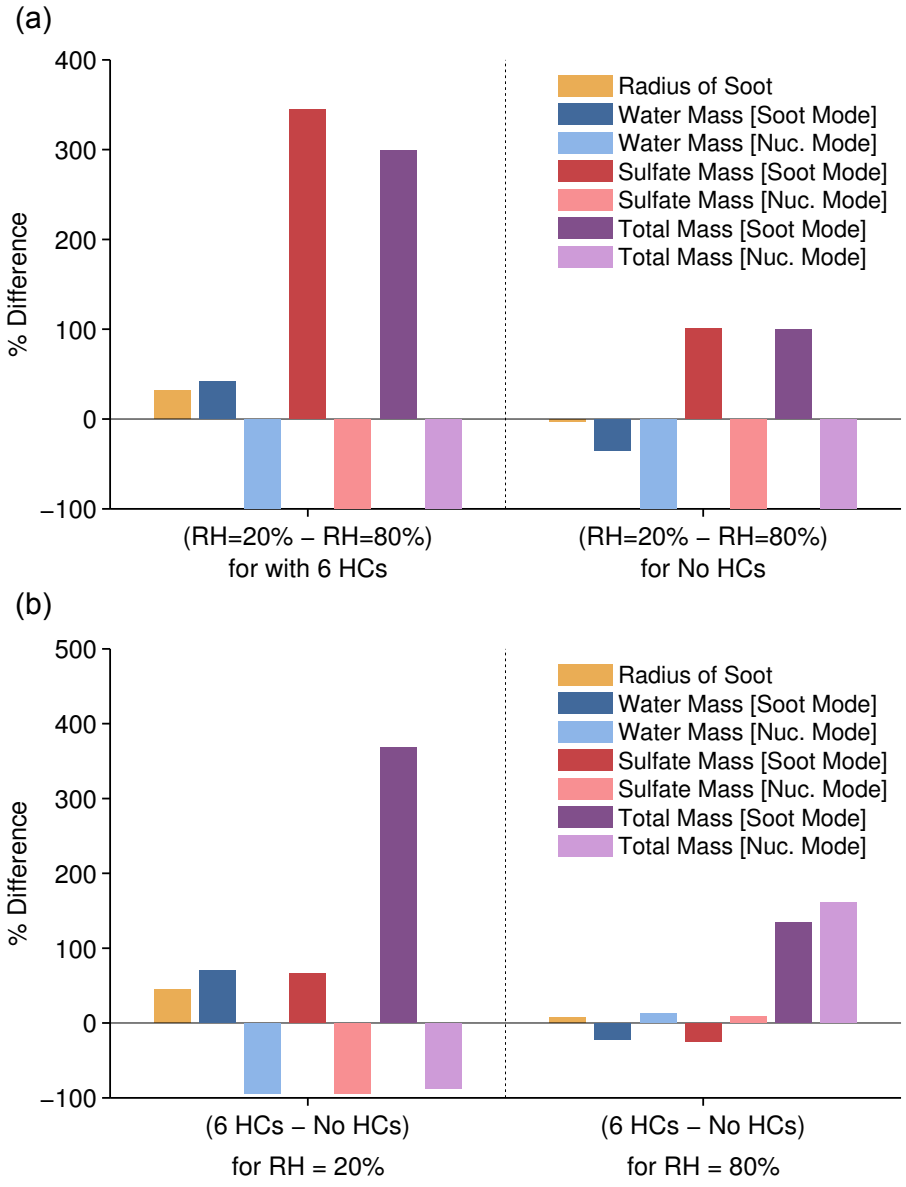

Figure 4-14: Effect of RH and Hydrocarbons

4.6 Summary

It is computationally expensive to simulate classical multi-component nucleation with increasing number of components. This chapter suggests nucleation approaches for hydrocarbons can be simplified by including only dominant effects which would be acceptable for aircraft emissions, and Figure 4-15 shows simplified pathways for the new particle formation in aircraft emissions. Depending on the solubility of species, possible interactions between nucleation and coagulation processes and proposed pathways for new particle formation are examined. These processes and pathways include independent unary nucleation of water-insoluble hydrocarbons and multi-component/binary/unary nucleation of water-soluble hydrocarbons. The results presented in this chapter demonstrate that homogeneous aerosol formation is driven primarily by binary $H_2SO_4-H_2O$ nucleation, and the contribution of hydrocarbons is negligible to the rate of new particle formation.

Coagulation of water-insoluble hydrocarbon clusters with $H_2SO_4-H_2O$ clusters is assumed to form hydrophobic films on aqueous cores. While the contribution

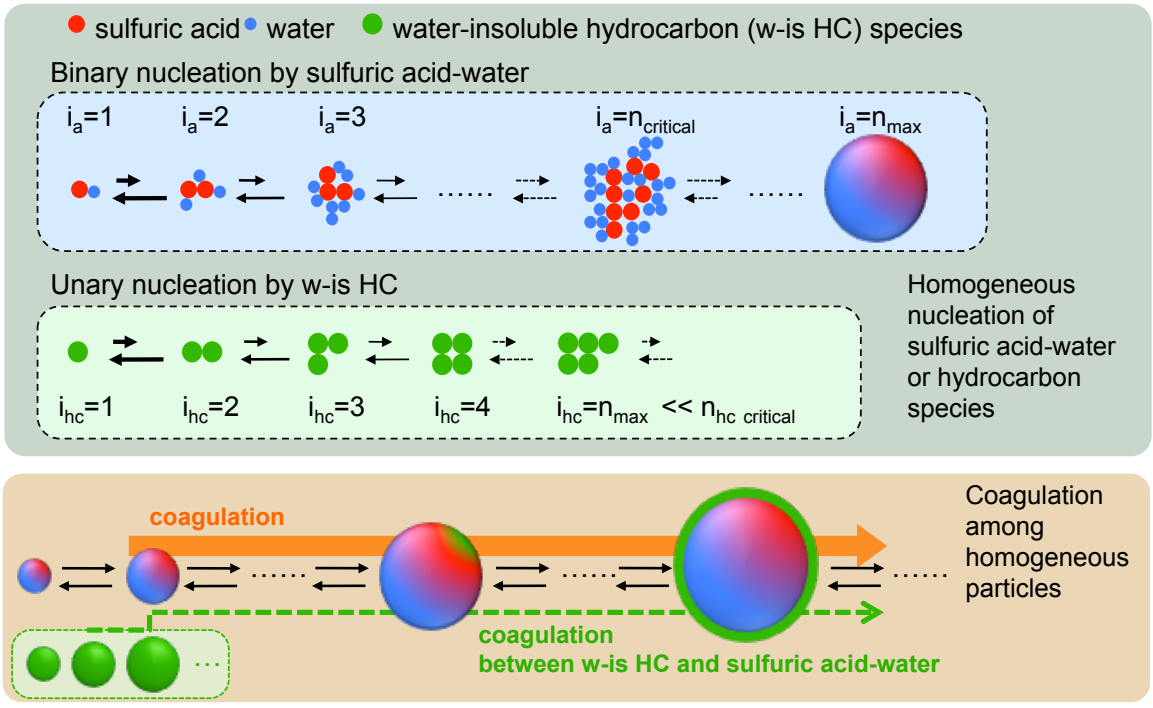

Figure 4-15: Simplified pathways for the new particle formation in aircraft emissions

of water-soluble hydrocarbons is negligible in nucleation and coagulation processes, water-insoluble hydrocarbons significantly contribute to the size growth of liquid particles. Competition between nucleation and soot modes is discussed and compared with the competition between hydrophobic and hydrophilic species discussed in the previous chapter. In summary, the contribution of hydrocarbons is important for the growth of particles in both nucleation and soot modes through condensation and coagulation of water-insoluble hydrocarbons and competitions induced by both types of hydrocarbons.

Chapter 5

Parametric Study

Chapter 3 provided parametric sensitivity studies of the soot particle growth without considering nucleation and Chapter 4 discussed the effect of relative humidity on both the nucleation mode and the soot mode in the presence of hydrocarbons. The previous chapters also identified important modeling parameters and discussed the role of hydrocarbons in the formation of aerosols in near-field aircraft emissions. This chapter discusses the sensitivity of the evolution of hydrocarbon-containing aerosols, both homogeneous particles and soot particles, by exploring parameter spaces of key factors. The focus of this chapter is on understanding competition between hydrocarbons and sulfuric acid, hydrophilic and hydrophobic effects, and nucleation and soot modes. Section 5.1 presents the effect of ambient conditions on the aerosol formation, Section 5.2 discusses the effect of hydrocarbon properties under different levels of ambient conditions, and Section 5.3 presents the effect of hydrocarbon concentrations to the evolution of mass distribution between nucleation and soot modes. Note that the analysis in this chapter presents simulation results at 1 km downstream with the baseline values described in Section 3.2.4 if no description is specified; for example, 100 ppb initial concentrations and 0.01 for the dry accommodation coefficients and 1 for the wet accommodation coefficients of both types of hydrocarbons.

5.1 Effect of Ambient Relative Humidity and Temperature

Figure 5-1 presents the mass budget of individual species in nucleation mode and soot mode at 1 km downstream under different levels of ambient conditions for near-field aircraft emissions. The nucleation mode is very sensitive to the ambient temperature and relative humidity. The low temperature and high relative humidity condition (toward the upper left corner) is required to exceed the critical sulfuric acid concentration in gas phase to trigger the critical $H_2SO_4-H_2O$ nucleation rate [4]. Consequently, there is the nucleation threshold as a function of ambient temperature and relative humidity, as shown in Figure 5-1. The soot mode is dominant at the higher ambient temperature and/or low ambient relative humidity conditions; above the threshold, however, the contribution of the soot mode decreases by competing with the nucleation mode for limited sulfate mass. The nucleation mode of hydrocarbons is also sensitive to the ambient conditions. Water-insoluble hydrocarbons contribute to the nucleation mode through coagulation with and/or condensation on the existing $H_2SO_4-H_2O$ nuclei, and thus they are sensitive to the nuclei population.

Figure 5-2 shows the sulfate mass distribution between nucleation mode and soot mode for the binary $H_2SO_4-H_2O$ aerosols under the identical simulation conditions except the presence of hydrocarbons. Overall, both results in Figure 5-1 and Figure 5-2 show a similar dependence to the ambient conditions, where nucleation is active at the low ambient temperature and high relative humidity conditions above the nucleation threshold, and condensation on soot is dominant at the high temperature and high relative humidity conditions. Incorporating hydrocarbons, however, enhanced the mass transfer of sulfate to soot coatings by increasing the hydrophilic soot surface activation by adsorption of water-soluble hydrocarbons and in turn, the contribution of soot mode became less sensitive to the ambient conditions.

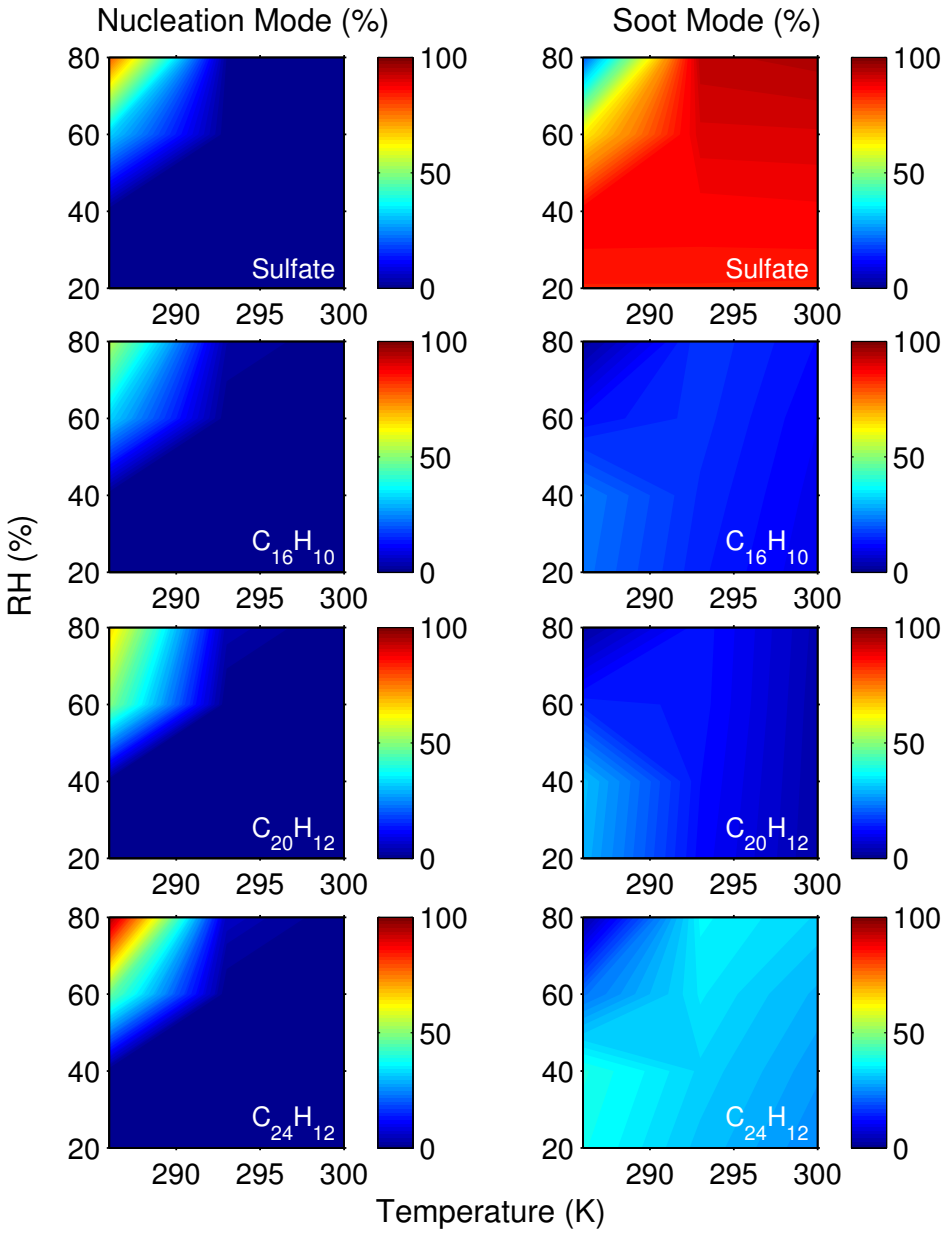

Figure 5-1: Mass distribution of sulfate and water-insoluble hydrocarbons between nucleation mode and soot mode as a function of ambient temperature and RH

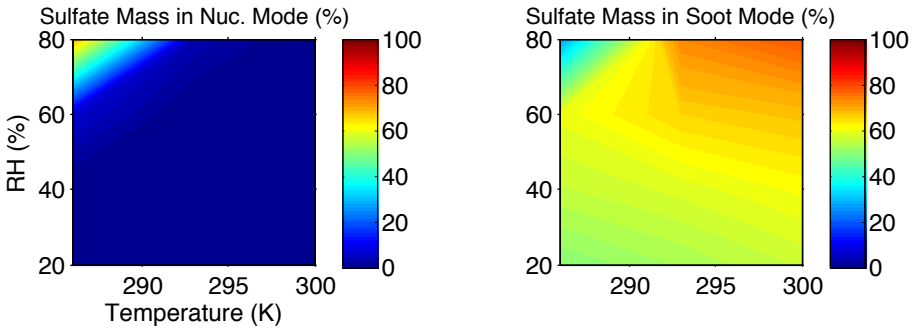

Figure 5-2: Mass distribution of sulfate in nucleation mode and soot mode for the binary $H_2SO_4-H_2O$ system

5.2 Effect of Accommodation Coefficients

Figure 5-3 and Figure 5-4 show mass distribution between nucleation and soot modes of condensable species as a function of the dry accommodation coefficients of hydrocarbons under the ambient temperature levels, 286K and 293K, and 60% ambient RH, where nucleation and soot modes would have comparable contributions. Increasing dry accommodation coefficient of water-soluble hydrocarbons enhanced the uptake of sulfate mass on soot particles while limiting $H_2SO_4-H_2O$ nucleation. However, it is not apparent that dry accommodation coefficients of hydrocarbons affect $H_2SO_4-H_2O$ nucleation directly. Increasing dry accommodation coefficient of water-insoluble hydrocarbon enhanced the uptake of water-insoluble hydrocarbons on soot particles as discussed in Section 3.2.4.

5.3 Effect of hydrocarbon concentrations

This section discusses the effect of hydrocarbon concentrations by varying their initial gaseous concentration at 80% ambient relative humidity and 286 K ambient temperature. Increasing the concentration of water-insoluble hydrocarbons and decreasing that of water-soluble hydrocarbons (toward the upper left corner) contributed to increasing sulfate mass in nucleation mode while decreasing that in soot mode, as shown in Figure 5-5. Increasing the concentration of water-soluble hydrocarbon enhanced the condensation of sulfuric acid by increasing the hydrophilic soot surface fraction

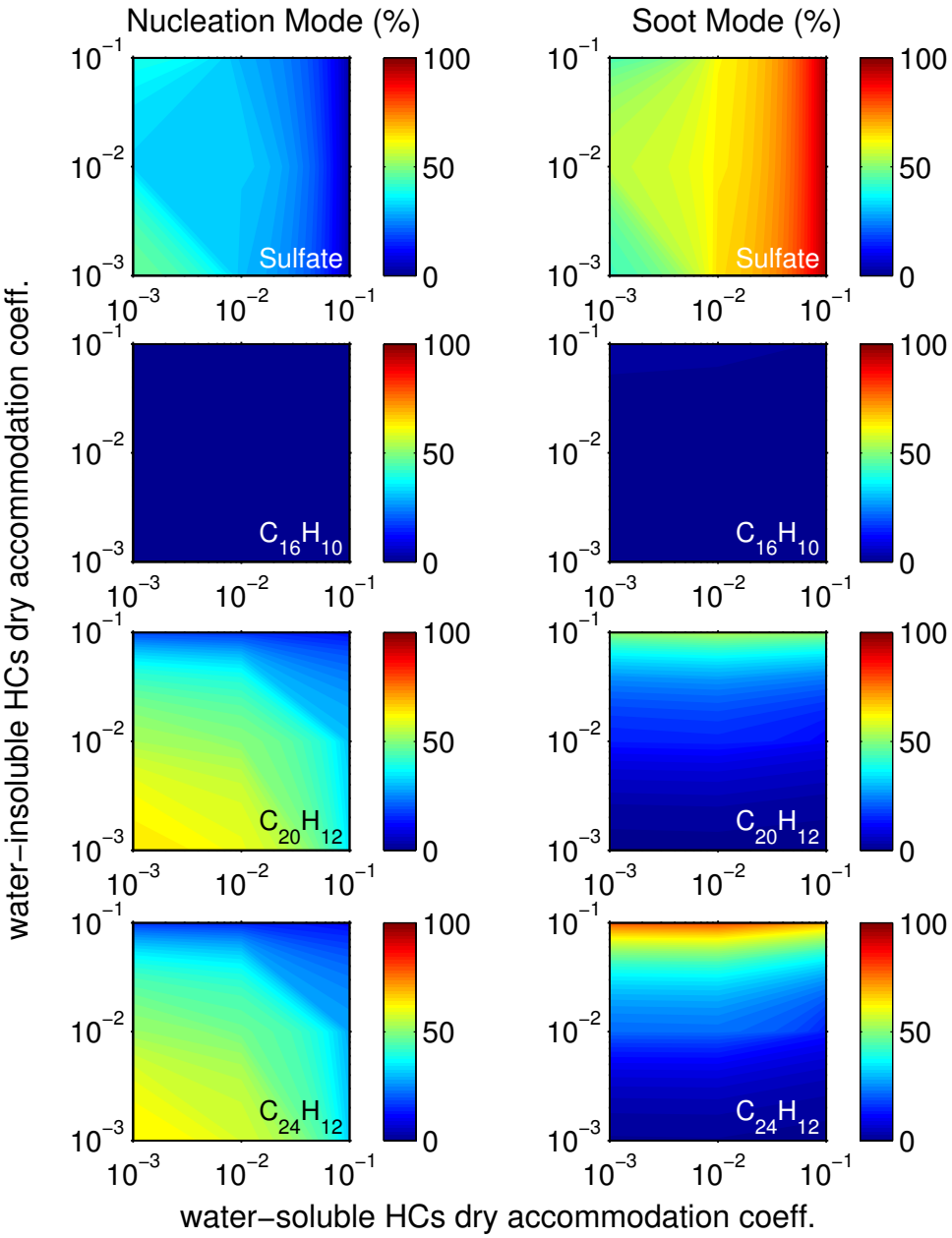

Figure 5-3: Mass distribution of sulfate and water-insoluble hydrocarbons between nucleation mode and soot mode at 286 K and RH=60%, as a function of dry accommodation coefficients of water-soluble hydrocarbons (shown in x-axis) and water-insoluble hydrocarbons (shown in y-axis)

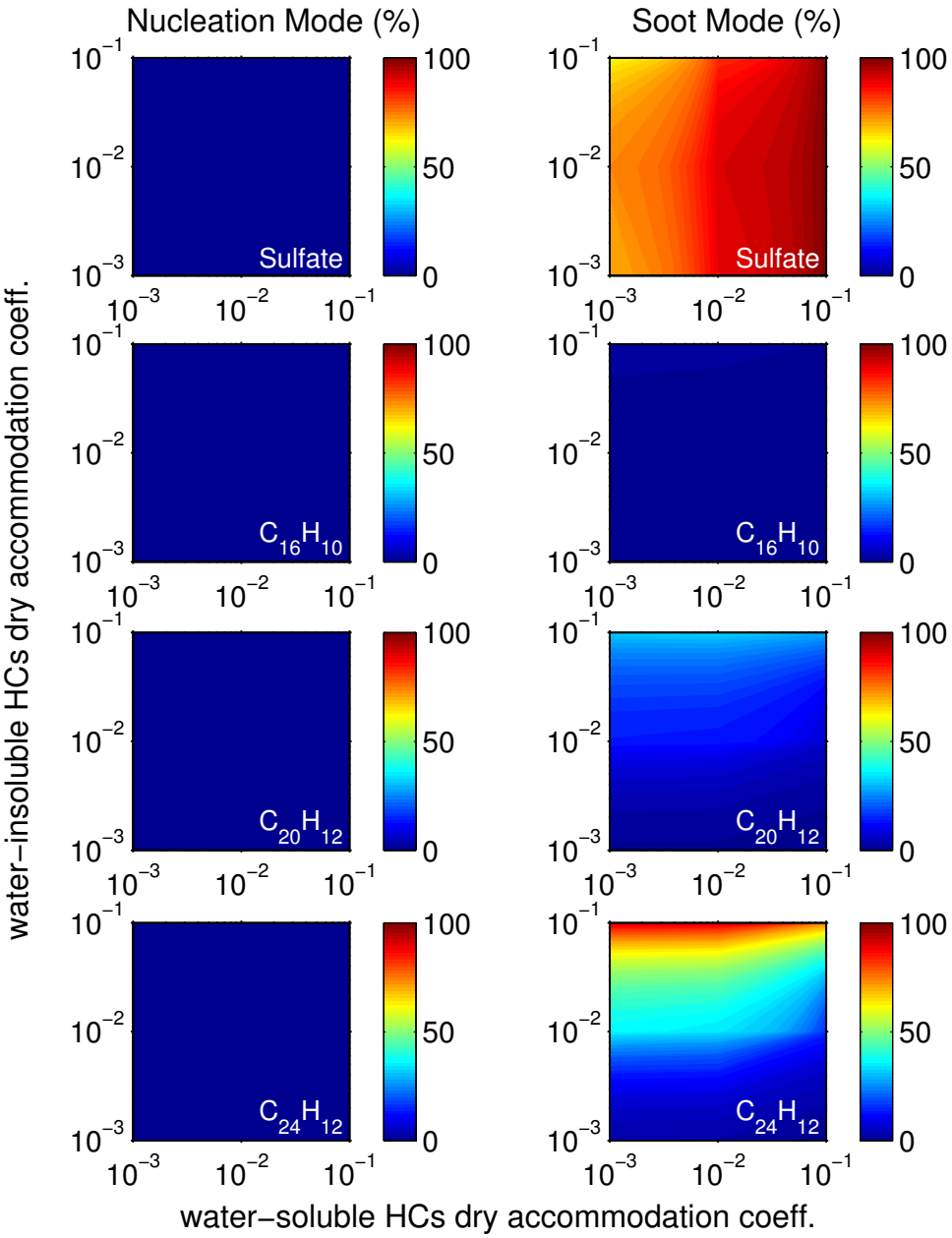

Figure 5-4: Mass distribution of sulfate and water-insoluble hydrocarbons between nucleation mode and soot mode at 293K and RH=60%, as a function of dry accommodation coefficients of water-soluble hydrocarbons (shown in x-axis) and water-insoluble hydrocarbons (shown in y-axis)

even under the high concentration levels of water-insoluble hydrocarbons. This suggests that soot surface activation by water-soluble hydrocarbons is important in the evolution of aerosols especially under the conditions undergoing competition between nucleation and soot modes.

It is interesting to note that the contribution of water-insoluble hydrocarbons to the nucleation mode is maximum around 100 ppb initial concentrations of water-insoluble hydrocarbons, suggesting that competition between soot and nucleation modes occurs. Water-insoluble hydrocarbons tended to condense on soot particles easily because of enhanced hydrophobic coatings on soot particles as the concentration of water-insoluble hydrocarbons increases. On the other hand, mass transfer of water-insoluble hydrocarbons to both nucleation and soot modes decreased by decreasing the gaseous concentration as a result of reduced partial pressures of hydrocarbons.

5.4 Summary

This chapter discusses the effect of ambient conditions at ground level, and dry accommodation coefficients and initial concentrations of hydrocarbons to the evolution of aerosols in nucleation and soot modes. Simulation results show that nucleation of sulfuric acid and water is sensitive to ambient temperature and relative humidity levels. The mass budget of water-insoluble hydrocarbons in the nucleation mode is also sensitive to the ambient conditions because their major pathways to the nucleation mode are coagulation with and/or condensation on the existing liquid aerosols.

The dry accommodation coefficients and initial concentrations of hydrocarbons induce competition between homogeneous droplets and soot coatings for sulfate mass while directly affecting to the uptake of water-insoluble hydrocarbons on soot particles. Although water-soluble hydrocarbon mass is negligible in both nucleation and soot modes, their contribution is important to the evolution of aerosols by inducing competition between hydrophilic and hydrophobic species and consequently competition between nucleation and soot modes for sulfuric acid.

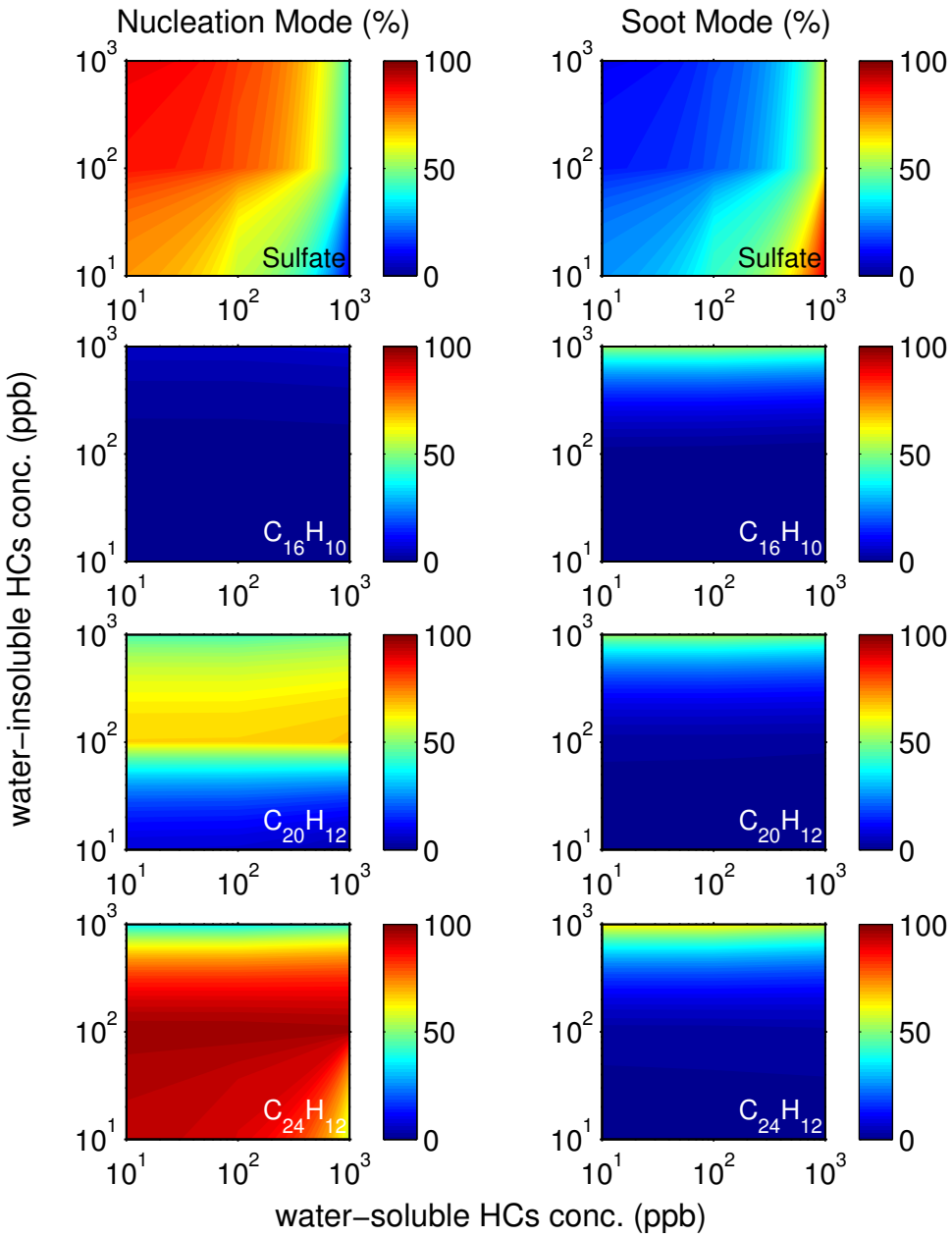

Figure 5-5: Mass distribution of sulfate and water-insoluble hydrocarbons between nucleation mode and soot mode at 286K and RH=80%, as a function of initial concentrations of water-soluble hydrocarbons (shown in x-axis) and water-insoluble hydrocarbons (shown in y-axis)

Chapter 6

Conclusions and Future Work

6.1 Summary and Conclusion

A one-dimensional kinetic microphysical model has been developed to study the formation of new particles and evolution of aircraft emitted aerosols. This thesis also explored the sensitivity of aerosol evolution to modeling parameters and ambient conditions. Incorporating hydrocarbon species into the binary sulfuric acid and water model started with modeling of hydrocarbon surrogates first. According to their solubility in water, hydrocarbons can be categorized in the microphysical processes as *water-soluble* or *water-insoluble* hydrocarbons. Water-soluble hydrocarbons were allowed to mix with sulfuric acid and water solutions, while water-insoluble hydrocarbons were assumed to exist a separate phase from aqueous solutions. General thermodynamic properties were estimated for pure substances first and then calculated for aqueous solutions or non-aqueous hydrocarbon mixture based on the mixing rule. For some properties requiring compound specific parameters or interactions, such as activity coefficient or saturation vapor pressure, this thesis used group contribution methods to employ a wide variety of hydrocarbon compounds in the simulations. Selected hydrocarbon surrogates in aircraft emissions include three water-soluble hydrocarbon oxygenates (C_3H_6O, $C_3H_6O_2$, $C_4H_8O_2$) and three water-insoluble hydrocarbons ($C_{16}H_{10}$, $C_{20}H_{12}$, $C_{24}H_{12}$), which cover a wide saturation vapor pressure region encompassing saturation vapor pressure of water and sulfuric acid. Based on

field measurements, the total concentration of hydrocarbon species was assumed to be 200 ppb in initial exhaust. Each hydrocarbon species then has comparable initial concentration with sulfuric acid precursors.

Microphysical processes incorporating hydrocarbon species into a binary sulfuric acid and water model have been explored with respect to the interactions with solid soot particles and with $H_2SO_4-H_2O$ liquid particles in Chapter 3 and Chapter 4 respectively. Soot particles emitted from aircraft engines are very hydrophobic initially but a substantial amount of water-soluble species has been observed far downstream locations in measured soot samples. This suggests that hydrophobic soot particles can turn to hydrophilic by undergoing microphysical processes. Solid soot surfaces can be activated by adsorption from collisions between gaseous molecules and soot particles, and in turn mass transfer from gas phase to liquid phase is allowed on the liquid activation layers. Condensation can contribute to surface activation as well. While water-insoluble hydrocarbons cover soot surface with hydrophobic films, adsorption of sulfuric acid or water-soluble hydrocarbons activate the hydrophobic soot surface to be hydrophilic. Interaction between water molecules and dry soot surfaces is not favorable, but water vapor can condense on the hydrophilic surfaces after activation. Sulfuric acid and low volatile water-insoluble hydrocarbons can condense on hydrophilic and hydrophobic soot coating respectively; however, volatile water-soluble hydrocarbons remain in vapor phase mostly.

Studies of potential nucleation pathways indicate that a major contributor to new particle formation is binary $H_2SO_4-H_2O$ nucleation regardless of involvement of hydrocarbons. Unary nucleation of water-insoluble hydrocarbons is not a favorable pathway to grow hydrocarbon clusters to bigger liquid particles. Nucleation pathways for water-soluble hydrocarbons were examined by considering interactions with water and/or sulfuric acid. All tested modeling approaches agreed that nucleation of water-soluble hydrocarbons is not a major pathway to contribute to the aerosol number density, similar to what was found for water-insoluble hydrocarbons. Clusters formed via nucleation can grow to nano-size particles via coagulation with other aqueous clusters or sub-critical hydrocarbon clusters. The hybrid bin approach was

employed in the modified coagulation model for multi-component aerosols having a hydrophobic hydrocarbon film and an aqueous core. The new particle formation from gaseous molecules to liquid particles was explored through the analysis of several possible pathways represented with involved interactions. While interactions related to water-soluble hydrocarbon are negligible in both nucleation and coagulation processes, interactions between water-insoluble hydrocarbon clusters and $H_2SO_4-H_2O$ clusters/droplets contribute the particle growth substantially.

Focusing on understanding the initial formation process of aircraft aerosols and the role of hydrocarbon compounds, a set of simulations with the developed kinetic microphysical model was conducted to 1 km downstream along plume centerline assuming organic-rich, near-field aircraft emissions at a low operating power setting. The simulation results demonstrate that low volatile hydrocarbons play an important role in the formation of aviation aerosols with interactions with both $H_2SO_4-H_2O$ aerosols and soot particles. Water-insoluble hydrocarbons contribute to the growth of aerosols while inducing competition with the uptake of water-soluble species. Light and volatile water-soluble hydrocarbons contribute to the uptake of water and sulfuric acid indirectly by increasing hydrophilic soot surface coverage. For both homogeneous liquid particles and solid soot particles, smaller particles tend to contain more hydrophobic organic fractions. Understanding of hydrocarbon interactions with the aerosols formation in aircraft emissions is important to estimate properties of aerosols, especially in small size.

Parametric studies provide a comprehensive evaluation of the sensitivity of the aerosol evolution to ambient conditions and modeling parameters including initial exhaust properties, properties of organic compounds, and properties of the soot surface. The size of soot particles is also an important factor to determine the particle growth and composition. Competition between hydrophilic and hydrophobic species is closely related to the contributions of some modeling parameters on the particle growth depending on the size of soot particles. Parameters directly affecting condensation of water-insoluble hydrocarbons have a strong effect on the soot particle growth regardless of the particle size. Soot particle growth is most sensitive to the

initial concentrations and dry accommodation coefficients of hydrocarbons while nucleation of homogeneous aerosols is sensitive to the ambient conditions. Competition between microphysical modes is also important to the evolution of aircraft emitted volatile particles in addition to competition between species. This thesis work concludes that both water-insoluble and water-soluble hydrocarbons contribute to the growth of homogenous liquid particles and soot particles under the near-field aircraft plume conditions of our interest.

6.2 Future Work

Further extension of the aerosol model in this work could be explored in future work.

One important area of future research would be to diversify the hydrocarbon surrogates to more realistically represent engine exhaust extending to other hydrocarbon species in aircraft emissions such as alkane and fatty acid compounds [29] as well as modeling surrogates of different types of fuels [71, 72]. Measurement results suggest the presence of lubricating oil from aircraft engines, and low volatile lubricating oil fragments composed with saturated long-chained hydrocarbons can contribute to the PM emissions [73]. Future work would involve incorporating lubricating oil as vapor or droplets to the current system with gaseous species and solid particles. Lubricating oil drops would change soot surface properties as well as serving as nuclei for hydrocarbon nucleation.

Considering the negative effect of hydrophobic films of hydrocarbons on the hygroscopic growth of $H_2SO_4-H_2O$ aerosols would be desirable since organic films may change the chemical and physical properties of aerosols. Several observations discussed that organic films can retard water condensation or evaporation while enhancing uptake of PAHs [74, 75]. Modeling the impeded water uptake of aqueous nuclei cores due to organic films will be helpful to understand aging of aerosols expected to have thick hydrophobic films. Some properties of organic films, such as thickness or molecular structure of organic compounds, are closely related to the retardation effect [68]. Also, another aspect of future work is to investigate soot aggregate in the

presence of thick liquid coating.

While the model developed in this thesis focused on the aerosol formation above the freezing point assuming near-field emission conditions, it is an interesting research area to study the evolution of aircraft emission undergoing ice nucleation as forming contrails. Future modeling work could extend the model to incorporate hydrocarbon species into the ice nucleation model. Understanding the role of hydrocarbons in ice nucleation will provide a better understanding of contrail formation.

Validating highly sensitive parameters such as accommodation coefficients with measurement data will be required also. Parametric studies in this thesis suggest that some hydrocarbon properties need to be assessed more accurately to eliminate large uncertainty. Dry or wet accommodation coefficients may need to be measured separately by controlling gaseous concentrations and the soot particle size. It will require designing the experimental conditions carefully to control competition between homogenous liquid aerosols and soot coatings. Model predictions with refined parameters from laboratory measurements will help to understand the parametric relationship between hydrocarbon properties, exhaust properties, ambient conditions, and aerosol composition and provide a better initial guess for organic fractions and particle distribution of aerosols along aircraft plume.

Appendix A

Activation of Curved Surfaces by Condensation

This section describes relationship between the rate of change of condensation mass and the rate of change of surface coverage (Θ). Figure A-1 shows an illustration of a liquid drop on the partially wettable solid surface. Surface area covered by a spherical cap shaped droplet can be expressed with corresponding geometric variable shown in Figure A-1 as:

$$\Theta = \frac{\Omega}{4\pi} = \frac{1 - \cos\theta_{act}}{2} \tag{A.1}$$

where Ω is the solid angle of a cone with apex $2\theta_{act}$.

Volume of the liquid drop (marked as blue color) can be calculated from the difference between the volume of the spherical cap with radius R_d (V_{A+B}, blue+orange) and the volume of the spherical cap with radius R_s (V_B, orange):

$$\begin{aligned} V =& V_{A+B} - V_B \\ =& \frac{\pi}{3}\left[R_d\left(1+\cos\theta_{cntr}\right)\right]^2\left[3R_d - R_d\left(1+\cos\theta_{cntr}\right)\right] \\ & - \frac{\pi}{3}\left[R_s\left(1-\cos\theta_{act}\right)\right]^2\left[3R_s - R_s\left(1-\cos\theta_{act}\right)\right] \\ =& \frac{\pi}{3}R_d^3\left(1+\cos\theta_{cntr}\right)^2\left(2-\cos\theta_{cntr}\right) - \frac{4\pi}{3}R_s^3\Theta^2\left(3-2\Theta\right) \end{aligned} \tag{A.2}$$

where R_d is the radius of the liquid drop, R_s is the radius of solid particle, and θ_{cntr}

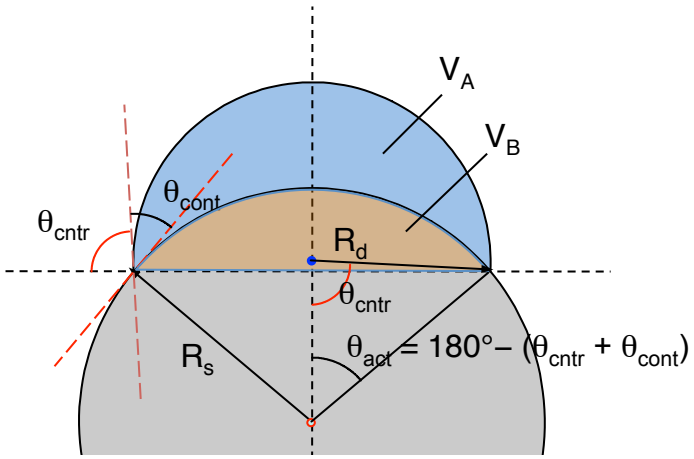

Figure A-1: Geometry for surface wetting

is the angle at the center of the droplet for the half arc corresponding to the opposite spherical sector of the droplet, θ_{act} is the angle at the center of the particle for the half arc corresponding to the spherical sector covered by the droplet.

Differentiating Equation (A.2) with respect to time,

$$\begin{aligned}\frac{dV}{dt} =& \frac{\pi}{3}\left[3R_d^2\frac{dR_d}{dt}\left(1+\cos\theta_{cntr}\right)^2\left(2-\cos\theta_{cntr}\right)\right.\\ &+2R_d^3\left(1+\cos\theta_{cntr}\right)\left(-\sin\theta_{cntr}\right)\frac{d\theta_{cntr}}{dt}\left(2-\cos\theta_{cntr}\right)\\ &\left.+R_d^3\left(1+\cos\theta_{cntr}\right)^2\sin\theta_{cntr}\frac{d\theta_{cntr}}{dt}\right]-\frac{\pi}{3}R_s^3\left[8\Theta\left(3-2\Theta\right)-8\Theta^2\right]\frac{d\Theta}{dt}\end{aligned} \tag{A.3}$$

With a constant contact angle, θ_{act}, θ_{cntr}, R_d, and their derivatives can be expressed in terms of θ_{cont}, Θ:

$$\begin{aligned}\cos\theta_{act} &= 1-2\Theta\\ \frac{d\theta_{act}}{dt} &= \frac{2}{\sin\theta_{act}}\frac{d\Theta}{dt}\end{aligned} \tag{A.4}$$

$$\begin{aligned}\theta_{cntr} &= \pi-\theta_{act}-\theta_{cont}\\ \frac{d\theta_{cntr}}{dt} &= -\frac{d\theta_{act}}{dt} = -\frac{2}{\sin\theta_{act}}\frac{d\Theta}{dt}\end{aligned} \tag{A.5}$$

$$
\begin{aligned}
R_d &= \frac{R_s \sin\theta_{act}}{\sin\theta_{cntr}} \\
\frac{dR_d}{dt} &= 2R_s \frac{\sin\theta_{cont}}{\sin\theta_{act}\sin^2\theta_{cntr}} \frac{d\Theta}{dt}
\end{aligned}
\tag{A.6}
$$

Rearranged Equation (A.3) gives a relationship between the rate of change of liquid droplet volume and the rate of change of surface coverage in terms of R_s, Θ, and θ_{cont}:

$$
\begin{aligned}
\frac{dV}{dt} =& \frac{\pi}{3}\left[6R_s^3 \frac{\sin\theta_{act}\sin\theta_{cont}}{\sin^4\theta_{cntr}}\left(1+\cos\theta_{cntr}\right)^2\left(2-\cos\theta_{cntr}\right)\right. \\
&\left. +4R_s^3 \frac{\sin^2\theta_{act}}{\sin^2_{cntr}}\left(1+\cos\theta_{cntr}\right)\left(2-\cos\theta_{cntr}\right) - 2R_s^3 \frac{\sin^2\theta_{act}}{\sin^2\theta_{cntr}}\left(1+\cos\theta_{cntr}\right)^2\right]\frac{d\Theta}{dt} \\
&- \frac{24}{3}\pi R_s^3\left(\Theta-\Theta^2\right)\frac{d\Theta}{dt} \\
=& f\left(R_s,\Theta,\theta_{cont}\right)\frac{d\Theta}{dt}
\end{aligned}
\tag{A.7}
$$

Finally, the rate of change of surface coverage by the rate of change of condensational mass can be given as:

$$
\frac{d\Theta}{dt} = \frac{1}{f\left(R_s,\Theta,\theta_{cont}\right)}\frac{dV}{dt} = \frac{1}{f\left(R_s,\Theta,\theta_{cont}\right)}\frac{1}{\rho}\frac{dm}{dt} \tag{A.8}
$$

$$
\left.\frac{d\Theta}{dt}\right|_{cond} = F\left(R_s,\Theta,\theta_{cont},\rho\right)\left.\frac{dm}{dt}\right|_{cond} \tag{A.9}
$$

Appendix B

Summary for the Role of Hydrocarbons in the Evolution of Aircraft Aerosols

This section provides a summary of key points for the role of hydrocarbons in the initial formation of aircraft emitted aerosols.

In soot microphysics,

- Hydrophobic soot surfaces need to be activated as hydrophilic for condensation of water-soluble species, where sulfuric acid and water-soluble organics can increase the hydrophilic fraction of soot surfaces.
- Hydrophobic soot surfaces need to be activated as hydrophobic for condensation of water-insoluble species by water-insoluble organics.
- Condensation contributes to the particle growth and increases the surface coverage as well.
- Small particles reach surface saturation faster and grow faster because of enhanced surface activation by condensation.
- Small soot particles are more hydrophobic because condensation of water-insoluble hydrocarbons increases the hydrophobic surface fraction while limiting hydrophilic

surface activation.

- In the soot coatings, water-soluble hydrocarbons appear in the young plume where the adsorption process is dominating and activate the soot surface as hydrophilic. Water-insoluble hydrocarbons contribute to the soot particle growth by both condensation and hydrophobic activation of the soot surface.

For the new particle formation,

- $H_2SO_4-H_2O$ nucleation determines the formation of homogeneous liquid particles, while hydrocarbon nucleation is not a favorable pathway to form larger homogeneous particles.

- Coagulation between water-insoluble hydrocarbons and $H_2SO_4-H_2O$ droplets is important to the homogeneous particle growth, while both nucleation and coagulation of water-soluble hydrocarbon are insignificant.

- For homogeneous particles, smaller liquid particles tend to be more organic-rich and hydrophobic.

In summary,

- Low volatility water-insoluble hydrocarbons contribute to the particle growth by condensation on both soot particles and liquid aerosols while inducing competition with water-soluble species.

- Light volatile water-soluble hydrocarbons remain in the vapor phase mostly, but they contribute to the enhanced uptake of water and sulfuric acid on soot particles by increasing hydrophilic surface activation.

Bibliography

[1] H. Vehkamäki, M. Kulmala, K. Lehtinen, and M. Noppel, "Modelling binary homogeneous nucleation of water-sulfuric acid vapours: parameterisation for high temperature emissions," *Environmental Science & Technology*, vol. 37, no. 15, pp. 3392–3398, 2003.

[2] B. E. Poling, J. M. Prausnitz, and J. P. O'Connell, "The properties of gases and liquids," *McGraw-Hill*, Jan 2000.

[3] I. Waitz, J. Townsend, J. Cutcher-Gershenfeld, E. Greitzer, and J. Kerrebrock, "Aviation and the environment," *Report to the United States Congress*, Dec 2004.

[4] J. H. Seinfeld and S. N. Pandis, "Atmospheric chemistry and physics: From air pollution to climate change," *John Wiley & Sons, New York*, Jan 2006.

[5] P. Buseck and K. Adachi, "Nanoparticles in the atmosphere," *Elements*, vol. 4, no. 6, pp. 389–394, 2008.

[6] W. Chameides and M. Bergin, "Soot takes center stage," *Science*, vol. 297, pp. 2214–2215, Jan 2002.

[7] R. Sausen, I. Isaksen, V. Grewe, D. Hauglustaine, D. S. Lee, G. Myhre, M. O. Kohler, G. Pitari, U. Schumann, F. Stordal, and C. Zerefos, "Aviation radiative forcing in 2000: An update on ipcc (1999)," *Meteorologische Zeitschrift*, vol. 14, pp. 555–561, Jan 2005.

[8] J. Schwarz, J. Spackman, D. Fahey, R. Gao, U. Lohmann, P. Stier, L. Watts, D. S. Thomson, D. Lack, L. Pfister, M. J. Mahoney, D. Baumgardner, J. C. Wilson, and J. M. Reeves, "Coatings and their enhancement of black carbon light absorption in the tropical atmosphere," *Journal of Geophysical Research*, vol. 113, Jan 2008.

[9] M. Kanakidou, J. H. Seinfeld, S. Pandis, I. Barnes, F. J. Dentener, M. C. Facchini, R. V. Dingenen, B. Ervens, A. Nenes, C. J. Nielsen, E. Swietlicki, J. P. Putaud, Y. Balkanski, S. Fuzzi, J. Horth, G. K. Moortgat, R. Winterhalter, C. E. L. Myhre, K. T. E. Vignati, E. G. Stephanou, and J. Wilson, "Organic aerosol and global climate modelling: a review," *Atmospheric Chemistry and Physics*, vol. 5, no. 4, pp. 1053–1123, 2005.

[10] A. Seaton, D. Godden, W. MacNee, and K. Donaldson, "Particulate air pollution and acute health effects," *The Lancet*, vol. 345, pp. 176–178, Jan 1995.

[11] C. A. Pope and D. Dockery, "Health effects of fine particulate air pollution: lines that connect," *Journal of the Air & Waste Manage. Assoc.*, vol. 56, pp. 709–742, Jan 2006.

[12] G. Oberdörster, E. Oberdörster, and J. Oberdörster, "Nanotoxicology: an emerging discipline evolving from studies of ultrafine particles," *Environmental Health Perspectives*, vol. 113, no. 7, p. 823, 2005.

[13] J. Lighty, J. Veranth, and A. Sarofim, "Combustion aerosols: factors governing their size and composition and implications to human health," *Journal of the Air & Waste Management Association*, vol. 50, no. 9, pp. 1565–1618, 2000.

[14] B. Kärcher and F. Yu, "Role of aircraft soot emissions in contrail formation," *Geophys. Res. Lett*, vol. 36, Jan 2009.

[15] H.-W. Wong and R. Miake-Lye, "Parametric studies of contrail ice particle formation in jet regime using microphysical parcel modeling," *Atmospheric Chemistry and Physics*, vol. 10, pp. 3261–3272, 2010.

[16] B. Koo, A. Ansari, and S. Pandis, "Integrated approaches to modeling the organic and inorganic atmospheric aerosol components," *Atmospheric Environment*, vol. 37, pp. 4757–4768, Jan 2003.

[17] Y. Ming and L. Russell, "Organic aerosol effects on fog droplet spectra," *J. Geophys. Res*, vol. 109, Jan 2004.

[18] D. Topping, G. McFiggans, and H. Coe, "A curved multi-component aerosol hygroscopicity model framework: Part 2–including organic compounds," *Atmospheric Chemistry and Physics*, vol. 5, pp. 1223–1242, Jan 2005.

[19] K. Adachi and P. Buseck, "Internally mixed soot, sulfates, and organic matter in aerosol particles from mexico city," *Atmospheric Chemistry and Physics*, vol. 8, pp. 6469–6481, Jan 2008.

[20] A. Petzold, M. Gysel, X. Vancassel, R. Hitzenberger, H. Puxbaum, S. Vrochticky, E. Weingartner, U. Baltensperger, and P. Mirabel, "On the effects of organic matter and sulphur-containing compounds on the ccn activation of combustion particles," *Atmospheric Chemistry and Physics*, vol. 5, pp. 3187–3203, Jan 2005.

[21] B. Svenningsson, J. Rissler, E. Swietlicki, M. Mircea, M. Bilde, M. Facchini, S. Decesari, S. Fuzzi, J. Zhou, J. Monster, and T. Rosenorn, "Hygroscopic growth and critical supersaturations for mixed aerosol particles of inorganic and organic compounds of atmospheric relevance," *Atmospheric Chemistry and Physics*, vol. 6, pp. 1937–1952, Jan 2006.

[22] H. Du and F. Yu, "Nanoparticle formation in the exhaust of vehicles running on ultra-low sulfur fuel," *Atmospheric Chemistry and Physics*, vol. 8, pp. 4729–4739, Jan 2008.

[23] J. Odum, T. Jungkamp, R. Griffin, H. Forstner, R. Flagan, and J. Seinfeld, "Aromatics, reformulated gasoline, and atmospheric organic aerosol formation," *Environ Sci Technol*, vol. 31, pp. 1890–1897, Jan 1997.

[24] M. Kulmala, V. Kerminen, T. Anttila, A. Laaksonen, and C. D. O'Dowd, "Organic aerosol formation via sulphate cluster activation," *J. Geophys. Res*, vol. 109, Jan 2004.

[25] M. Jacobson, "Analysis of aerosol interactions with numerical techniques for solving coagulation, nucleation, condensation, dissolution, and reversible chemistry among multiple size distributions," *Journal of Geophysical Research-Atmospheres*, vol. 107, p. 4366, Jan 2002.

[26] B. J. Turpin, P. Saxena, and E. Andrews, "Measuring and simulating particulate organics in the atmosphere: problems and prospects," *Atmospheric Environment*, vol. 34, pp. 2983–3013, 2000.

[27] H.-W. Wong, P. E. Yelvington, M. T. Timko, T. B. Onasch, R. C. Miake-Lye, J. Zhang, and I. A. Waitz, "Microphysical modeling of ground-level aircraft-emitted aerosol formation: Roles of sulfur-containing species," *Journal of Propulsion and Power*, vol. 24, pp. 590–602, Jan 2008.

[28] P. E. Yelvington, S. C. Herndon, J. C. Wormhoudt, J. T. Jayne, R. C. Miake-Lye, W. B. Knighton, and C. Wey, "Chemical speciation of hydrocarbon emissions from a commercial aircraft engine," *Journal of Propulsion and Power*, vol. 23, pp. 912–918, Jan 2007.

[29] W. B. Knighton, T. M. Rogers, B. E. Anderson, S. C. Herndon, P. E. Yelvington, and R. C. Miake-Lye, "Quantification of aircraft engine hydrocarbon emissions using proton transfer reaction mass spectrometry," *Journal of Propulsion and Power*, vol. 23, pp. 949–958, Jan 2007.

[30] A. L. Robinson, N. M. Donahue, M. K. Shrivastava, E. A. Weitkamp, A. M. Sage, A. P. Grieshop, T. E. Lane, J. R. Pierce, and S. N. Pandis, "Rethinking organic aerosols: semivolatile emissions and photochemical aging," *Science*, vol. 315, pp. 1259–62, Mar 2007.

[31] N. Donahue, A. Robinson, C. Stanier, and S. Pandis, "Coupled partitioning, dilution, and chemical aging of semivolatile organics," *Environ Sci Technol*, vol. 40, pp. 02635–2643, Jan 2006.

[32] U.S.EPA, "Estimation programs interface suite™for microsoft®windows, v 4.00," *United States Environmental Protection Agency, Washington, DC, USA*, 2009.

[33] Y. Nannoolal, J. Rarey, and D. Ramjugernath, "Estimation of pure component properties part 1. estimation of the normal boiling point of non-electrolyte organic compounds via group contributions and group interactions," *Fluid Phase Equilibria*, vol. 226, pp. 45–63, Jan 2004.

[34] Y. Nannoolal, J. Rarey, and D. Ramjugernath, "Estimation of pure component properties part 2. estimation of critical property data by group contribution," *Fluid Phase Equilibria*, vol. 252, pp. 1–27, Jan 2007.

[35] S. Clegg and J. Seinfeld, "Thermodynamic models of aqueous solutions containing inorganic electrolytes and dicarboxylic acids at 298.15 k. 1. the acids as nondissociating components," *J. Phys. Chem. A*, vol. 110, pp. 5692–5717, Jan 2006.

[36] B. Larsen, P. Rasmussen, and A. Fredenslund, "A modified unifac group-contribution model for prediction of phase equilibria and heats of mixing," *Industrial & engineering chemistry research*, vol. 26, pp. 2274–2286, Jan 1987.

[37] D. Taleb, J. Ponche, and P. Mirabel, "Vapor pressures in the ternary system water-nitric acid-sulfuric acid at low temperature: A reexamination," *Journal of Geophysical Research-Atmospheres*, vol. 101, no. D20, pp. 25967–25977, 1996.

[38] T. Jensen, A. Fredenslund, and P. Rasmussen, "Pure-component vapor pressures using unifac group contribution," *Industrial & Engineering Chemistry Fundamentals*, vol. 20, pp. 239–246, Jan 1981.

[39] W. Asher and J. Pankow, "Vapor pressure prediction for alkenoic and aromatic organic compounds by a unifac-based group contribution method," *Atmospheric Environment*, vol. 40, pp. 3588–3600, Jan 2006.

[40] J. Pankow and W. Asher, "Simpol. 1: a simple group contribution method for predicting vapor pressures and enthalpies of vaporization of multifunctional organic compounds," *Atmospheric Chemistry and Physics*, vol. 8, pp. 2773–2796, Jan 2008.

[41] Y. Nannoolal, J. Rarey, and D. Ramjugernath, "Estimation of pure component properties part 3. estimation of the vapor pressure of non-electrolyte organic compounds via group contributions and group interactions," *Fluid Phase Equilibria*, vol. 269, pp. 117–133, Jan 2008.

[42] P. C. Hiemenz and R. Rajagopalan, "Principles of colloid and surface chemistry," *Marcel Dekker, Inc.*, Jan 1997.

[43] S. Brunauer, P. Emmett, and E. Teller, "Adsorption of gases in multimolecular layers," *J Am Chem Soc*, vol. 60, pp. 309–319, Jan 1938.

[44] T. HILL, "Theory of physical adsorption," *Advances in Catalysis and Related Subjects*, vol. 4, pp. 211–258, Jan 1952.

[45] H. Kohler, "The nucleus in and the growth of hygroscopic droplets," *T Faraday Soc*, vol. 32, pp. 1152–1161, Jan 1936.

[46] B. Henson, "An adsorption model of insoluble particle activation: Application to black carbon," *J. Geophys. Res*, vol. 112, Jan 2007.

[47] R. Sorjamaa and A. Laaksonen, "The effect of h2o adsorption on cloud drop activation of insoluble particles: a theoretical framework," *Atmospheric Chemistry and Physics*, vol. 7, pp. 6175–6180, Jan 2007.

[48] O. Popovicheva, N. Persiantseva, N. K. Shonija, P. DeMott, K. Koehler, M. Petters, S. Kreidenweis, V. Tishkova, B. Demirdjian, and J. Suzanne, "Water interaction with hydrophobic and hydrophilic soot particles," *Physical Chemistry Chemical Physics*, vol. 10, pp. 2332–2344, Jan 2008.

[49] B. Kärcher, "Physicochemistry of aircraft-generated liquid aerosols, soot, and ice particles 1. model description," *Journal of Geophysical Research-Atmospheres*, vol. 103, no. D14, pp. 17111–17128, 1998.

[50] N. Fuchs, *The mechanics of aerosols*. Pergamon Press, Oxford, 1964.

[51] N. Persiantseva, O. Popovicheva, and N. K. Shonija, "Wetting and hydration of insoluble soot particles in the upper troposphere," *Journal of Environmental Monitoring*, vol. 6, pp. 939–945, Jan 2004.

[52] B. Kärcher, T. Peter, and U. Biermann, "The initial composition of jet condensation trails," *Journal of the Atmospheric Sciences*, vol. 53, pp. 3066–3083, Jan 1996.

[53] M. JACOBSON, "Development and application of a new air pollution modeling system –ii. aerosol module structure and design," *Atmospheric Environment*, vol. 31, pp. 131–144, Jan 1997.

[54] B. Demirdjian, D. Ferry, J. Suzanne, O. Popovicheva, N. Persiantseva, and N. Shonija, "Heterogeneities in the microstructure and composition of aircraft engine combustor soot: impact on the water uptake," *Journal of Atmospheric Chemistry*, vol. 56, no. 1, pp. 83–103, 2007.

[55] M. Kulmala, L. Pirjola, and J. Mäkelä, "Stable sulphate clusters as a source of new atmospheric particles," *Nature*, vol. 404, no. 6773, pp. 66–69, 2000.

[56] F. Yu and R. Turco, "From molecular clusters to nanoparticles: Role of ambient ionization in tropospheric aerosol formation," *Journal of Geophysical Research*, vol. 106, pp. 4797–4814, 2001.

[57] R. Zhang, I. Suh, J. Zhao, D. Zhang, E. Fortner, X. Tie, L. Molina, and M. Molina, "Atmospheric new particle formation enhanced by organic acids," *Science*, vol. 304, no. 5676, p. 1487, 2004.

[58] F. Yu, "Quasi-unary homogeneous nucleation of H_2SO_4−H_2O," *The Journal of Chemical Physics*, vol. 122, p. 074501, 2005.

[59] F. Yu, "Improved quasi-unary nucleation model for binary H_2SO_4−H_2O homogeneous nucleation," *The Journal of Chemical Physics*, vol. 127, p. 054301, 2007.

[60] H. Du and F. Yu, "Kinetic modeling of nucleation experiments involving SO_2 and OH: new insights into the underlying nucleation mechanisms," *Atmospheric Chemistry and Physics*, vol. 9, pp. 7913–7922, 2009.

[61] B. Gorbunov, "From binary and ternary to multicomponent nucleation: Atmospheric aerosol formation," *The Journal of Chemical Physics*, vol. 115, p. 2641, 2001.

[62] T. Onasch, J. Jayne, S. Herndon, D. Worsnop, R. Miake-Lye, I. Mortimer, and B. Anderson, "Chemical properties of aircraft engine particulate exhaust emissions," *Journal of Propulsion and Power*, vol. 25, no. 5, pp. 1121–1137, 2009.

[63] M. Timko, T. Onasch, M. Northway, J. Jayne, M. Canagaratna, S. Herndon, E. Wood, R. Miake-Lye, and W. Knighton, "Gas turbine engine emissions—part ii: Chemical properties of particulate matter," *Journal of Engineering for Gas Turbines and Power*, vol. 132, p. 061505, 2010.

[64] G. Ellison, A. Tuck, and V. Vaida, "Atmospheric processing of organic aerosols," *Journal of Geophysical Research*, vol. 104, no. D9, pp. 11633–11641, 1999.

[65] J. Gilman, H. Tervahattu, and V. Vaida, "Interfacial properties of mixed films of long-chain organics at the air-water interface," *Atmospheric Environment*, vol. 40, no. 34, pp. 6606–6614, 2006.

[66] H. Tervahattu, J. Juhanoja, V. Vaida, A. Tuck, J. Niemi, K. Kupiainen, M. Kulmala, H. Vehkamäki, *et al.*, "Fatty acids on continental sulfate aerosol particles," *Journal of Geophysical Research*, vol. 110, 2005.

[67] P. Gill, T. Graedel, and C. Weschler, "Organic films on atmospheric aerosol particles, fog droplets, cloud droplets, raindrops, and snowflakes," *Reviews of Geophysics and Space Physics*, vol. 21, no. 4, pp. 903–920, 1983.

[68] J. Xiong, M. Zhong, C. Fang, L. Chen, and M. Lippmann, "Influence of organic films on the hygroscopicity of ultrafine sulfuric acid aerosol," *Environmental science & technology*, vol. 32, no. 22, pp. 3536–3541, 1998.

[69] R. Garland, M. Wise, M. Beaver, H. DeWitt, A. Aiken, J. Jimenez, and M. Tolbert, "Impact of palmitic acid coating on the water uptake and loss of ammonium sulfate particles," *Atmospheric Chemistry and Physics*, vol. 5, no. 7, pp. 1951–1961, 2005.

[70] M. Jacobson and R. Turco, "Simulating condensational growth, evaporation, and coagulation of aerosols using a combined moving and stationary size grid," *Aerosol science and technology*, vol. 22, no. 1, pp. 73–92, 1995.

[71] E. Corporan, M. J. DeWitt, V. Belovich, R. Pawlik, A. C. Lynch, J. R. Gord, and T. R. Meyer, "Emissions characteristics of a turbine engine and research combustor burning a fischer-tropsch jet fuel," *Energy & Fuels*, vol. 21, pp. 2615–2626, 2007.

[72] M. T. Timko, Z. Yu, T. B. Onasch, H.-W. Wong, R. C. Miake-Lye, A. J. Beyersdorf, B. E. Anderson, K. L. Thornhill, E. L. Winstead, E. Corporan, M. J. DeWitt, C. D. Klingshirn, C. Wey, K. Tacina, D. S. Liscinsky, R. Howard, and A. Bhargava, "Particulate emissions of gas turbine engine combustion of a fischer-tropsch synthetic fuel," *Energy & Fuels*, vol. 24, pp. 5883–5896, 2010.

[73] Z. Yu, D. S. Liscinsky, E. L. Winstead, B. S. True, M. T. Timko, A. Bhargava, S. C. Herndon, R. C. Miake-Lye, and B. E. Anderson, "Characterization of lubrication oil emissions from aircraft engines," *Environmental Science & Technology*, vol. 44, pp. 9530–9534, 2010.

[74] D. J. Donaldson and V. Vaida, "The influence of organic films at the air-aqueous boundary on atmospheric processes," *Chemical reviews*, vol. 106, no. 4, pp. 1445–1461, 2006.

[75] B. T. Mmereki, S. R. Chaudhuri, and D. J. Donaldson, "Enhanced uptake of pahs by organic-coated aqueous surfaces," *The Journal of Physical Chemistry A*, vol. 107, no. 13, pp. 2264–2269, 2003.